

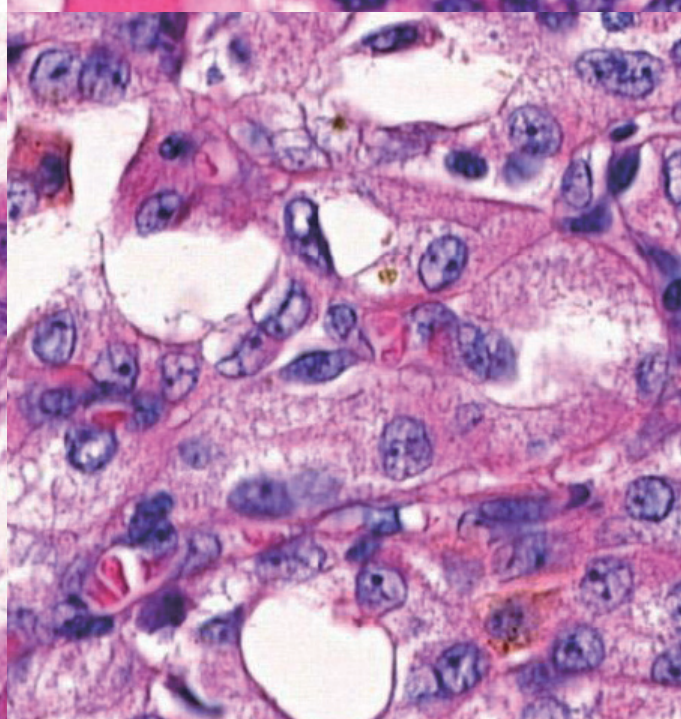
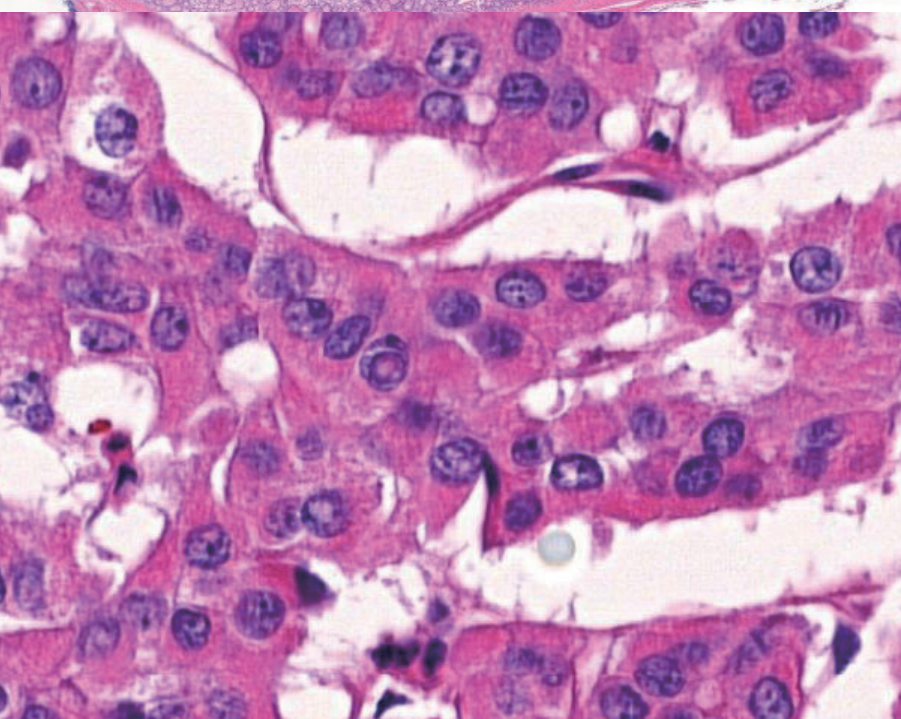
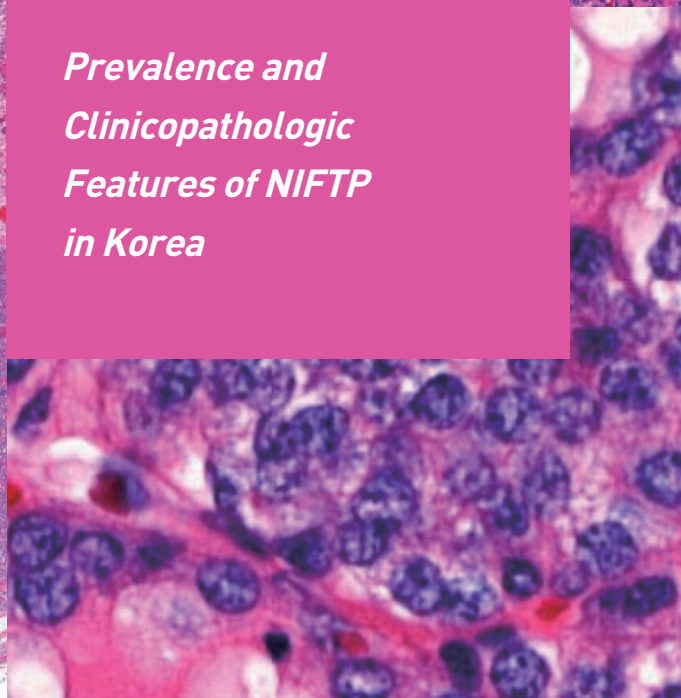
JPTM

**Journal of Pathology
and Translational Medicine**

November 2019
Vol. 53 / No.6
jpatholm.org
pISSN: 2383-7837
eISSN: 2383-7845



*Prevalence and
Clinicopathologic
Features of NIFTP
in Korea*



Aims & Scope

The *Journal of Pathology and Translational Medicine* is an open venue for the rapid publication of major achievements in various fields of pathology, cytopathology, and biomedical and translational research. The Journal aims to share new insights into the molecular and cellular mechanisms of human diseases and to report major advances in both experimental and clinical medicine, with a particular emphasis on translational research. The investigations of human cells and tissues using high-dimensional biology techniques such as genomics and proteomics will be given a high priority. Articles on stem cell biology are also welcome. The categories of manuscript include original articles, review and perspective articles, case studies, brief case reports, and letters to the editor.

Subscription Information

To subscribe to this journal, please contact the Korean Society of Pathologists/the Korean Society for Cytopathology. Full text PDF files are also available at the official website (<http://jpatholtm.org>). *Journal of Pathology and Translational Medicine* is indexed by Emerging Sources Citation Index (ESCI), PubMed, PubMed Central, Scopus, KoreaMed, KoMCI, WPRIM, Directory of Open Access Journals (DOAJ), and CrossRef. Circulation number per issue is 700.

Editors-in-Chief

Jung, Chan Kwon, MD (*The Catholic University of Korea, Korea*) <https://orcid.org/0000-0001-6843-3708>
Park, So Yeon, MD (*Seoul National University, Korea*) <https://orcid.org/0000-0002-0299-7268>

Senior Editors

Hong, Soon Won, MD (*Yonsei University, Korea*) <https://orcid.org/0000-0002-0324-2414>
Kim, Chong Jai, MD (*University of Ulsan, Korea*) <https://orcid.org/0000-0002-2844-9446>

Associate Editors

Shin, Eunah, MD (*CHA University, Korea*) <https://orcid.org/0000-0001-5961-3563>
Kim, Haeryoung, MD (*Seoul National University, Korea*) <https://orcid.org/0000-0002-4205-9081>

Editorial Board

Avila-Casado, Maria del Carmen (*University of Toronto, Toronto General Hospital UHN, Canada*)

Bae, Young Kyung (*Yonsei University, Korea*)

Bongiovanni, Massimo (*Lausanne University Hospital, Switzerland*)

Bychkov, Andrey (*Chulalongkorn University, Thailand Kameda Medical Center, Japan Nagasaki University Hospital, Japan*)

Choi, Yeong-Jin (*The Catholic University of Korea, Korea*)

Chong, Yo Sep (*The Catholic University of Korea, Korea*)

Chung, Jin-Haeng (*Seoul National University, Korea*)

Fadda, Guido (*Catholic University of Rome-Foundation Agostino Gemelli University Hospital, Italy*)

Gong, Gyungyub (*University of Ulsan, Korea*)

Ha, Seung Yeon (*Gachon University, Korea*)

Han, Jee Young (*Inha University, Korea*)

Jain, Deepali (*All India Institute of Medical Sciences, India*)

Jang, Se Jin (*University of Ulsan, Korea*)

Jeong, Jin Sook (*Dong-A University, Korea*)

Jun, Sun-Young (*The Catholic University of Korea, Korea*)

Kang, Gyeong Hoon (*Seoul National University, Korea*)

Kim, Aeree (*Korea University, Korea*)

Kim, Jang-Hee (*Ajou University, Korea*)

Kim, Jung Ho (*Seoul National University, Korea*)

Kim, Kyu Rae (*University of Ulsan, Korea*)

Kim, Se Hoon (*Yonsei University, Korea*)

Kim, Woo Ho (*Seoul National University, Korea*)

Ko, Young Hye (*Sungkyunkwan University, Korea*)

Koo, Ja Seung (*Yonsei University, Korea*)

Lai, Chiung-Ru (*Taipei Veterans General Hospital, Taiwan*)

Lee, C. Soon (*University of Western Sydney, Australia*)

Lee, Hye Seung (*Seoul National University, Korea*)

Liu, Zhiyan (*Shandong University, China*)

Lkhagvadorj, Sayamaa (*Mongolian National University of Medical Sciences, Mongolia*)

Moon, Woo Sung (*Chonbuk University, Korea*)

Paik, Jin Ho (*Seoul National University, Korea*)

Park, Chan-Sik (*University of Ulsan, Korea*)

Park, Young Nyun (*Yonsei University, Korea*)

Shahid, Pervez (*Aga Khan University, Pakistan*)

Song, Joon Seon (*University of Ulsan, Korea*)

Sung, Chang Ohk (*University of Ulsan, Korea*)

Tan, Puay Hoon (*National University of Singapore, Singapore*)

Than, Nandor Gabor (*Semmelweis University, Hungary*)

Tse, Gary M. (*The Chinese University of Hong Kong, Hong Kong*)

Yatabe, Yasushi (*Aichi Cancer Center, Japan*)

Yoon, Sun Och (*Yonsei University, Korea*)

Zhu, Yun (*Jiangsu Institution of Nuclear Medicine, China*)

Consulting Editors

Huh, Sun (*Hallym University, Korea*)

Kakudo, Kennichi (*Kindai University, Japan*)

Ro, Jae Y. (*Cornell University, The Methodist Hospital, U.S.A.*)

Ethic Editor

Choi, In-Hong (*Yonsei University, Korea*)

Statistics Editors

Kim, Dong Wook (*National Health Insurance Service Ilsan Hospital, Korea*)

Lee, Hye Sun (*Yonsei University, Korea*)

Manuscript Editor

Chang, Soo-Hee (*InfoLumi Co., Korea*)

Layout Editor

Kim, Haeja (*iMiS Company Co., Ltd., Korea*)

Website and JATS XML File Producers

Cho, Yoosang (*M2Community Co., Korea*)

Im, Jeonghee (*M2Community Co., Korea*)

Administrative Assistants

Jung, Ji Young (*The Korean Society of Pathologists*)

Jeon, Anmi (*The Korean Society for Cytopathology*)

Contact the Korean Society of Pathologists/the Korean Society for Cytopathology

Publishers: Lee, Kyo Young, MD, Hong, Soon Won, MD

Editors-in-Chief: Jung, Chan Kwon, MD, Park, So Yeon, MD

Published by the Korean Society of Pathologists/the Korean Society for Cytopathology

Editorial Office

Room 1209 Gwanghwamun Officia, 92 Saemunan-ro, Jongno-gu, Seoul 03186, Korea

Tel: +82-2-795-3094 Fax: +82-2-790-6635 E-mail: office@jpatholtm.org

#1508 Renaissancetower, 14 Mallijae-ro, Mapo-gu, Seoul 04195, Korea

Tel: +82-2-593-6943 Fax: +82-2-593-6944 E-mail: office@jpatholtm.org

Printed by iMiS Company Co., Ltd. (JMC)

Jungang Bldg. 18-8 Wonhyo-ro 89-gil, Yongsan-gu, Seoul 04314, Korea

Tel: +82-2-717-5511 Fax: +82-2-717-5515 E-mail: ml@smileml.com

Manuscript Editing by InfoLumi Co.

210-202, 421 Pangyo-ro, Bundang-gu, Seongnam 13522, Korea

Tel: +82-70-8839-8800 E-mail: infolumi.chang@gmail.com

Front cover image: Histologic features of non-invasive follicular thyroid neoplasm with papillary-like nuclear features (Fig. 1). p380.

© Copyright 2019 by the Korean Society of Pathologists/the Korean Society for Cytopathology

© Journal of Pathology and Translational Medicine is an Open Access journal under the terms of the Creative Commons Attribution Non-Commercial License (<https://creativecommons.org/licenses/by-nc/4.0/>).

© This paper meets the requirements of KS X ISO 9706, ISO 9706-1994 and ANSI/NISO Z.39.48-1992 (Permanence of Paper).

This journal was supported by the Korean Federation of Science and Technology Societies Grant funded by the Korean Government.

CONTENTS

ORIGINAL ARTICLES

- 347 **Interobserver Reproducibility of PD-L1 Biomarker in Non-small Cell Lung Cancer: A Multi-Institutional Study by 27 Pathologists**
Sunhee Chang, Hyung Kyu Park, Yoon-La Choi, Se Jin Jang, Cardiopulmonary Pathology Study Group of the Korean Society of Pathologists
- 354 **MicroRNA-374a Expression as a Prognostic Biomarker in Lung Adenocarcinoma**
Yeseul Kim, Jongmin Sim, Hyunsung Kim, Seong Sik Bang, Seungyun Jee, Sungeon Park, Kiseok Jang
- 361 **Molecular and Clinicopathological Features of Gastrointestinal Stromal Tumors in Vietnamese Patients**
Quoc Dat Ngo, Quoc Thang Pham, Dang Anh Thu Phan, Anh Vu Hoang, Thi Ngoc Ha Hua, Sao Trung Nguyen
- 369 **Comparison of Squamous Cell Carcinoma of the Tongue between Young and Old Patients**
Gyuheon Choi, Joon Seon Song, Seung-Ho Choi, Soon Yuhl Nam, Sang Yoon Kim, Jong-Lyel Roh, Bu-Kyu Lee, Kyung-Ja Cho
- 378 **A Multi-institutional Study of Prevalence and Clinicopathologic Features of Non-invasive Follicular Thyroid Neoplasm with Papillary-like Nuclear Features (NIFTP) in Korea**
Ja Yeong Seo, Ji Hyun Park, Ju Yeon Pyo, Yoon Jin Cha, Chan Kwon Jung, Dong Eun Song, Jeong Ja Kwak, So Yeon Park, Hee Young Na, Jang-Hee Kim, Jae Yeon Seok, Hee Sung Kim, Soon Won Hong
- 386 **Clinical Utility of a Fully Automated Microsatellite Instability Test with Minimal Hands-on Time**
Miseon Lee, Sung-Min Chun, Chang Ohk Sung, Sun Y. Kim, Tae W. Kim, Se Jin Jang, Jihun Kim
- 393 **Cytomorphological Features of Hyperchromatic Crowded Groups in Liquid-Based Cervicovaginal Cytology: A Single Institutional Experience**
Youngeun Lee, Cheol Lee, In Ae Park, Hyoung Jin An, Haeryoung Kim

CASE REPORTS

- 399 **Concurrent Anti-glomerular Basement Membrane Nephritis and IgA Nephropathy**
Kwang-Sun Suh, Song-Yi Choi, Go Eun Bae, Dae Eun Choi, Min-Kyung Yeo

403 Adenocarcinoma Arising in an Ectopic Hamartomatous Thymoma with HER2 Overexpression

Harim Oh, Eojin Kim, Bokyung Ahn, Jeong Hyeon Lee, Youngseok Lee, Yang Seok Chae, Chul Hwan Kim, Yoo Jin Lee

407 Peritoneal Fluid Cytology of Disseminated Large Cell Neuroendocrine Carcinoma Combined with Endometrioid Adenocarcinoma of the Endometrium

Yong-Moon Lee, Min-Kyung Yeo, Song-Yi Choi, Kyung-Hee Kim, Kwang-Sun Suh

LETTERS TO THE EDITOR

411 Comment on “Prognostic Role of Claudin-1 Immunohistochemistry in Malignant Solid Tumors: A Meta-Analysis”

Bolin Wang, Yan Huang

412 Response to Comment on “Prognostic Role of Claudin-1 Immunohistochemistry in Malignant Solid Tumors: A Meta-Analysis”

Jung-Soo Pyo, Nae Yu Kim, Won Jin Cho

CORRIGENDUM

415 Correction of Ethics Statement: Metastatic Insulinoma Presenting as a Liver Cyst

Hua Li, Tony El Jabbour, Ankesh Nigam, Hwajeong Lee

Instructions for Authors for *Journal of Pathology and Translational Medicine* are available at <http://jpatholm.org/authors/authors.php>

Interobserver Reproducibility of PD-L1 Biomarker in Non-small Cell Lung Cancer: A Multi-Institutional Study by 27 Pathologists

Sunhee Chang*, Hyung Kyu Park^{1*}, Yoon-La Choi², Se Jin Jang³,
Cardiopulmonary Pathology Study Group of the Korean Society of Pathologists

Department of Pathology, Inje University Ilsan Paik Hospital, Goyang; ¹Department of Pathology, Konkuk University Medical Center, Konkuk University School of Medicine, Seoul; ²Department of Pathology and Translational Genomics, Samsung Medical Center, Sungkyunkwan University School of Medicine, Seoul; ³Department of Pathology, Asan Medical Center, University of Ulsan College of Medicine, Seoul, Korea

Background: Assessment of programmed cell death-ligand 1 (PD-L1) immunohistochemical staining is used for treatment decisions in non-small cell lung cancer (NSCLC) regarding use of PD-L1/programmed cell death protein 1 (PD-1) immunotherapy. The reliability of the PD-L1 22C3 pharmDx assay is critical in guiding clinical practice. The Cardiopulmonary Pathology Study Group of the Korean Society of Pathologists investigated the interobserver reproducibility of PD-L1 staining with 22C3 pharmDx in NSCLC samples. **Methods:** Twenty-seven pathologists individually assessed the tumor proportion score (TPS) for 107 NSCLC samples. Each case was divided into three levels based on TPS: <1%, 1%–49%, and ≥50%. **Results:** The intraclass correlation coefficient for TPS was 0.902 ± 0.058 . Weighted κ coefficient for 3-step assessment was 0.748 ± 0.093 . The κ coefficients for 1% and 50% cut-offs were 0.633 and 0.834, respectively. There was a significant association between interobserver reproducibility and experience (formal PD-L1 training, more experience for PD-L1 assessment, and longer practice duration on surgical pathology), histologic subtype, and specimen type. **Conclusions:** Our results indicate that PD-L1 immunohistochemical staining provides a reproducible basis for decisions on anti-PD-1 therapy in NSCLC.

Key Words: Programmed cell death-ligand 1; Reproducibility; Observer variation; Immunohistochemistry

Received: July 15, 2019 **Revised:** September 1, 2019 **Accepted:** September 26, 2019

Corresponding Author: Yoon-La Choi, MD, Department of Pathology, Samsung Medical Center, Sungkyunkwan University School of Medicine, 81 Irwon-ro, Gangnam-gu, Seoul 06351, Korea

Tel: +82-2-3410-2797, Fax: +82-2-3410-6396, E-mail: ylchoi@skku.edu

*Sunhee Chang and Hyung Kyu Park contributed equally to this work.

Immunotherapies with checkpoint inhibitor programmed death-ligand 1 (PD-L1)/programmed cell death protein 1 (PD-1) antibodies have shown encouraging results in patients with advanced non-small cell lung cancer (NSCLC).¹⁻⁴ Assessment of PD-L1 immunohistochemical staining has been developed for pathology laboratories to aid in selecting patients who will benefit from PD-1/PD-L1–targeted therapy.^{1,5} PD-L1 immunohistochemistry is currently the most useful biomarker because of the wide availability of formalin-fixed, paraffin-embedded tissues, the relatively low cost, and widespread use in pathology laboratories, particularly in contrast to molecular pathology-based methods.^{1,6}

Pembrolizumab (Keytruda, Merck & Co., Inc., Kenilworth, NJ, USA), approved by the U.S. Food and Drug Administration (FDA) and Korea Ministry of Food and Drug Safety (MFDS), is a first-

line therapy PD-1 inhibitor for patients with advanced NSCLC.¹ Dako PD-L1 immunohistochemical (IHC) 22C3 pharmDx was used to determine PD-L1 expression in patients with advanced NSCLC during the clinical phase 1 trial (KEYNOTE-001).^{2,7} The PD-L1 IHC 22C3 pharmDx assay is the first companion diagnostic assay for PD-L1 approved by the FDA and MFDS.^{1,5} Currently, four PD-L1 assays using four different PD-L1 antibodies (22C3, 28-8, SP263, and SP142) on two different IHC platforms (Dako and Ventana) are approved by the FDA and Korea Food & Drug Administration. Each assay has its own scoring system. In the era of immunotherapy, reliability of assay results is critical to predict the likelihood of response to anti-PD-1 or anti-PD-L1 therapy. A few studies have investigated the reproducibility of assessing PD-L1 tests in NSCLC tissue samples.⁸⁻¹⁰

This study aimed to investigate the interobserver reproducibility of assessing PD-L1 expression in NSCLC tissue samples. Furthermore, association with observer factors and reproducibility of PD-L1 assessment was also investigated.

MATERIALS AND METHODS

Study material

A total of 107 cases of NSCLC were selected from the archives of the Department of Pathology of Samsung Medical Center from October 2016 and December 2016. Of these, 22 tissue samples were from resections, 66 tissue samples were from computed tomography-guided core biopsy, and 19 tissue samples were cell blocks of endobronchial ultrasound-guided transbronchial needle aspirate (EBUS-TBNA). The study material comprised 66 adenocarcinomas, 33 squamous cell carcinomas, and eight other non-small cell lung cancers. Selected tumor samples contained more than 100 cells per sample.

Immunohistochemical staining and evaluation

Tissue samples were stained for PD-L1 with the 22C3 phar-

mDx Kit (Agilent Technologies, Santa Clara, CA, USA) on the Dako Autostainer Link 48 platform (Agilent Technologies). Deparaffinization, rehydration, and target retrieval procedures were performed using EnVision FLEX Target Retrieval solution (1×, low pH) and EnVision FLEX wash buffer (1×). The tissue samples were then placed on the Autostainer Link 48. This instrument performed the staining process by applying appropriate reagent, monitoring incubation time, and rinsing slides between reagents. The reagent times were preprogrammed in the Dako Link software. A sample with primary antibody omitted was used as a negative control. Samples were subsequently counterstained with hematoxylin and mounted in non-aqueous, permanent mounting media. The stained slides were scanned by a Aperio scanner (Leica Biosystems, Buffalo Grove, IL, USA). Pathologists scored the virtual images using ImageScope software (Leica Biosystems).

Tumor proportion score (TPS) was defined as the percentage of viable tumor cells with any perceptible membrane staining irrespective of staining intensity. Normal cells and tumor-associated immune cells were excluded from scoring. Each case was divided into three levels based on TPS: < 1% (no PD-L1 expression), 1%–49% (PD-L1 expression), or ≥ 50% (high PD-L1 expression) (Fig. 1).

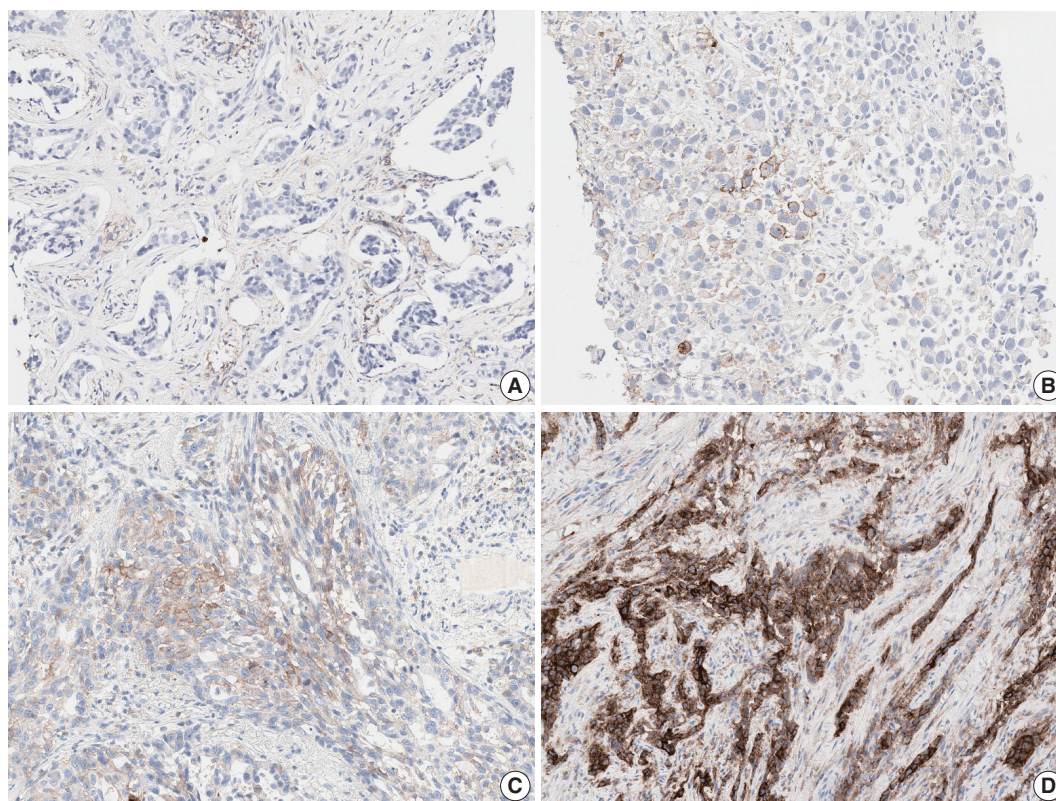


Fig. 1. Programmed cell death-ligand 1 (PD-L1) immunohistochemistry results in non-small cell lung cancer patients using 22C3 antibody on fully automated Dako Autostainer Link 48 platform. (A) Negative staining for PD-L1. (B) PD-L1 tumor proportion score (TPS) of 10%. (C) PD-L1 TPS of 70%. (D) PD-L1 TPS of 100%.

Participating pathologists

All slides were independently evaluated by 20 pulmonary pathology specialists and seven surgical pathology fellows. Eleven experts participated in a 1-day training course by Dako (Agilent Technologies, Santa Clara, CA, USA) relating to evaluation of the PD-L1 22C3 assay. Participant practice duration ranged from 1 to 37 years with a median of 13 years. Sixteen of the 27 pathologists gained experience in PD-L1 assessment by practicing daily with two to 500 cases per day for 2 months before starting this study, and four of the 16 pathologists had assessed more than 100 cases.

Statistical analysis

The gold standard PD-L1 TPS was established as TPS and assessed by highly trained and experienced experts. To assess the concordance of TPS between the 27 pathologists and the gold standard, intraclass correlation coefficients (ICCs) were calculated. The weighted kappa (κ) coefficient was calculated to evaluate concordance of the 3-step assessment between pathologists and the gold standard. Agreement for 1% and 50% cut-offs was assessed using overall percent agreement (OPA), positive and negative percent agreement, and Cohen's κ coefficient. Correlations between TPS and experience for PD-L1 test experience or practice duration were investigated using Spearman's rank correlation coefficient. Correlations between the 3-step assessment and PD-L1 test experience or practice duration were also investigated using Spearman's rank correlation coefficient. Differences in the concordance of TPS, 3-step assessment, and 1% and 50% cut-offs were compared between the expert group and fellow group using Wilcoxon rank sum tests. Correlations between TPS or 3-step assessment and training were assessed using Wilcoxon rank sum test. Correlations between TPS or 3-step assessment and histologic subtype or specimen type were assessed using Kruskal-Wallis Test.

An ICC is interpreted as follows: below 0.3 indicates poor agreement, 0.5 indicates moderate agreement, 0.7 indicates strong agreement, and 0.85 or more indicates almost perfect agreement. A κ coefficient of 0.4 or less is poor to fair agreement, greater than 0.4 to 0.6 is moderate agreement, greater than 0.6 to 0.8

is substantial agreement, and greater than 0.8 is almost perfect agreement. Spearman's rank correlation coefficient is interpreted as follows: below 0.3 indicates little if any (linear) correlation, between 0.3 and 0.5 indicates low correlation, between 0.5 and 0.7 indicates moderate correlation, between 0.7 and 0.9 indicates high correlation, and 0.9 or more indicates very high correlation. A p-value of $<.05$ was considered statistically significant. Statistical analyses were performed using SAS ver. 9.4 (SAS Institute Inc., Cary, NC, USA).

Ethics statement

This study was approved by the Institutional Review Board of Inje University Ilsan Paik Hospital with a waiver of informed consent (2018-08-009).

RESULTS

Interobserver reproducibility

Among 107 samples, 22 samples (20.6%) had a TPS $<1\%$, 40 samples (37.4%) had a TPS between 1% and 49%, and 45 samples (42.1%) had a TPS $\geq 50\%$. The ICC for TPS was 0.902 ± 0.058 , indicating almost perfect agreement (Table 1). Weighted κ coefficient for the 3-step assessment was 0.748 ± 0.093 , indicating substantial agreement. Using $\geq 1\%$ stained tumor cells as the cut-off for a positive test, the κ coefficient was calculated as 0.633 ± 0.111 , and OPA was $86.2 \pm 5.5\%$ (Table 2). The κ coefficient was 0.834 ± 0.095 , and the OPA was $92.1 \pm 4.4\%$ for cut-off $\geq 50\%$. These results indicate substantial agreement for 1% and almost perfect agreement for 50% cut-offs. The interobserver reproducibility was greater at the 50% cut-off than at the 1% cut-off.

Factors influencing interobserver reproducibility

There was significant association between interobserver reproducibility and specimen type (Table 3). The ICC for TPS was significantly higher in the resection group (0.926 ± 0.050) than in the EBUS-TBNA group (0.887 ± 0.099). The κ coefficient for the 3-step assessment was significantly higher in the biopsy group (0.776 ± 0.104) than in the EBUS-TBNA group (0.669 ± 0.089).

Table 1. Intraclass correlation coefficient of the tumor proportion score

	ICC for TPS	p-value	Weighted Kappa for 3 tiered assessment	p-value
Total (n=26)	0.902 ± 0.058		0.748 ± 0.093	
Expert (n=19)	0.919 ± 0.034	.037	0.772 ± 0.073	.043
Fellow (n=7)	0.859 ± 0.088		0.680 ± 0.115	

ICC, Intraclass correlation coefficient; TPS, tumor proportion score.

The EBUS-TBNA group showed almost perfect agreement for the 50% cut-off, but fair agreement for the 1% cut-off.

ICCs for TPS were influenced by histologic subtype (Table 4). The squamous cell carcinoma group showed higher agreement than the adenocarcinoma group. There was no significant difference between κ coefficients for the 3-step assessment.

There was significant association between interobserver reproducibility and experience (formal PD-L1 training, more experience for PD-L1 test, and longer practice duration on surgical pathology). The ICC for TPS was significantly higher in the trained group (0.922 ± 0.034) than in the untrained group (0.875 ± 0.074) (Table 5). The κ coefficient for the 3-step assessment was also significantly higher in the trained group (0.776 ± 0.079) than in the untrained group (0.709 ± 0.101). There was low linear correlation between ICC for TPS and experience for PD-L1 assessment (Spearman correlation coefficient = 0.422) (Table 6). There was no correlation between the κ coefficient for the 3-step assessment and experience for PD-L1 assessment. The ICC for TPS was significantly higher in the expert group ($91.9\% \pm 3.4\%$) than in the fellow group ($85.9\% \pm 8.8\%$) (Table 1). The κ coefficient for the 3-step assessment was also significantly higher in the expert

group (0.772 ± 0.073) than in the fellow group (0.680 ± 0.115). The κ coefficient for the 3-step assessment was significantly different in biopsy specimens between the expert group (0.807 ± 0.034) and the fellow group (0.693 ± 0.129) ($p = 0.0013$). In EBUS-TBNA and resection specimens, the κ coefficient of the expert group was slightly higher than that of the fellow group but there was no statistically significant difference between the two groups. There were no differences in κ coefficients at 1% and 50% cut-offs between the expert group and fellow group (Table 2).

DISCUSSION

We investigated the interobserver reproducibility of assessment of PD-L1 expression in NSCLC and observed good interobserver agreement for PD-L1 scoring. Pathologists were highly concordant for TPS with an ICC of 0.902. Rimm et al.⁸ examined the interobserver reproducibility for 22C3, 28-8, SP142, and E1L3N PD-L1 assays. Ninety samples were assessed by 13 pathologists. ICC was 0.882 for the 22C3 assay. The ICCs for 28-8, SP142, and E1L3N assays were 0.832, 0.869, and 0.859, respectively, showing high concordance. The findings suggest that PD-L1 assay is a reliable method for assessing PD-L1 expression in tumor cells.

We report good interobserver agreement for 1% and 50% cut-offs with κ coefficients of 0.633 and 0.834, respectively (Table 7). Cooper et al.⁹ investigated the interobserver reproducibility for

Table 2. Interobserver reproducibility of the cut-off

	1% Cut-off	p-value	50% Cut-off	p-value
Cohen's κ coefficient				
Total (n=26)	0.633±0.111		0.834±0.095	
Expert (n=19)	0.656±0.104	.068	0.858±0.072	.082
Fellow (n=7)	0.570±0.113		0.768±0.123	
OPA (%)				
Total (n=26)	86.2±5.5		92.1±4.4	
Expert (n=19)	87.3±4.6	.067	93.2±3.3	.075
Fellow (n=7)	83.2±6.8		89.1±5.5	
NPA (%)				
Total (n=26)	85.7±16.0		95.4±4.3	
Expert (n=19)	86.8±17.1	.150	95.3±4.5	.884
Fellow (n=7)	82.5±13.5		95.4±4.0	
PPA (%)				
Total (n=26)	86.3±8.4		87.5±12.0	
Expert (n=19)	87.4±7.6	.385	9.2±9.2	.149
Fellow (n=7)	83.4±1.2		8.3±16.4	

OPA, overall percent agreement; NPA, negative percent agreement; PPA, positive percent agreement.

Table 3. Impact of specimen type on interobserver reproducibility

	EBUS-TBNA (n=19)	Biopsy (n=66)	Resection (n=22)	p-value
ICC for TPS	0.887±0.099	0.899±0.061	0.926±0.050	.023
κ for 3-step evaluation	0.669±0.089	0.776±0.104	0.716±0.126	.001
κ for 1% cutoff	0.383±0.134	0.713±0.137	0.538±0.209	
κ for 50% cutoff	0.832±0.128	0.830±0.097	0.839±0.118	

EBUS-TBNA, Endobronchial ultrasound-guided transbronchial needle aspiration; ICC, intraclass correlation coefficient; TPS, tumor proportion score.

Table 4. Impact of histologic subtype on interobserver reproducibility

	SCC (n=33)	ADC (n=66)	p-value
ICC for TPS	0.877±0.071	0.917±0.053	.024
κ for 3-step evaluation	0.757±0.107	0.753±0.089	.073

SCC, squamous cell carcinoma; ADC, adenocarcinoma; ICC, intraclass correlation coefficient; TPS, tumor proportion score.

Table 5. Impact of training on interobserver reproducibility

	Training		p-value
	Yes (n=15)	No (n=11)	
ICC for TPS	0.922±0.034	0.875±0.074	.043
κ for 3-step assessment	0.776±0.079	0.709±0.101	.026

ICC, intraclass correlation coefficient; TPS, tumor proportion score.

Table 6. Impact of experience on interobserver reproducibility

	ICC for TPS		κ coefficient for 3-step evaluation	
	Spearman correlation	p-value	Spearman correlation	p-value
PD-L1 test experience	0.422	.032	0.277	.170
Practice duration	0.477	.014	0.527	.005

ICC, intraclass correlation coefficient; TPS, tumor proportion score; PD-L1, programmed cell death-ligand 1.

Table 7. Summary of the interobserver reproducibility study

	Sample	Observer	1% Cut-off	50% Cut-off
Rimm et al. ⁸	90	13	$\kappa = 0.537^a$	$\kappa = 0.749^a$
Cooper et al. ⁹	108	10	$\kappa = 0.68$	$\kappa = 0.58$
Brunnström et al. ¹⁰	55	7	2%–20% ^b	0%–2% ^b
Current study	107	27	$\kappa = 0.633$	$\kappa = 0.834$

^aFor the mean of all four assay (22C3, 28-8, SP142, and E1L3N); ^bDifferently classified cases by any one pathologist compared with consensus.

assessment of the 22C3 PD-L1 assay. Two separate sample sets of 60 samples each were designed for the 1% and 50% cut-offs that contained equally distributed PD-L1 positive and negative samples. The sample set for the 1% cut-off contained 10 positive samples close to the cut-off, and the sample set for the 50% cut-off contained 20 negative or positive samples close to the cut-off. Ten pathologists assessed a sample set of 108 samples obtained after pooling the 1% cut-off and the 50% cut-off sample sets together. The κ coefficient was 0.68 for the 1% cut-off and 0.58 for the 50% cut-off. Brunnström et al. examined interobserver reproducibility for the 28-8, 22C3, SP142, and SP263 assays.¹⁰ Seven pathologists assessed 55 samples. For the 22C3 assay, 2%–20% of cases were differently classified by any one pathologist compared to the consensus at the 1% cut-off, and 0%–2% of the cases were differently classified by any one pathologist compared to the consensus at the 50% cut-off. For all four assays, there were 0%–20% and 0%–5% differently classified cases at 1% and 50% cut-offs, respectively. Variation in the number of differently classified cases by any one pathologist compared to the consensus was statistically significant between cut-offs. The number of differently classified cases was significantly lower for the SP142 assay compared to that for the other three assays. This difference was probably because there were many obviously negative cases for SP142.¹⁰ Rimm et al.⁸ reported that κ coefficients for the mean of all 4 assays were 0.537 and 0.749 at 1% and 50% cut-offs, respectively. Interobserver concordance for the PD-L1 assay was higher at the 50% cut-off than at the 1% cut-off, except for the results of Cooper et al.⁹ It is possible that Cooper et al.⁹ used sample sets to artificially enrich with samples close to the cut-offs, which is not possible in clinical practice.

The interobserver concordance for TPS and the 3-step assess-

ment correlated with practice duration and was higher in the expert group than in the fellow group. This is probably because pulmonary pathologists were familiar with the varied morphologies of cancer and cancer-associated immune cells and had experience assessing other immunohistochemistry biomarkers, such as anaplastic lymphoma kinase, human epidermal growth factor receptor 2, and estrogen receptor.⁹ There was no difference in concordance between the expert group and fellow group for 1% and 50% cut-offs, similar to the results of Brunnström et al.¹⁰ Experience in conducting the PD-L1 test impacted interobserver concordance for TPS but not for 3-step assessment. These analyses suggested that the currently used 1% and 50% cut-offs are relatively reliable regardless of pathologist experience.

Our study reported that 1-day training improved interobserver reproducibility, whereas 1-hour training had no or very little impact on interobserver reproducibility.⁹ Therefore, 1-day training may be more effective than 1-hour training.

Tumor histologic subtype and specimen type influenced interobserver reproducibility, which was not previously reported. EBUS-TBNA showed lower interobserver agreement than resection and biopsy specimens at the 1% cut-off. Although squamous cell carcinoma showed higher agreement for TPS than adenocarcinoma, no significant difference was observed for the 3-step assessment. Strong membranous staining of macrophages, non-specific cytoplasmic staining of tumor cells, weak and/or partial membranous staining of tumors cells, heterogeneous staining intensities, and patchy staining are well-known interpretation pitfalls in assessing any PD-L1 assay (Fig. 2).⁸⁻¹⁰ While using the 1% cut-off, misinterpretation of very few or even single cells may lead to false positive or false negative results. Training and an external quality assessment program should be organized with special focus on difficult cases and on assessing the 1% cut-off. Guidelines including examples and strategies for difficult cases should be developed.

The limitations of our study include the lack of a “true gold standard” and outcome data for therapy. However, gold standard assessment was undertaken by highly trained experienced specialists. The following were strengths of the present study: it is more representative of real clinical practice than previous studies,

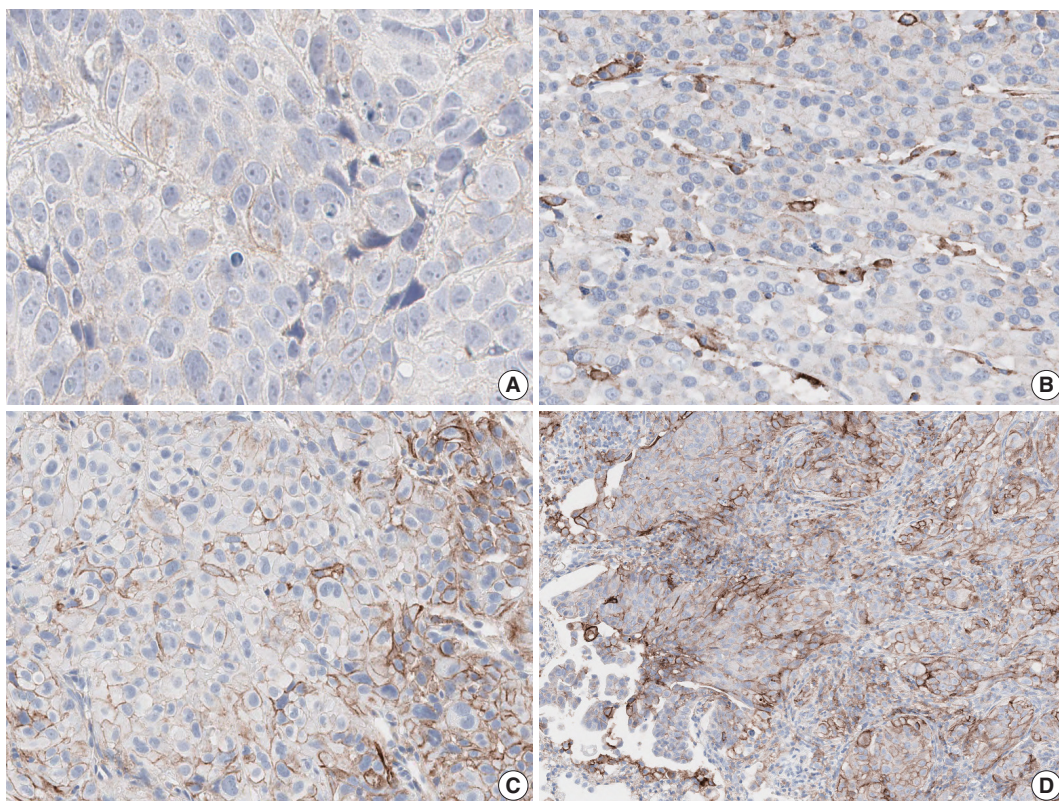


Fig. 2. (A) Few tumor cells show weak and partial membrane staining for programmed cell death-ligand 1 (PD-L1) antibody. (B) Tumor associated immune cells show strong staining with lack of PD-L1 staining in tumor cells. (C) Tumor cells show heterogeneous membrane staining pattern with various staining intensities. (D) Tumor shows patchy membrane staining pattern.

whole sections from many samples were used to evaluate the reproducibility of PD-L1 assays, more observers than previous studies, and participating pathologists worked in different centers and had different levels of experience.

In conclusion, our results indicate that PD-L1 staining provides a reliable basis for decisions regarding anti-PD-1 therapy in NSCLC. Although interobserver agreement for the 1% cut-off was relatively lower, it was substantial and acceptable. Better training, longer assay experience, and an external quality assessment program could improve interobserver reproducibility for the 1% cut-off.

ORCID

Sunhee Chang: <https://orcid.org/0000-0002-7775-4711>

Hyung Kyu Park: <https://orcid.org/0000-0002-5972-3516>

Yoon-La Choi: <http://orcid.org/0000-0002-5788-5140>

Se Jin Jang: <http://orcid.org/0000-0001-8239-4362>

Author Contributions

Conceptualization: YLC.

Data curation: SC, HKP, YLC.

Formal analysis: HKP, YLC.

Funding acquisition: SC, SJJ.

Investigation: SC, HKP, YLC.

Methodology: SC, HKP, YLC.

Project administration: YLC.

Resources: YLC.

Supervision: YLC, SJJ.

Validation: SC, HKP, YLC.

Visualization: SC, HKP, YLC.

Writing—original draft: SC.

Writing—review & editing: SC, YLC, SJJ.

Conflicts of Interest

The authors declare that they have no potential conflicts of interest.

Funding

This research was supported by 2017 The Korean Society of Pathologists Grant.

REFERENCES

1. Guan J, Lim KS, Mekhail T, Chang CC. Programmed death ligand-1 (PD-L1) expression in the programmed death receptor-1 (PD-1)/PD-L1 blockade: a key player against various cancers. *Arch Pathol Lab Med* 2017; 141: 851-61.
2. Reck M, Rodríguez-Abreu D, Robinson AG, et al. Pembrolizumab versus chemotherapy for PD-L1-positive non-small-cell lung cancer. *N Engl J Med* 2016; 375: 1823-33.
3. Langer CJ, Gadgeel SM, Borghaei H, et al. Carboplatin and pemetrexed with or without pembrolizumab for advanced, non-squamous non-small-cell lung cancer: a randomised, phase 2 cohort of the open-label KEYNOTE-021 study. *Lancet Oncol* 2016; 17: 1497-508.
4. Gettinger S, Rizvi NA, Chow LQ, et al. Nivolumab monotherapy for first-line treatment of advanced non-small-cell lung cancer. *J Clin Oncol* 2016; 34: 2980-7.
5. Roach C, Zhang N, Corigliano E, et al. Development of a companion diagnostic PD-L1 immunohistochemistry assay for pembrolizumab therapy in non-small-cell lung cancer. *Appl Immunohistochem Mol Morphol* 2016; 24: 392-7.
6. Cree IA, Booton R, Cane P, et al. PD-L1 testing for lung cancer in the UK: recognizing the challenges for implementation. *Histopathology* 2016; 69: 177-86.
7. Herbst RS, Baas P, Kim DW, et al. Pembrolizumab versus docetaxel for previously treated, PD-L1-positive, advanced non-small-cell lung cancer (KEYNOTE-010): a randomised controlled trial. *Lancet* 2016; 387: 1540-50.
8. Rimm DL, Han G, Taube JM, et al. A prospective, multi-institutional, pathologist-based assessment of 4 immunohistochemistry assays for PD-L1 expression in non-small cell lung cancer. *JAMA Oncol* 2017; 3: 1051-8.
9. Cooper WA, Russell PA, Cherian M, et al. Intra- and interobserver reproducibility assessment of PD-L1 biomarker in non-small cell lung cancer. *Clin Cancer Res* 2017; 23: 4569-77.
10. Brunnström H, Johansson A, Westbom-Fremer S, et al. PD-L1 immunohistochemistry in clinical diagnostics of lung cancer: interpathologist variability is higher than assay variability. *Mod Pathol* 2017; 30: 1411-21.

MicroRNA-374a Expression as a Prognostic Biomarker in Lung Adenocarcinoma

Yeseul Kim, Jongmin Sim¹, Hyunsung Kim, Seong Sik Bang, Seungyun Jee, Sungeon Park, Kiseok Jang

Department of Pathology, Hanyang University College of Medicine, Seoul; ¹Department of Pathology, Samsung Medical Center, Seoul, Korea

Background: Lung cancer is the most common cause of cancer-related death, and adenocarcinoma is the most common histologic subtype. MicroRNA is a small non-coding RNA that inhibits multiple target gene expression at the post-transcriptional level and is commonly dysregulated in malignant tumors. The purpose of this study was to analyze the expression of microRNA-374a (miR-374a) in lung adenocarcinoma and correlate its expression with various clinicopathological characteristics. **Methods:** The expression level of miR-374a was measured in 111 formalin-fixed paraffin-embedded lung adenocarcinoma tissues using reverse transcription-quantitative polymerase chain reaction assays. The correlation between miR-374a expression and clinicopathological parameters, including clinical outcome, was further analyzed. **Results:** High miR-374 expression was correlated with advanced pT category (chi-square test, $p = .004$) and pleural invasion (chi-square test, $p = .034$). Survival analysis revealed that patients with high miR-374a expression had significantly shorter disease-free survival relative to those with low miR-374a expression (log-rank test, $p = .032$). **Conclusions:** miR-374a expression may serve as a potential prognostic biomarker for predicting recurrence in early stage lung adenocarcinoma after curative surgery.

Key Words: Lung neoplasms; Adenocarcinoma; Stage; Recurrence; MicroRNAs

Received: July 17, 2019 **Revised:** September 27, 2019 **Accepted:** October 1, 2019

Corresponding Author: Kiseok Jang, MD, PhD, Department of Pathology, Hanyang University College of Medicine, 222-1 Wangsimni-ro, Seongdong-gu, Seoul 04763, Korea
Tel: +82-2-2290-8248, Fax: +82-2-2296-7502, E-mail: medartisan@hanyang.ac.kr

Lung cancer is one of the most frequently diagnosed cancers and is a leading cause of morbidity and mortality globally.¹ Of the various lung cancer types, the most common histologic subtype is adenocarcinoma, which accounts for 40%–50% of diagnoses.² Despite recent advances in immunotherapy and targeted therapy, patients with lung cancer still have a poor prognosis with an average 5-year survival rate of about 55%, even when diagnosed at stage I.¹

MicroRNA (miRNA) is a single-stranded, non-coding, regulatory RNA of 19–25 nucleotides in length.³ miRNAs are one of the components of the RNA-induced silencing complex that inhibits target gene expression either by causing mRNA degradation or suppressing mRNA translation.⁴ As miRNAs can bind mRNA by incomplete complementarity of sequences, a single miRNA can regulate multiple target genes.⁴ Previous miRNA expression profiling studies have shown that up- and down-regulation of miRNA expression is commonly observed in malignant tumor tissues compared to normal counterparts.⁵ This miRNA dysregulation is involved in carcinogenesis and tumor progression.⁵

miRNA expression profiling studies of various human malignancies have identified potential biomarkers for early diagnosis, classification, prognosis, and therapeutic response.⁶

MicroRNA-374a (miR-374a) has been investigated due to its involvement in the carcinogenesis and tumor progression of solid tumors and hematologic malignancies. Previous studies demonstrated that miR-374a promotes cell proliferation and metastasis of osteosarcoma, hepatocellular carcinoma, pancreatic cancer, breast cancer, and esophageal cancer by targeting various tumor suppressors, including Axin2, MIG-6, SRCIN1, LACTB, and ARRB1.^{7–13} However, some studies demonstrated the tumor suppressive role of miR-374a in colon cancer, T-cell lymphoblastic lymphoma, and non-small cell lung cancer (NSCLC) by targeting cyclin D1, PTEN, and AKT.^{14–16}

In this study, miR-374a expression was measured using the quantitative real-time polymerase chain reaction (qRT-PCR) technique with RNA extracted from formalin-fixed, paraffin-embedded (FFPE) tumor tissues of 111 lung adenocarcinoma samples. The expression of miR-374a was correlated with con-

ventional clinicopathologic parameters as well as patient survival.

MATERIALS AND METHODS

Patients and tumor samples

A total of 184 consecutive cases of curative surgery for primary lung adenocarcinoma conducted at Hanyang University Hospital, Seoul, Korea, from 2003 to 2014 were retrospectively selected. Of the total 184 cases, 37 (20.1%) were excluded due to the lack of a suitable FFPE sample and 36 of the remaining patients were excluded because of the poor quality of FFPE RNAs. Finally, qRT-PCR for miR-374a and the U6 control was successful in 111 cases and further statistical analyses were performed. None of the patients received preoperative therapy. Clinicopathological data were collected and reviewed from the medical records and histopathological reports, and additional review of archived pathologic slides was conducted. The clinicopathological parameters included patient age, sex, tumor size, T category, pleural invasion, lymph node metastasis, American Joint Committee on Cancer (AJCC) tumor stage, histological grade, lymphovascular invasion, and perineural invasion. Histologic grading was determined by conventional histological criteria, including architectural abnormalities and cytologic atypia. Most cases with histologic grade 1 were categorized as lepidic predominant subtype, cases with grade 2 were categorized as acinar or papillary predominant subtype, and cases with grade 3 were categorized as solid or micropapillary predominant subtype based on the new 2015 World Health Organization classification. Disease-free survival (DFS) was measured from the date of operation until recurrence or death. Overall survival (OS) was measured from the date of operation until the time of death or the last follow-up.

RNA extraction and qRT-PCR

To identify areas most representative of tumors and non-necrotic tumor sections, we reviewed and marked histologic slides. Three or four 10- μ m-thick tissue sections from each block were collected. Total RNA was isolated from the FFPE tumor tissues using miRNeasy FFPE kits (Qiagen, Hilden, Germany) according to the manufacturer's instruction. The concentration and purity of extracted RNA was measured using a NanoDrop 2000 spectrophotometer (NanoDrop Technologies, Waltham, MA, USA).

Universal cDNA synthesis kits (Exiqon, Vedbaek, Denmark) were used to convert RNA into cDNA. qRT-PCR experiments were performed with a mixture of diluted cDNA samples, an miR-374a specific primer set (Exiqon), and an ExiLENT SYBR

Green Master mix (Exiqon). PCR was performed using a CFX96 thermocycler (Bio-Rad, Hercules, CA, USA) under the following conditions: 95°C for 15 minutes followed by 45 cycles of 95°C for 10 seconds and 60°C for 1 minute. After PCR amplification, melting curve analysis was performed to confirm the specificity of PCR products. The expression level of miR-374a was calculated using the $2^{-\Delta\Delta C_t}$ method relative to the U6 small nuclear RNA (RNU6B).

Statistical analysis

Statistical analysis was performed using SPSS ver. 21.0 software (IBM Corp., Armonk, NY, USA). Chi-square tests were used to evaluate associations between miR-374a expression and various clinicopathological parameters of pulmonary adenocarcinoma patients. Kaplan-Meier survival curves for both DFS and OS were plotted, and the log-rank test was applied to establish the level of significance. The Cox proportional hazard regression model was employed in both univariable and multivariable survival analyses. A p-value of $< .05$ was defined as statistically significant.

Ethics statement

This study was approved by the Institutional Review Board (IRB) of Hanyang University Hospital (IRB file no. 2016-07-038) with a waiver of informed consent.

RESULTS

Clinicopathological characteristics of patients enrolled in the study

Two-thirds of patients were over 60 years of age ($n = 68$, 61.3%) and more females than men ($n = 65$, 58.6%) were included in the study. Most of the cases were categorized as histologic grade 2 ($n = 78$, 69.6%) and AJCC stage I ($n = 76$, 68.5%). Lymph node metastasis was found in 25 cases (22.5%), pleural invasion in 46 cases (41.4%), lymphovascular invasion in 40 cases (36.0%), and perineural invasion in 21 cases (18.9%). The clinicopathological characteristics are summarized in Table 1.

Correlations between miR-374a expression and clinicopathological characteristics in pulmonary adenocarcinoma

The quantitative measures of relative miR-374a expression in all 111 lung adenocarcinoma samples were as follows: mean, 0.048; median, 0.066; standard deviation, 1.585; and range, 0.000–11.794. The patients were divided into two groups (low

Table 1. Summary of clinicopathological characteristics in pulmonary adenocarcinoma patients

Characteristic	No. (%) (n=111)
Age (yr)	
<60	43 (38.7)
≥60	68 (61.3)
Sex	
Male	46 (41.4)
Female	65 (58.6)
Histological grade	
Grade 1	23 (20.7)
Grade 2	78 (70.3)
Grade 3	10 (9.0)
T category	
pT1	51 (45.9)
pT2	53 (47.7)
pT3	5 (4.5)
pT4	2 (1.8)
AJCC stage group	
I	76 (68.5)
II	17 (15.3)
III	18 (16.2)
Lymph node metastasis	
pN0	86 (77.5)
pN1	10 (9.0)
pN2	13 (11.7)
pN3	2 (1.8)
Pleural invasion	
PL0	65 (58.6)
PL1	35 (31.5)
PL2	10 (9.0)
PL3	1 (0.9)
Lymphovascular invasion	
Absent	71 (64.0)
Present	40 (36.0)
Perineural invasion	
Absent	90 (81.1)
Present	21 (18.9)

AJCC, American Joint Committee on Cancer.

vs high) according to the median value of miR-374a expression. We analyzed the associations between miR-374a expression and clinicopathological characteristics, including age, sex, AJCC stage group, primary tumor (T category), lymph node metastasis, pleural invasion, histologic grade, lymphovascular invasion, and perineural invasion. High miR-374a expression was correlated with advanced T category (chi-square test, $p = .004$) and the presence of pleural invasion (chi-square test, $p = .034$) (Table 2).

Prognostic value of miR-374a expression in pulmonary adenocarcinoma

The median follow-up interval of patients for OS and DFS was 27.3 months (range, 0.9 to 118.6 months) and 25.7 months

(range, 0.9 to 85.0 months), respectively. Local recurrence or metastasis was found in 18 patients, and 9 patients died during the follow-up period. On univariate survival analysis, AJCC stage, T category, lymph node metastasis, histologic grade, lymphovascular invasion, and perineural invasion were revealed as prognostic factors for DFS and/or OS (Table 3). Patients with high miR-374a expression showed shorter DFS compared to those with low miR-374a expression, and the difference was statistically significant (log-rank test, $p = .032$) (Fig. 1). However, miR-374a expression level was not an independent prognostic factor in multivariable survival analysis. The OS of the patients with high miR-374a expression was also inferior to those with low expression; however, the difference failed to demonstrate a statistical significance. In addition, stage-stratified survival analyses revealed that high miR-374a expression was significantly associated with shorter DFS only in patients with AJCC stage I (log-rank test, $p = .006$).

DISCUSSION

Fresh frozen tissue has been mostly used for high-throughput miRNA expression profiling for human cancers. However, sampling and long-term storage of fresh tumor tissue is laborious and expensive in daily clinical practice. As tumor specimens are routinely stored as FFPE blocks after diagnostic process in pathology archives and can be linked with medical records, emerging interest has been directed toward whether FFPE tissue can be used for studies of miRNA biomarkers. Interestingly, miRNAs appear to be stable in FFPE samples, even exhibiting near total mRNA degradation.¹⁷ Preservation of miRNA in FFPE tumor samples has been confirmed in previous studies, and the results obtained from qRT-PCR analyses, miRNA expression profiling, and even next-generation sequencing studies are consistent with those of fresh frozen tissue.¹⁸⁻²¹ These results suggest that quantifying miRNA expression level using FFPE tissue can enable the identification of clinically-available miRNA biomarkers in human malignancies.

One of the clinical significances of measuring miRNA expression level in resected tumor tissues is to identify patients at high risk of recurrence or cancer-related death after curative surgery. Zheng et al.²² reported that NSCLC patients with low miR-195 expression showed poor overall survival. In the study of Chen et al.,²³ low miRNA-148a expression was significantly correlated with high histologic grade, frequent lymph node metastasis, and a poor OS in NSCLC. Further, miR-21, as an oncogenic miRNA, has been reported as a biomarker for predicting recur-

rence, metastasis, and resistance of radiation and chemotherapy in NSCLC.²⁴⁻²⁶ In our study, high miR-374a expression correlated with advanced pT category, pleural invasion, and poor DFS in lung adenocarcinoma. Zhao et al.¹⁶ investigated miR-374a expression level in 158 NSCLC tissues by in situ hybridization.

They found that miR-374a was highly expressed in NSCLC relative to non-neoplastic tissues and correlated with lymph node metastasis and poor clinical outcome.¹⁶ However, in the study of 38 Estonian NSCLC cases (18 squamous cell carcinomas and 20 adenocarcinomas), low miR-374a expression, as by miRNA

Table 2. Correlation between miR-374a expression and various clinicopathological factors in lung adenocarcinoma (n = 111)

Clinicopathological characteristic	No.	miR-374a expression		Chi-square test
		Low	High	p-value
Age (yr)				.437
<60	43	19 (44.2)	24 (55.8)	
≥60	68	36 (52.9)	32 (47.1)	
Sex				.337
Male	46	20 (43.5)	26 (56.5)	
Female	65	35 (53.8)	30 (46.2)	
AJCC stage group				.221
I	76	41 (53.9)	35 (46.1)	
II, III	35	14 (40.0)	21 (60.0)	
Primary tumor				.004
pT1	51	33 (64.7)	18 (35.3)	
pT2, pT3, pT4	60	22 (36.7)	38 (63.3)	
LN metastasis				>.99
Negative	86	43 (50.0)	43 (50.0)	
Positive	25	12 (48.0)	13 (52.0)	
Pleural invasion				.034
Negative	65	38 (58.5)	27 (41.5)	
Positive	46	17 (37.0)	29 (63.0)	
Histological grade				.490
Grade 1	23	13 (56.5)	10 (43.5)	
Grade 2 and 3	88	42 (47.7)	46 (52.3)	
Lymphovascular invasion				.695
Absent	71	34 (47.9)	37 (52.1)	
Present	40	21 (52.5)	19 (47.5)	
Perineural invasion				.234
Absent	90	42 (46.7)	48 (53.3)	
Present	21	13 (61.9)	8 (38.1)	

Values are presented as number (%).

AJCC, American Joint Committee on Cancer; LN, lymph node.

Table 3. Univariate Cox regression analysis of clinicopathological parameters and patient survival in lung adenocarcinoma

	Disease-free survival			Overall survival		
	HR	95% CI	p-value	HR	95% CI	p-value
Age (<60 yr vs ≥60 yr)	1.129	0.607–1.129	.702	2.231	0.856–5.817	.101
Sex (male vs female)	0.694	0.376–1.282	.244	0.469	0.200–1.099	.081
AJCC stage (I vs II, III and IV)	4.975	2.535–9.764	<.001	4.606	1.800–11.789	.001
T category (pT1 vs pT2, pT3, and pT4)	2.661	1.391–5.089	.003	4.663	1.713–12.694	.003
LN metastasis (absent vs present)	4.314	2.313–8.045	<.001	3.087	1.331–7.157	.009
Pleural invasion (absent vs present)	1.397	0.702–2.782	.341	3.488	1.406–8.656	.007
Histologic grade (grade 1 vs grade 2 and 3)	3.667	1.130–11.898	.030	2.367	0.552–10.149	.246
LVI (absent vs present)	3.969	2.053–7.673	<.001	3.677	1.488–9.085	.005
Perineural invasion (absent vs present)	2.363	1.172–4.762	.016	3.855	1.524–9.751	.004
miR-374a expression (low vs high)	2.740	1.054–7.125	.039	1.485	0.395–5.590	.559
miR-374a (low vs high), stage I only	5.676	1.434–22.462	.013	2.844	0.464–17.433	.250

HR, hazard ratio; CI, confidence interval; AJCC, American Joint Committee on Cancer; LN, lymph node; LVI, lymphovascular invasion.

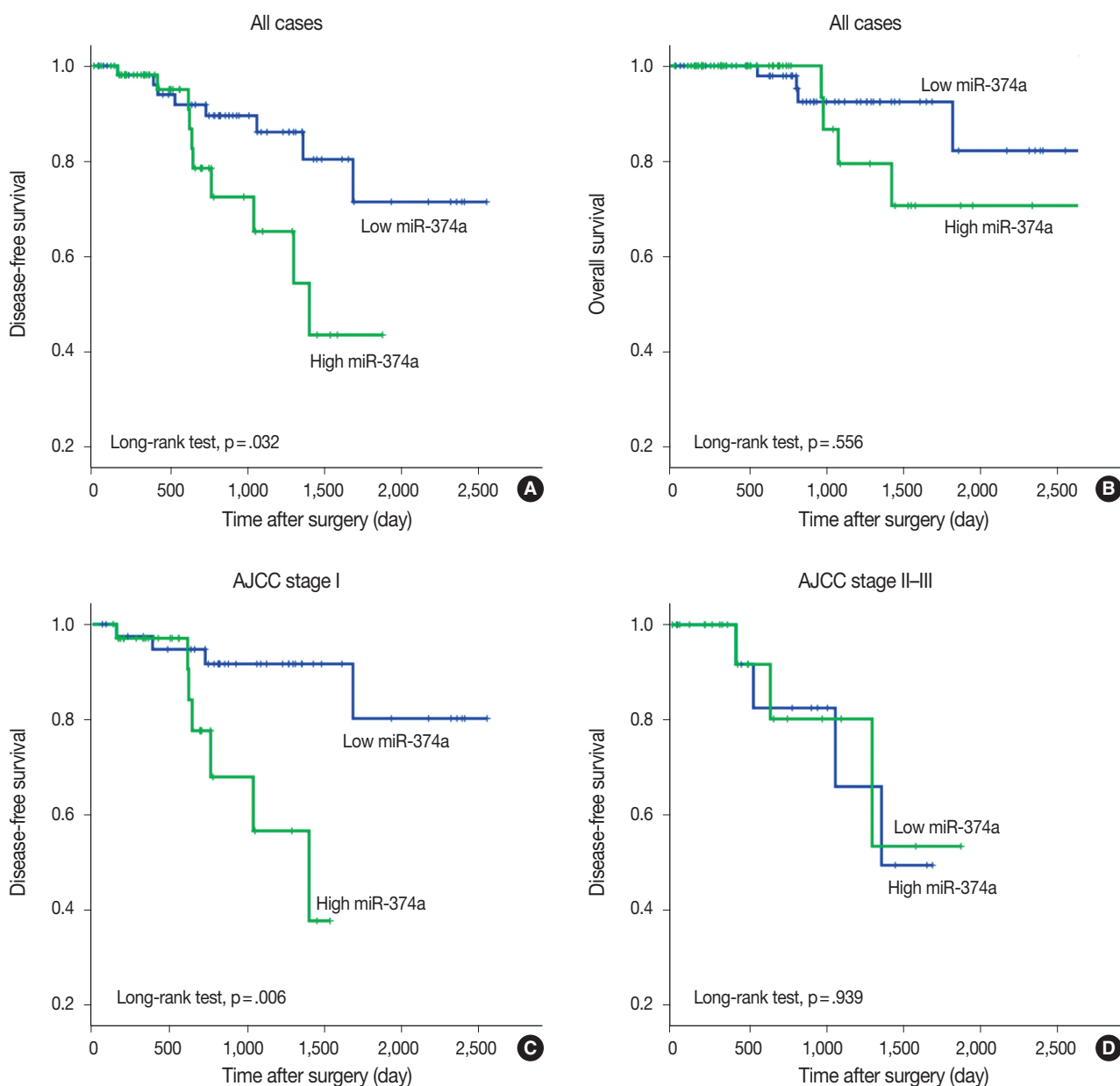


Fig. 1. Kaplan-Meier survival curves of lung adenocarcinoma patients stratified based on miR-374a expression level. (A) Disease-free survival according to miR-374a expression (log-rank test, $p = .032$). (B) Overall survival according to miR-374a expression (log-rank test, $p = .556$). (C) Disease-free survival according to miR-374a expression only in American Joint Committee on Cancer (AJCC) stage I patients (log-rank test, $p = .006$). (D) Disease-free survival according to miR-374a expression in AJCC stage II-III (log-rank test, $p = .939$).

microarray, was associated with poor survival. This discrepancy may result from the difference in miRNA detection methods and study population, such as ethnicity and histologic type. Lack of reproducibility between studies suggests that further validation with a larger case series and optimization of detection methods is needed for clarification.

Most previous studies have reported miR-374a as an oncogenic miRNA in various cancer types. In studies with osteosarcoma

cell lines, tumor cells transiently transfected with miR-374a mimic showed an increase in cell proliferation and colony formation by downregulating FOXO1 and/or Axin2.^{7,27} Downregulation of miR-374a inhibited cell proliferation, migration, and invasion in breast cancer cell lines (MDA-MB-23a and MCF-7) by targeting LACTB.¹¹ In triple-negative breast cancer, ARRB1 was a direct target of miR-374a, and knockdown of miR-374a attenuated cell proliferation and migration in vitro.¹³ Down-

regulation of miR-374a inhibited tumor growth and decreased Ki-67 proliferation index in xenograft mice.¹³ However, some studies have reported miR-374a as a tumor suppressive miRNA. Induced overexpression of miR-374a in colon cancer cell lines inhibited cell proliferation and invasion based on in vitro assays and a xenograft model by targeting cyclin D1.¹⁴ Nasopharyngeal cancer cells transfected with miR-374a mimic inhibited cell proliferation and invasion in vitro, and showed a decreased number of metastatic lesions in a mouse model.²⁸ These results suggest that miR-374a may have dual roles in tumor progression, and the role depends on the major target pathway in a given cancer subtype.

In conclusion, our data show that high miR-374a expression correlates with advanced pT category and pleural invasion. High expression of miR-374a may serve as a potential prognostic biomarker for predicting recurrence in early stage lung adenocarcinoma after curative surgery. Further validation studies for a prognostic biomarker and related mechanism should be explored.

ORCID

Yeseul Kim: <http://orcid.org/0000-0001-8273-884X>
 Jongmin Sim: <http://orcid.org/0000-0002-7106-1279>
 Hyunsung Kim: <http://orcid.org/0000-0002-8935-7414>
 Seong Sik Bang: <http://orcid.org/0000-0002-6872-5986>
 Seungyun Jee: <http://orcid.org/0000-0003-3895-817X>
 Sungeon Park: <http://orcid.org/0000-0001-9224-2979>
 Kiseok Jang: <http://orcid.org/0000-0002-6585-3990>

Author Contributions

Conceptualization: KJ.
 Data curation: YK, JS, HK, SSB, SJ, SP.
 Formal analysis: JS, YK, KJ.
 Funding acquisition: KJ.
 Investigation: JS, YK, KJ.
 Methodology: KJ.
 Project administration: KJ.
 Resources: JS, KJ.
 Supervision: KJ.
 Validation: JS, YK, KJ.
 Visualization: YK, KJ.
 Writing—original draft preparation: YK, KJ.
 Writing—review & editing: YK, KJ.

Conflicts of Interest

The authors declare that they have no potential conflicts of

interest.

Funding

This work was supported by a National Research Foundation of Korea (NRF) grant funded by the Korean government (Ministry of Science, ICT & Future Planning) (NRF-2015R1C1A1A01056091) and Basic Science Research Program through the National Research Foundation of Korea (NRF) funded by the Ministry of Education (NRF-2018R1D1A1B07048798).

Acknowledgments

We would like to thank Jeongyun Eom and Jisook Kim (Department of Pathology, Hanyang University Hospital) for excellent technical assistance.

REFERENCES

1. Cronin KA, Lake AJ, Scott S, et al. Annual report to the nation on the status of cancer, part I: national cancer statistics. *Cancer* 2018; 124: 2785-800.
2. Kim HC, Jung CY, Cho DG, et al. Clinical characteristics and prognostic factors of lung cancer in Korea: a pilot study of data from the Korean Nationwide Lung Cancer Registry. *Tuberc Respir Dis* 2019; 82: 118-25.
3. Chen K, Rajewsky N. The evolution of gene regulation by transcription factors and microRNAs. *Nat Rev Genet* 2007; 8: 93-103.
4. Bartel DP. MicroRNAs: genomics, biogenesis, mechanism, and function. *Cell* 2004; 116: 281-97.
5. Calin GA, Croce CM. MicroRNA signatures in human cancers. *Nat Rev Cancer* 2006; 6: 857-66.
6. Trang P, Weidhaas JB, Slack FJ. MicroRNAs as potential cancer therapeutics. *Oncogene* 2008; 27 Suppl 2: S52-7.
7. Lu T, Zhang C, Chai MX, An YB, Jia JL. MiR-374a promotes the proliferation of osteosarcoma cell proliferation by targeting Axin2. *Int J Clin Exp Pathol* 2015; 8: 10776-83.
8. Wang Y, Xin H, Han Z, Sun H, Gao N, Yu H. MicroRNA-374a promotes esophageal cancer cell proliferation via Axin2 suppression. *Oncol Rep* 2015; 34: 1988-94.
9. Cai J, Guan H, Fang L, et al. MicroRNA-374a activates Wnt/ β -catenin signaling to promote breast cancer metastasis. *J Clin Invest* 2013; 123: 566-79.
10. Li H, Chen H, Wang H, et al. MicroRNA-374a promotes hepatocellular carcinoma cell proliferation by targeting mitogen-inducible gene 6 (MIG-6). *Oncol Res* 2018; 26: 557-63.
11. Zhang J, He Y, Yu Y, et al. Upregulation of miR-374a promotes tumor metastasis and progression by downregulating LACTB and pre-

- dicts unfavorable prognosis in breast cancer. *Cancer Med* 2018 May 23 [Epub]. <https://doi.org/10.1002/cam4.1576>.
12. Ma L, Shao Z, Zhao Y. MicroRNA-374a promotes pancreatic cancer cell proliferation and epithelial to mesenchymal transition by targeting SRCIN1. *Pathol Res Pract* 2019; 215: 152382.
 13. Son D, Kim Y, Lim S, et al. MiR-374a-5p promotes tumor progression by targeting ARRB1 in triple negative breast cancer. *Cancer Lett* 2019; 454: 224-33.
 14. Chen Y, Jiang J, Zhao M, et al. MicroRNA-374a suppresses colon cancer progression by directly reducing CCND1 to inactivate the PI3K/AKT pathway. *Oncotarget* 2016; 7: 41306-19.
 15. Qian D, Chen K, Deng H, et al. MicroRNA-374b suppresses proliferation and promotes apoptosis in T-cell lymphoblastic lymphoma by repressing AKT1 and Wnt-16. *Clin Cancer Res* 2015; 21: 4881-91.
 16. Zhao M, Xu P, Liu Z, et al. Dual roles of miR-374a by modulated c-Jun respectively targets CCND1-inducing PI3K/AKT signal and PTEN-suppressing Wnt/ β -catenin signaling in non-small-cell lung cancer. *Cell Death Dis* 2018; 9: 78.
 17. Hall JS, Taylor J, Valentine HR, et al. Enhanced stability of microRNA expression facilitates classification of FFPE tumour samples exhibiting near total mRNA degradation. *Br J Cancer* 2012; 107: 684-94.
 18. Zhang X, Chen J, Radcliffe T, Lebrun DP, Tron VA, Feilolter H. An array-based analysis of microRNA expression comparing matched frozen and formalin-fixed paraffin-embedded human tissue samples. *J Mol Diagn* 2008; 10: 513-9.
 19. Weng L, Wu X, Gao H, et al. MicroRNA profiling of clear cell renal cell carcinoma by whole-genome small RNA deep sequencing of paired frozen and formalin-fixed, paraffin-embedded tissue specimens. *J Pathol* 2010; 222: 41-51.
 20. Glud M, Klausen M, Gniadecki R, et al. MicroRNA expression in melanocytic nevi: the usefulness of formalin-fixed, paraffin-embedded material for miRNA microarray profiling. *J Invest Dermatol* 2009; 129: 1219-24.
 21. Hui AB, Shi W, Boutros PC, et al. Robust global micro-RNA profiling with formalin-fixed paraffin-embedded breast cancer tissues. *Lab Invest* 2009; 89: 597-606.
 22. Zheng J, Xu T, Chen F, Zhang Y. MiRNA-195-5p functions as a tumor suppressor and a predictive of poor prognosis in non-small cell lung cancer by directly targeting CIAPIN1. *Pathol Oncol Res* 2019; 25: 1181-90.
 23. Chen Y, Min L, Ren C, et al. MiRNA-148a serves as a prognostic factor and suppresses migration and invasion through Wnt1 in non-small cell lung cancer. *PLoS One* 2017; 12: e0171751.
 24. Zheng W, Zhao J, Tao Y, et al. MicroRNA-21: a promising biomarker for the prognosis and diagnosis of non-small cell lung cancer. *Oncol Lett* 2018; 16: 2777-82.
 25. Wang XC, Wang W, Zhang ZB, Zhao J, Tan XG, Luo JC. Overexpression of miRNA-21 promotes radiation-resistance of non-small cell lung cancer. *Radiat Oncol* 2013; 8: 146.
 26. Gao W, Lu X, Liu L, Xu J, Feng D, Shu Y. MiRNA-21: a biomarker predictive for platinum-based adjuvant chemotherapy response in patients with non-small cell lung cancer. *Cancer Biol Ther* 2012; 13: 330-40.
 27. He W, Feng L, Xia D, Han N. MiR-374a promotes the proliferation of human osteosarcoma by downregulating FOXO1 expression. *Int J Clin Exp Med* 2015; 8: 3482-9.
 28. Zhen Y, Fang W, Zhao M, et al. MiR-374a-CCND1-pPI3K/AKT-c-JUN feedback loop modulated by PDCD4 suppresses cell growth, metastasis, and sensitizes nasopharyngeal carcinoma to cisplatin. *Oncogene* 2017; 36: 275-85.

Molecular and Clinicopathological Features of Gastrointestinal Stromal Tumors in Vietnamese Patients

Quoc Dat Ngo, Quoc Thang Pham, Dang Anh Thu Phan, Anh Vu Hoang¹, Thi Ngoc Ha Hua, Sao Trung Nguyen

Department of Pathology, ¹Center for Molecular Biomedicine, University of Medicine and Pharmacy at Ho Chi Minh City, Ho Chi Minh City, Vietnam

Background: Gastrointestinal stromal tumors (GISTs) are the most frequent mesenchymal neoplasms of the gastrointestinal tract. Management of GIST patients is currently based on clinicopathological features and associated genetic changes. However, the detailed characteristics and molecular genetic features of GISTs have not yet been described in the Vietnamese population. **Methods:** We first identified 155 patients with primary GIST who underwent surgery with primary curative intent between 2011 and 2014 at University Medical Center at Ho Chi Minh City, Vietnam. We evaluated the clinicopathological features and immunohistochemical reactivity to p53 and Ki-67 in these patients. Additionally, *KIT* genotyping was performed in 100 cases. **Results:** The largest proportion of GISTs was classified as high-risk (43.2%). Of the 155 GISTs, 52 (33.5%) were positive for Ki-67, and 58 (37.4%) were positive for p53. The expression of Ki-67 and p53 were correlated with mitotic rate, tumor size, risk assessment, and tumor stage. Out of 100 GIST cases, *KIT* mutation was found in 68%, of which 62 (91.2%) were found in exon 11, two (2.9%) in exon 9, and four (5.8%) in exon 17. No mutation in exon 13 was identified. Additionally, *KIT* mutations did not correlate with any clinicopathological features. **Conclusions:** The expression of Ki-67 and p53 were associated with high-risk tumors. Mutations in exon 11 were the most commonly found, followed by exon 17 and exon 9. Additionally, *KIT* mutation status was not correlated with any recognized clinicopathological features.

Key Words: Gastrointestinal stromal tumors; Ki-67; p53; *KIT* mutation

Received: April 23, 2019 **Revised:** July 7, 2019 **Accepted:** August 27, 2019

Corresponding Author: Quoc Dat Ngo, MD, PhD, Department of Pathology, University of Medicine and Pharmacy at Ho Chi Minh City, 217 Hong Bang Street, Ward 11, District 5, Ho Chi Minh City, Vietnam

Tel: +84-838-558-411, Fax: +84-838-552-304, E-mail: ngoquocdat@ump.edu.vn

Gastrointestinal stromal tumors (GISTs) are the most frequent mesenchymal neoplasms of the gastrointestinal (GI) tract,¹ with an incidence reported at 10–15 per million persons.² GISTs can be found anywhere within the GI tract, most commonly in the stomach (55.6%) and small intestine (31.8%).^{1,2} The cell of origin and diagnostic criteria were highly debated until gain-of-function mutations in *KIT* were confirmed in 1998.^{3–5} GISTs have a wide morphological spectrum, and although spindle cell tumors are the most common, 20%–25% of GIST cases present an epithelioid pattern, and some cases show mixed histology. Currently, diagnosis is based on morphology, ancillary tests including immunohistochemistry (95% express CD117 and 98% express DOG1), and molecular profiling.^{6–10} Among clinicopathological features, the most universally applicable prognostic factors for GISTs are tumor size and mitotic rate per 50 high power fields (HPF).^{1,7,8}

Nearly 80% of GISTs harbor a mutation in *KIT*, and another

5%–10% of cases have platelet-derived growth factor receptor (*PDGFR*) mutation.⁶ However, approximately 10%–15% of GISTs have no mutation in either of these genes and were previously known as wild-type GISTs.⁶ However, the terminology “wild-type GISTs” is progressively being abandoned as mutations have been identified in *BRAF* and succinate dehydrogenase (*SDH*) genes.^{9,10} In tumors with a *KIT* mutation, the most commonly affected region is exon 11 (juxtamembrane domain; 70%), followed by exon 9 (extracellular domain; 10%–15%), exon 13 (tyrosine kinase 1 domain; 1%–2%), and exon 17 (activation loop; 1%).^{11–14} Secondary mutations in exons 13, 14, or 17 are usually present in imatinib-resistant patients.¹⁵

Management of GIST patients is currently based not only on clinicopathological features (e.g., risk assessment and tumor stage), but also genetic changes including *KIT*-, *PDGFRA*-, and *SDH* mutations.⁸ To our knowledge, however, the detailed characteristics and molecular genetic features of GISTs have not yet been

described in the Vietnamese population.

In this study, we conducted a standard clinicopathological risk assessment and evaluated the relationships between expression of Ki-67 and p53 and the clinicopathological features of GISTs in Vietnamese patients. Furthermore, we investigated the common regions of *KIT* mutation, comprising exon 11, exon 9, exon 13, and exon 17.

MATERIALS AND METHODS

Tissue samples

In a descriptive study design, 155 primary GISTs were collected from patients who underwent surgical resection between 2011 and 2014 at the University Medical Center at Ho Chi Minh City (Ho Chi Minh City, Vietnam). Patients treated with preoperative imatinib were not enrolled in the study. The diagnosis was confirmed based on the histological features and immunoreactivity of CD117.

Clinicopathological data of age, sex, tumor location, tumor size, and tumor stage were recorded. Localized GISTs were those that were confined to the primary organ of origin, and locally advanced GISTs were those with contiguous organ involvement. Morphological features, such as pattern (spindle cell, epithelioid, or mixed) and mitotic activity (per 50 HPFs with a total area of 5 mm²) were evaluated. For risk assessment, tumors were categorized into very low-, low-, intermediate-, and high-risk groups based on the National Institute of Health (NIH) classification criteria.¹⁶

For immunohistochemical analysis, we used archival formalin-fixed, paraffin-embedded (FFPE) tissues from the 155 GISTs. One or two representative tumor blocks from each case were examined using immunohistochemistry.

For *KIT* genotyping, 100 FFPE tissues were available for *KIT* mutation analysis. Genomic DNA was isolated from paraffin-embedded tissues and tested at *KIT* exons 9, 11, 13, and 17.

Immunohistochemistry

Three-micrometer-thick slides were used for immunohistochemical analysis. Primary antibodies for CD117 (1:400, polyclonal, Ventana, Oro Valley, AZ, USA), Ki-67 (1:25, MIB-1 monoclonal, Dako, Carpinteria, CA, USA), p53 (1:50, DO-7 monoclonal, Dako), smooth muscle actin (SMA; 1:2,000, 1A4, monoclonal, Dako), and neuron-specific enolase (NSE; 1:50, VI-H14, Dako) were used to detect protein expression. Immunostaining for CD117, Ki-67, p53, SMA, and NSE was performed using an automated staining machine (VENTANA

BenchMark, Ventana) according to the manufacturer's instructions. For the markers (CD117, SMA, and NSE), immunostaining was defined as positive if $\geq 10\%$ of tumor cells were stained and negative if $< 10\%$ of tumor cells were stained. The labeling index (LI) (%) for Ki-67 and p53 expression was evaluated based on a count of at least 1,000 tumor cells in the highest-density immunoreactivity areas of the positive tumor nuclei. Ki-67 and p53 were defined as positive if the LI was higher than 10%¹⁷ or 5%,¹⁸ respectively. Two senior surgical pathologists without knowledge of the clinicopathological features of the patients independently reviewed the immunostaining slides. Interobserver differences were resolved by consensus review using a double-headed microscope after independent review.

KIT genotyping

Genomic DNA was extracted from paraffin-embedded tissues of 100 patients using the ReliaPrep FFPE gDNA Miniprep System kit (Promega, Madison, WI, USA) according to the manufacturer's protocol. Amplifications of *KIT* exons 9, 11, 13, and 17 were performed using TaKaRa Taq HotStart Polymerase (Takara Bio, Shiga, Japan) with primers as previously published.¹⁹ Polymerase chain reaction (PCR) fragments were sequenced and analyzed in both sense and antisense directions using a BigDye Terminator v3.1 kit on an ABI 3130 Genetic Analyzer (Applied Biosystems, Foster City, CA, USA). Mutations were confirmed through a second independent PCR amplification and sequencing.

Statistical analysis

Associations between clinicopathological features and Ki-67 expression, p53 expression, and *KIT* mutations were analyzed using the chi-square test and Fisher's exact test. Differences were considered significant at $p < .05$. All statistical analyses were performed using SPSS software ver. 16.0 (SPSS Inc., IBM, Chicago, IL, USA).

Ethics statement

This study was approved by the Board of Ethics in Biomedical Research at the University of Medicine and Pharmacy at Ho Chi Minh City, Vietnam (approval number: 54/UMP-BOARD; Date: December 22, 2012). Informed consent was obtained from all individual participants included in the study.

RESULTS

Clinicopathological characteristics of GISTs

We included 72 (46.5%) male and 83 (53.5%) female patients in this study, with a male: female ratio of 1:1.2, and the median age at diagnosis was 55 years (range, 15 to 88 years). Tumor size ranged from 1.0 to 29 cm in the largest dimension, with a median size of 6 cm. The GISTs presented in a wide distribution both within and outside the GI tract (Table 1). The most common location was the stomach (52.3%), followed by the jejunum-ileum (27.7%). GISTs were also found outside the GI tract including the omentum (5.8%) and retroperitoneum (3.2%).

Most cases showed spindle cell (72.3%) or epithelioid cell morphology (14.8%), and mixed type accounted for 12.9% of cases (Table 1, Fig. 1A–C). Tumor cells were positive for CD117 (Fig. 1D). Many GISTs were positive for SMA (20%) (Fig. 1E) or for NSE (67.7%) (Fig. 1F). Sixty-seven of 155 cases (43.2%) were classified as high risk, 42 (27.1%) as low risk, 40 (25.8%) as intermediate risk, and 6 (3.9%) as very low risk (Supplementary Table S1). Most tumors located in the jejunum-ileum (55.8%) or the colorectum (44.4%) fell into the high-risk category (Table 2). Of the 14 cases of extra-intestinal GISTs, 13 (92.9%) were classified as the high-risk group.

We next evaluated Ki-67 and p53 expression in the GISTs (Fig. 1G, H). Of the 155 cases, 52 (33.5%) were positive for

Ki-67, and 58 (37.4%) were positive for p53 (Table 1). Expression of Ki-67 correlated with mitotic rate ($p < .001$), tumor size ($p = .014$), risk assessment ($p < .001$), and tumor stage ($p < .001$) (Table 3). Similarly, expression of p53 correlated with mitotic rate ($p < .001$), tumor risk assessment ($p < .001$), and tumor stage ($p < .001$). In contrast, expression of Ki-67 and p53 was not associated with GIST phenotype ($p = .482$ and $p = .102$, respectively).

KIT mutation analysis

KIT mutations were detected in 68 of 100 GIST cases (68%). Sixty-two of the 68 *KIT* mutations (91.2%) were found in *KIT* exon 11 (Table 4). There were two cases (2.9%) with mutations in *KIT* exon 9 and 4 cases (5.8%) with mutations in *KIT* exon 17. No mutations were found in *KIT* exon 13. We detected a variety of *KIT* mutation types in exons 9, 11, and 17 including point mutations, insertions, deletions, duplications, and complex mutations.

Among the cases with mutations in *KIT* exon 11, in-frame deletion was the most common type (35/62, 56.5%) (Fig. 2A), followed by point mutation (19/62, 30.6%) (Fig. 2B). Complex mutations were detected in six of 62 cases (9.7%). The two cases with mutation in the extracellular membrane region encoded by exon 9 were insertions (Y503_F504insAY) (Fig. 2C) and were found in tumors of the jejunum-ileum. All mutations in *KIT* exon 17 were point mutations, and three of four cases (75%) had an N822K substitution (Fig. 2D). We further investigated the relationships between *KIT* mutation status and other clinicopathological characteristics; however, no significant correlation was found (Supplementary Table S2).

DISCUSSION

A systematic review of 29 studies on nearly 14,000 GIST patients reported a median age of 60 years, and the incidence was similar for males and females.² Our study showed a slightly higher incidence rate in females and a median age lower than in other studies. However, our average age was higher than that of the Korean sub-population reported in the systemic review mentioned above.² Although many studies have reported the presence of GISTs in the esophagus,^{1,2} no esophageal GISTs were present in our study. Our results showed that GISTs were most predominant in the stomach, followed by the small intestine, which was consistent with the findings in most of the literature. Interestingly, our results revealed that extra-intestinal GISTs accounted for 9% of cases. According to a study in Singapore from

Table 1. Characteristics of 155 patients with GISTs

Characteristic	No. (%) (n=155)
Age, median (yr)	55 (15–88)
Sex	
Female	83 (53.5)
Male	72 (46.5)
Tumor location	
Stomach	81 (52.3)
Duodenum	8 (5.2)
Jejunum-ileum	43 (27.7)
Colorectum	9 (5.8)
Omentum	9 (5.8)
Retroperitoneum	5 (3.2)
Histology	
Spindle	112 (72.3)
Epithelioid	23 (14.8)
Mixed	20 (12.9)
Immunohistochemical profiles	
SMA	31 (20.0)
NSE	105 (67.7)
Ki-67	52 (33.5)
p53	58 (37.4)

GISTs, gastrointestinal stromal tumors; SMA, smooth muscle actin; NSE, neuron-specific enolase.

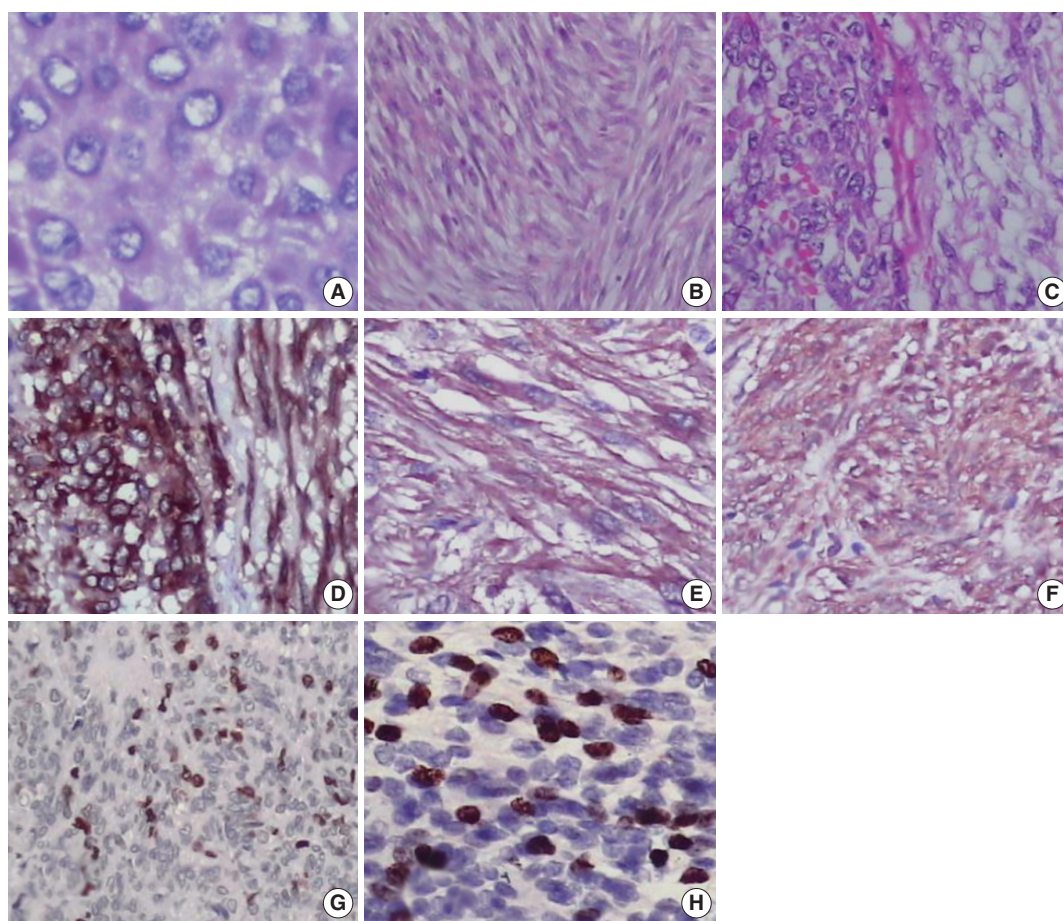


Fig. 1. Histopathological and immunohistochemical analysis of gastrointestinal stromal tumor. (A) Epithelioid cell morphology. (B) Spindle cell morphology. (C) Mixed type. Immunohistochemical expression of CD117 (D), smooth muscle actin (E), neuron-specific enolase (F), p53 (G), and Ki-67 (H).

Table 2. Location and risk stratification of 155 GISTs

	Very low risk	Low risk	Intermediate risk	High risk
Stomach	6 (7.4)	30 (37.0)	22 (27.2)	23 (28.4)
Duodenum	0	1 (12.5)	4 (50.0)	3 (37.5)
Jejunum-ileum	0	9 (20.9)	10 (23.3)	24 (55.8)
Colorectum	0	1 (11.1)	4 (44.4)	4 (44.4)
Omentum	0	1 (11.1)	0	8 (88.9)
Retroperitoneum	0	0	0	5 (100)

Values are presented as number (%).
GISTs, gastrointestinal stromal tumors.

1998 to 2008, the frequency of extra-intestinal GISTs has increased since CD117 immunohistochemistry has been applied for diagnosis.²⁰

According to the literature, most GISTs have high-risk features, followed by intermediate- and low-risk groups.^{2,17,18,20,21} Our study also had a majority of GISTs classified as high-risk, followed by low-risk, intermediate-, and very low-risk groups. Our study

revealed that most jejunum-ileum and colorectal GISTs fell into the high-risk group. These results were compatible with a previous study in which non-gastric GISTs were mostly classified in the high-risk group.²² Our study showed an extremely high ratio of extra-intestinal GISTs in the high-risk group. In contrast, another study with 29 extra-intestinal GIST cases showed seven cases (24.1%) in the high-risk group using the criteria of mitotic rate per 50 high power fields $\geq 5/50$ HPF and Ki-67 $\geq 10\%$.²³ Recently reported evidence proposed that retroperitoneal GISTs could be derived from a GI tract origin.²⁴

In our study, Ki-67 expression correlated with risk assessment and other clinicopathological features, as in previous studies.^{17,18,25,26} Although the cut-off value for Ki-67 expression varied among studies, it is clear that Ki-67 expression is a prognostic factor and a good marker for biological behavior such as metastatic tendency.^{17,18,25,26} Furthermore, *TP53*, the most mutated gene in human cancer,²⁷ has also been proposed to be a predictive

Table 3. Relationship between Ki-67 expression, p53 expression and clinicopathological characteristics of GISTs

	Ki-67 expression			p53 expression		
	Positive	Negative	p-value	Positive	Negative	p-value
Mitotic rate (per 50 HPFs)			<.001 ^a			.001 ^a
≤5	19 (20.2)	75 (79.8)		25 (26.6)	69 (73.4)	
6–10	5 (25.0)	15 (75.0)		7 (35.0)	13 (65.0)	
>10	28 (68.3)	13 (31.7)		26 (63.4)	15 (36.6)	
Tumor size (cm)			.014 ^a			.148 ^a
0–5	16 (24.2)	50 (75.8)		20 (30.3)	46 (69.7)	
>5–10	17 (32.1)	36 (67.9)		20 (37.7)	33 (62.3)	
>10	19 (52.8)	17 (47.2)		18 (50.0)	18 (50.0)	
Risk stratification			<.001 ^a			<.001 ^a
Very low/low risk	6 (12.5)	42 (87.5)		8 (16.7)	40 (83.3)	
Intermediate risk	10 (25.0)	30 (75.0)		15 (37.5)	25 (62.5)	
High risk	36 (53.7)	31 (46.3)		35 (52.2)	32 (47.8)	
Histology			.482 ^a			.102 ^a
Spindle	77 (68.8)	35 (31.2)		75 (67.0)	37 (33.0)	
Epithelioid	15 (65.2)	8 (34.8)		10 (43.5)	13 (56.5)	
Mixed	11 (55.0)	9 (45.0)		12 (60.0)	8 (40.0)	
Tumor necrosis			.475 ^b			.012 ^b
No	32 (31.4)	70 (68.6)		31 (30.4)	71 (69.6)	
Yes	20 (37.7)	33 (62.3)		27 (50.9)	26 (49.1)	
Stage ^c			<.001 ^b			<.001 ^b
Localized	12 (17.4)	57 (82.6)		14 (20.3)	55 (79.7)	
Locally advanced	29 (50.9)	28 (49.1)		30 (52.6)	27 (47.4)	

Values are presented as number (%).

GISTs, gastrointestinal stromal tumors; HPFs, high-power fields.

^aChi-square test; ^bFisher's exact test; ^c29 GISTs patients were excluded from the analysis as they were missing tumor stage information.

Table 4. Summary of *KIT* mutation status in 100 GIST patients

	<i>KIT</i> mutation				<i>KIT</i> wild-type
	Exon 9	Exon 11	Exon 13	Exon 17	
Tumor location					
Stomach	0	39	0	2	14
Duodenum	0	3	0	0	1
Jejunum-ileum	2	14	0	1	7
Colorectum	0	1	0	0	6
Omentum	0	3	0	1	3
Retroperitoneum	0	2	0	0	1
Type of mutation					
In-frame deletion	0	35	0	0	0
Single point	0	19	0	4	0
Complex	0	6	0	0	0
Insertion	2	1	0	0	0
Duplication	0	1	0	0	0

GIST, gastrointestinal stromal tumor.

marker for risk of malignancy in GISTs.^{17,28} The cut-off value for p53 expression varied among studies.^{17,18,28} One study from Japan that used the same cut-off values for p53 expression and risk assessment as our study showed less frequent p53 expression in the high-risk group.¹⁸ However, in our study, there was a significant correlation between p53 expression and high-risk assessment.

Pauser et al.²⁸ reported that expression of p53 was related to epithelioid morphology. However, our study showed that p53 expression was not correlated with the morphologic phenotypes of GISTs.

In the current study, *KIT* mutations were found in 60%–80% of GISTs and were most frequently detected in exon 11, which is consistent with previous reports.^{1,4,6,29,30} Additionally, *KIT* mutations were not associated with the clinicopathological features of GISTs. According to the National Comprehensive Cancer Network (NCCN) panel, the presence and type of *KIT* mutation are not strongly correlated with prognosis.⁸ However, another study showed that GISTs with *KIT* exon 11 deletions and high mitotic rates were negatively correlated with recurrence-free survival.³¹ In the American College of Surgeons Oncology Group (ACOSOG) Z9001 trial, GIST patients with *KIT* exon 11 deletion mutations had longer recurrence-free survival than those with other mutation types (genotypes) when treated with adjuvant imatinib.³²

Interestingly, the second most frequent region of *KIT* mutation in this study was exon 17. Two of four cases with *KIT* exon 17 mutations were identified in the stomach. Other studies have reported that primary mutations in *KIT* exon 17 were fre-

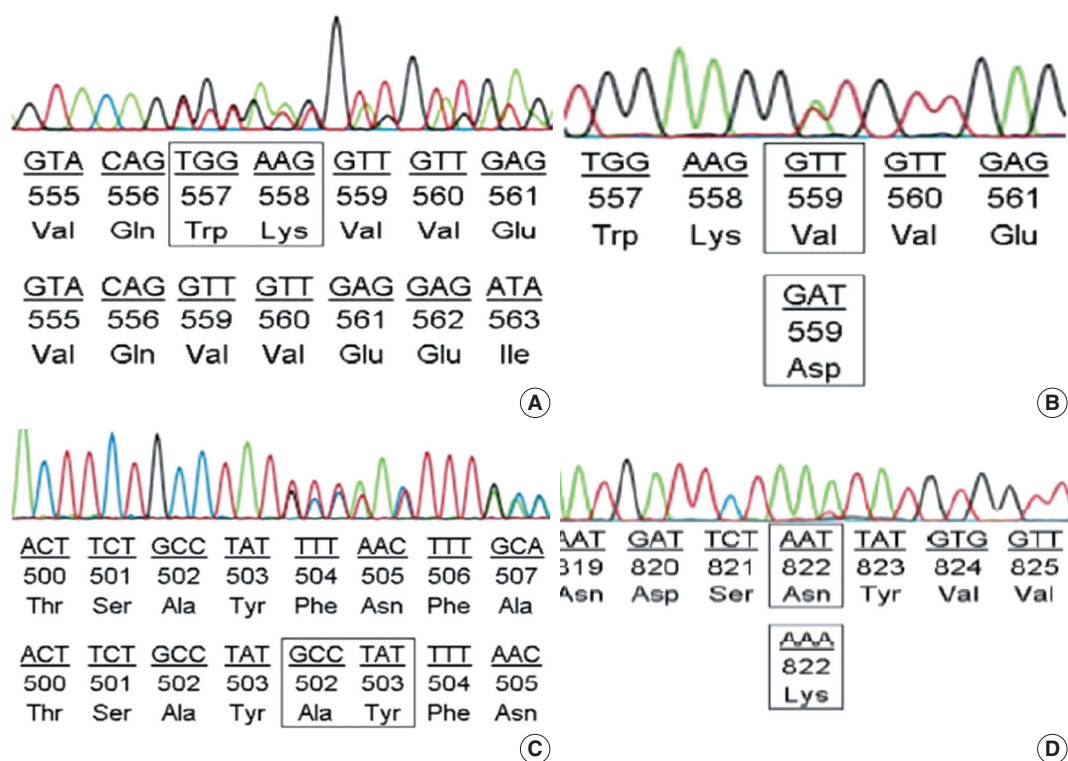


Fig. 2. *KIT* mutation in gastrointestinal stromal tumor. (A) In-frame deletion in exon 11. (B) Point mutation in exon 11. (C) Insertion mutation in exon 9. (D) Point mutation in exon 17.

quently detected in tumors of the small intestine,^{11,35} and approximately 1% of newly diagnosed GISTs had detectable mutations in *KIT* exon 17.¹¹ Furthermore, *KIT* exon 17 mutations as a secondary mutation (including N822K substitution) were often found in cases with acquired imatinib resistance.^{34,35} Our study did not detect any mutations in *KIT* exon 13, and mutations in *KIT* exon 9 were only identified in two cases. According to the NCCN guidelines, patients with advanced GISTs with *KIT* exon 9 mutations who are treated with double the standard dose of imatinib have an improved likelihood of response.⁸

Our study has several limitations. Because it is a descriptive study, it lacks clinical outcome information for the patients, which would enable us to determine overall and disease-free survival. Furthermore, additional analysis to investigate the status of *PDG-FRA* and *SDH* mutations in the “wild-type” GIST cases (32%) to reveal a more comprehensive picture of the molecular alterations in Vietnamese GIST patients would be helpful but was not feasible at this point.

In conclusion, this study demonstrated the clinicopathological features, immunohistochemical characteristics, and *KIT* mutation status of 155 Vietnamese GIST patients. The stomach was the most common site of GISTs, followed by the small intestine,

outside the GI tract, and colorectum. The majority of GISTs outside the GI tract fell into the high-risk group. Expression of Ki-67 and p53 was associated with high-risk assessment. Mutations in *KIT* exon 11 were the most frequently detected, followed by mutations in *KIT* exons 17 and 9. However, *KIT* mutations were not associated with clinicopathological or morphological features.

Electronic Supplementary Material

Supplementary materials are available at Journal of Pathology and Translational Medicine (<https://jpatholm.org>).

ORCID

Quoc Dat Ngo: <https://orcid.org/0000-0003-1461-0216>

Quoc Thang Pham: <https://orcid.org/0000-0001-8787-367X>

Dang Anh Thu Phan: <https://orcid.org/0000-0002-4062-0904>

Sao Trung Nguyen: <https://orcid.org/0000-0002-3847-4717>

Author Contributions

Conceptualization: QDN.

Data curation: QDN, QTP, AVH.

Formal analysis: QDN, QTP.
 Investigation: QDN.
 Methodology: QDN, QTP, DATP.
 Project administration: QDN, TNHH, STN.
 Resources: QDN.
 Supervision: TNHH, STN.
 Validation: QDN, TNHH, STN.
 Visualization: QDN, QTP.
 Writing—original draft: QDN, QTP, DATP.
 Writing—review & editing: QDN, QTP, DATP.

Conflicts of Interest

The authors declare that they have no potential conflicts of interest.

Funding

No funding to declare.

Acknowledgments

We thank Professor Lewis Hassell, Department of Pathology, Oklahoma University Health Sciences Center for English proof-reading.

REFERENCES

- Miettinen M, Fletcher CD, Kindblom LG, Tsui WM. Mesenchymal tumours of the stomach. In: Bosman FT, Carneiro F, Hruban RH, Theise ND, eds. WHO classification of tumours of the digestive system. 3rd ed. Lyon: IARC, 2010; 74-9.
- Søreide K, Sandvik OM, Søreide JA, Giljaca V, Jureckova A, Bulusu VR. Global epidemiology of gastrointestinal stromal tumours (GIST): a systematic review of population-based cohort studies. *Cancer Epidemiol* 2016; 40: 39-46.
- Mazur MT, Clark HB. Gastric stromal tumors: reappraisal of histogenesis. *Am J Surg Pathol* 1983; 7: 507-19.
- Hirota S, Isozaki K, Moriyama Y, et al. Gain-of-function mutations of c-kit in human gastrointestinal stromal tumors. *Science* 1998; 279: 577-80.
- Joensuu H. Gastrointestinal stromal tumor (GIST). *Ann Oncol* 2006; 17 Suppl 10: x280-6.
- Von Mehren M, Randall RL, Benjamin RS, et al. Gastrointestinal stromal tumors, version 2.2014. *J Natl Compr Canc Netw* 2014; 12: 853-62.
- Miettinen M, Lasota J. Gastrointestinal stromal tumors. *Gastroenterol Clin North Am* 2013; 42: 399-415.
- Soft tissue sarcoma, version 1.2018. National Comprehensive Cancer Network: Clinical Practice Guidelines in Oncology [Internet]. Plymouth Meeting: National Comprehensive Cancer Network, 2018 [cited 2017 Dec 14]. Available from: https://www.nccn.org/professionals/physician_gls/pdf/sarcoma.pdf.
- Agaram NP, Wong GC, Guo T, et al. Novel V600E *BRAF* mutations in imatinib-naive and imatinib-resistant gastrointestinal stromal tumors. *Genes Chromosomes Cancer* 2008; 47: 853-9.
- Gaal J, Stratakis CA, Carney JA, et al. SDHB immunohistochemistry: a useful tool in the diagnosis of Carney-Stratakis and Carney triad gastrointestinal stromal tumors. *Mod Pathol* 2011; 24: 147-51.
- Patrikidou A, Domont J, Chabaud S, et al. Long-term outcome of molecular subgroups of GIST patients treated with standard-dose imatinib in the BFR14 trial of the French Sarcoma Group. *Eur J Cancer* 2016; 52: 173-80.
- Heinrich MC, Owzar K, Corless CL, et al. Correlation of kinase genotype and clinical outcome in the North American Intergroup Phase III Trial of imatinib mesylate for treatment of advanced gastrointestinal stromal tumor: CALGB 150105 Study by Cancer and Leukemia Group B and Southwest Oncology Group. *J Clin Oncol* 2008; 26: 5360-7.
- Lasota J, Miettinen M. Clinical significance of oncogenic *KIT* and *PDGFRA* mutations in gastrointestinal stromal tumours. *Histopathology* 2008; 53: 245-66.
- Heinrich MC, Rankin C, Blanke CD, et al. Correlation of long-term results of imatinib in advanced gastrointestinal stromal tumors with next-generation sequencing results: analysis of phase 3 SWOG intergroup trial S0033. *JAMA Oncol* 2017; 3: 944-52.
- Heinrich MC, Maki RG, Corless CL, et al. Primary and secondary kinase genotypes correlate with the biological and clinical activity of sunitinib in imatinib-resistant gastrointestinal stromal tumor. *J Clin Oncol* 2008; 26: 5352-9.
- Joensuu H. Risk stratification of patients diagnosed with gastrointestinal stromal tumor. *Hum Pathol* 2008; 39: 1411-9.
- Hu TH, Chuah SK, Lin JW, et al. Expression and prognostic role of molecular markers in 99 *KIT*-positive gastric stromal tumors in Taiwanese. *World J Gastroenterol* 2006; 12: 595-602.
- Nakamura N, Yamamoto H, Yao T, et al. Prognostic significance of expressions of cell-cycle regulatory proteins in gastrointestinal stromal tumor and the relevance of the risk grade. *Hum Pathol* 2005; 36: 828-37.
- Vu HA, Xinh PT, Kikushima M, et al. A recurrent duodenal gastrointestinal stromal tumor with a frameshift mutation resulting in a stop codon in *KIT* exon 13. *Genes Chromosomes Cancer* 2005; 42: 179-83.
- Chiang NJ, Chen LT, Tsai CR, Chang JS. The epidemiology of gastrointestinal stromal tumors in Taiwan, 1998-2008: a nation-wide

- cancer registry-based study. *BMC Cancer* 2014; 14: 102.
21. Brabec P, Sufliarsky J, Linke Z, et al. A whole population study of gastrointestinal stromal tumors in the Czech Republic and Slovakia. *Neoplasma* 2009; 56: 459-64.
 22. Tryggvason G, Gíslason HG, Magnússon MK, Jónasson JG. Gastrointestinal stromal tumors in Iceland, 1990-2003: the Icelandic GIST study, a population-based incidence and pathologic risk stratification study. *Int J Cancer* 2005; 117: 289-93.
 23. Yamamoto H, Oda Y, Kawaguchi K, et al. c-kit and *PDGFRA* mutations in extragastrointestinal stromal tumor (gastrointestinal stromal tumor of the soft tissue). *Am J Surg Pathol* 2004; 28: 479-88.
 24. Miettinen M, Felisiak-Golabek A, Wang Z, Inaguma S, Lasota J. GIST manifesting as a retroperitoneal tumor: clinicopathologic immunohistochemical, and molecular genetic study of 112 cases. *Am J Surg Pathol* 2017; 41: 577-85.
 25. Belev B, Brčić I, Prejac J, et al. Role of Ki-67 as a prognostic factor in gastrointestinal stromal tumors. *World J Gastroenterol* 2013; 19: 523-7.
 26. Ohdaira H, Ohyama S, Yamaguchi T, Yanagisawa A, Kato Y, Urashima M. Ki67 and tumor size as prognostic factors of gastrointestinal stromal tumors. *Japan Med Assoc J* 2005; 48: 586-92.
 27. Kandath C, McLellan MD, Vandin F, et al. Mutational landscape and significance across 12 major cancer types. *Nature* 2013; 502: 333-9.
 28. Pauser U, Schmedt Auf der Günne N, Klöppel G, Merz H, Feller AC. P53 expression is significantly correlated with high risk of malignancy and epithelioid differentiation in GISTs: an immunohistochemical study of 104 cases. *BMC Cancer* 2008; 8: 204.
 29. Corless CL, Heinrich MC. Molecular pathobiology of gastrointestinal stromal sarcomas. *Annu Rev Pathol* 2008; 3: 557-86.
 30. Tzen CY, Wang MN, Mau BL. Spectrum and prognostication of *KIT* and *PDGFRA* mutation in gastrointestinal stromal tumors. *Eur J Surg Oncol* 2008; 34: 563-8.
 31. Joensuu H, Wardelmann E, Sihto H, et al. Effect of *KIT* and *PDGFRA* mutations on survival in patients with gastrointestinal stromal tumors treated with adjuvant imatinib: an exploratory analysis of a randomized clinical trial. *JAMA Oncol* 2017; 3: 602-9.
 32. Corless CL, Ballman KV, Antonescu CR, et al. Pathologic and molecular features correlate with long-term outcome after adjuvant therapy of resected primary GI stromal tumor: the ACOSOG Z9001 trial. *J Clin Oncol* 2014; 32: 1563-70.
 33. Lasota J, Corless CL, Heinrich MC, et al. Clinicopathologic profile of gastrointestinal stromal tumors (GISTs) with primary *KIT* exon 13 or exon 17 mutations: a multicenter study on 54 cases. *Mod Pathol* 2008; 21: 476-84.
 34. Garner AP, Gozgit JM, Anjum R, et al. Ponatinib inhibits polyclonal drug-resistant *KIT* oncoproteins and shows therapeutic potential in heavily pretreated gastrointestinal stromal tumor (GIST) patients. *Clin Cancer Res* 2014; 20: 5745-55.
 35. Gao J, Tian Y, Li J, Sun N, Yuan J, Shen L. Secondary mutations of c-*KIT* contribute to acquired resistance to imatinib and decrease efficacy of sunitinib in Chinese patients with gastrointestinal stromal tumors. *Med Oncol* 2013; 30: 522.

Comparison of Squamous Cell Carcinoma of the Tongue between Young and Old Patients

Gyuheon Choi, Joon Seon Song, Seung-Ho Choi¹, Soon Yuhl Nam¹, Sang Yoon Kim¹, Jong-Lyel Roh¹, Bu-Kyu Lee², Kyung-Ja Cho

Departments of Pathology, ¹Otolaryngology, and ²Oral and Maxillofacial Surgery, Asan Medical Center, University of Ulsan College of Medicine, Seoul, Korea

Background: The worldwide incidence of squamous cell carcinoma of the tongue (SCCOT) in young patients has been increasing. We investigated clinicopathologic features of this unique population and compared them with those of SCCOT in the elderly to delineate its pathogenesis. **Methods:** We compared clinicopathological parameters between patients under and over 45 years old. Immunohistochemical assays of estrogen receptor, progesterone receptor, androgen receptor, p53, p16, mdm2, cyclin D1, and glutathione S-transferase P1 were also compared between them. **Results:** Among 189 cases, 51 patients (27.0%) were under 45 years of age. A higher proportion of women was seen in the young group, but was not statistically significant. Smoking and drinking behaviors between age groups were similar. Histopathological and immunohistochemical analysis showed no significant difference by age and sex other than higher histologic grades observed in young patients. **Conclusions:** SCCOT in young adults has similar clinicopathological features to that in the elderly, suggesting that both progress via similar pathogenetic pathways.

Key Words: Mouth neoplasms; Young adult; Smoking; Drinking; Immunohistochemistry

Received: July 10, 2019 **Revised:** August 30, 2019 **Accepted:** September 16, 2019

Corresponding Author: Kyung-Ja Cho, MD, PhD, Department of Pathology, Asan Medical Center, University of Ulsan College of Medicine, 88 Olympic-ro 43-gil, Songpa-gu, Seoul 05505, Korea

Tel: +82-2-3010-4545, Fax: +82-2-472-7898, E-mail: kjc@amc.seoul.kr

Risk factors for squamous cell carcinoma of the tongue (SCCOT) are well known and include a history of smoking and alcohol consumption. Most incidences occur in older men;¹ however, several reports indicate that the global incidence of SCCOT in young, non-smoking women has been rising,²⁻⁴ a trend also observed in the Korean population. A study by Choi et al.⁵ also found that the incidence of SCCOT in younger patients, particularly women, has been increasing. SCCOT in young patients presents with similar clinical outcomes to those for older patients.^{6,7} Distinct epidemiological features are apparent for these two cohorts, such as weaker association with smoking and drinking in younger patients,^{4,8,9} suggesting that biology and pathogenesis in these groups might also be distinct.

This study was designated to compare a set of clinicopathological parameters between sexes (male and female) and age groups (young and old). Young was defined as adults under 45; no standard definition of young regarding SCCOT has been established; however, a cutoff of 45 is frequently used in related studies.^{7,10,11}

Expression levels of several proteins were also compared through

immunohistochemical (IHC) staining. Targeted proteins include p16, p53, mdm2, cyclin D1, glutathione S-transferase P1 (GSTP1), and estrogen receptor (ER), all of which were associated with tumorigenesis of SCCOT in previous studies.¹²⁻¹⁷ p16, p53, mdm2, and cyclin D1 are essential to regulation of the cell cycle and apoptosis. Abnormal expression of these proteins in oral squamous cell carcinoma (SCC) has frequently been reported, implying an association with the pathogenesis and prognosis of SCCOT. Some reports have shown that expression levels vary by age groups.^{12,15,18-20} GSTP1 is a member of the glutathione S-transferase enzyme superfamily that participates in detoxification processes. Exposure to toxic substances such as tobacco, alcohol, and betel is a major risk factor for SCCOT,¹ and impaired GSTP1 function has been associated with an increased cancer risk.²¹

The increasing proportion of women under 45 years old with SCCOT suggests potential involvement with sexual hormone receptors, and increased ER expression in SCCOT has been reported for oral SCC.^{13,14} Recent studies found a relationship be-

tween oropharyngeal SCC and hormone receptor expression.^{22,23} We performed IHC stains for ER, progesterone receptor (PR), and androgen receptor (AR) to evaluate previous results and further analyze other clinicopathological features associated with hormone receptor expression.

MATERIALS AND METHODS

Study population

After searching an anonymized research database at Asan Medical Center, 295 cases of histologically confirmed SCCOT were found from 2005 to 2012. Ninety-six cases were excluded due to the lack of an available tissue block or clinical data, and 189 cases were finally retrieved for this retrospective study.

Clinical data collection

Clinical parameters collected from electronic medical records included age at onset, sex, smoking status, alcohol consumption level, treatment history, recurrence, and survival. Patients under 45 years old were classified as young patients. Smoking status was classified as non- or ex-smoker (no smoking for at least 1 year), or current smoker. Smokers were further categorized into light (< 1 pack of cigarettes/day) and heavy smokers (≥ 1 pack of cigarettes/day). Drinkers with a history of more than seven drinks per week were considered heavy drinkers. A drink was defined as roughly 14 g of pure alcohol regardless of beverage type, equivalent to approximately 12 ounces of regular beer. Cutoff values of heavy smoking and drinking were set by as described in previous work²⁴⁻²⁶ wherein patients over these cutoff values showed a significantly increased risk of oral epithelial dysplasia or cancer. Disease-free survival (DFS) was calculated from the date of initial pathological diagnosis to the date of radiological or clinical recurrence, while overall survival (OS) was calculated to the date of patient death.

Pathological review and tissue microarray construction

All available hematoxylin and eosin slides were reviewed to obtain pathological parameters, such as tumor size, histologic grade, depth of invasion (DOI), stromal tumor-infiltrating lymphocytes (TIL) group, lymphovascular invasion (LVI), perineural invasion (PNI), and TNM stage. TNM stage for each case was revised based on the American Joint Committee on Cancer (AJCC), 8th edition.²⁷ TIL assessment criteria followed the International Immuno-Oncology Biomarker Working Group guidelines.^{28,29} Each tumor was assigned to low, intermediate, or high TIL group according to the percentage of stromal area occupied

by lymphocytic infiltrate (low, < 20%; intermediate, 20%–50%; high, > 50%). For the construction of tissue microarray (TMA) blocks, two tissue cores of approximately 2 mm were excised from the central area of the SCCOT and from tumor margins with normal mucosa.

Immunohistochemistry

IHC staining for p16 (1:6, clone E6H4, mouse mAb, Ventana Medical Systems, Tucson, AZ, USA), p53 (1:1,500, clone M7001, mouse mAb, Dako, Glostrup, Denmark), ER (1:200, clone 6F11, mouse mAb, Novocastra, Newcastle upon Tyne, UK), PR (1:200, clone 16, mouse mAb, Novocastra), AR (1:100, clone SP107, rabbit mAb, Cell Marque, Rocklin, CA, USA), mdm2 (1:50, clone SMP14, mouse mAb, Zeta, Arcadia, CA, USA), cyclin D1 (1:100, clone SP4, mouse mAb, Cell Marque), and GSTP1 (1:6,000, clone 3F2, mouse mAb, Cell Signaling, Danvers, MA, USA) was conducted in accordance with the manufacturer's manual on a Ventana BenchMark XT Autostainer (Ventana Medical Systems). Serially cut 4- μ m sections of the TMA block were deparaffinized, and antigen retrieval was carried out with EDTA buffer (cell conditioner #1) for 32 minutes (p16, p53, PR, AR, cyclin D1, and GSTP1) or 64 minutes (mdm2 and ER). After inactivation of endogenous peroxidase and rinsing with Tris buffer (reaction buffer), diluted primary antibodies were added and incubated for 16 minutes (p16, p53, PR, AR, cyclin D1, and GSTP1) or 32 minutes (mdm2 and ER) at 37°C.

Expression levels of p53, p16, mdm2, and cyclin D1 were analyzed by a semiquantitative score based on the proportion of stained area (%) using criteria outlined in Table 1 and in reference to previous reports.^{19,30,31} GSTP1 was interpreted as weak or strong by cytoplasmic staining intensity. IHC stains for ER,

Table 1. Interpretation criteria for immunohistochemical analysis of p53, mdm2, cyclin D1, and p16

Marker	Score	Cells stained (%)
p53	0	0
	1+	<10
	2+	10 to <50
	3+	≥50
mdm2	0	0
	1+	<10
	2+	10 to <50
	3+	≥50
Cyclin D1	Low	<50
	High	≥50
p16	0	0
	1+	<5
	2+	5 to <25
	3+	≥25

PR, and AR were considered as positive when nuclear expression was noted regardless of cellular proportion.

Statistical analysis

Statistical analysis was performed using SPSS ver. 25.0 (IBM Corp., Armonk, NY, USA). Results for age, tumor size, and DOI were described with mean and 95% confidence interval. The Mann-Whitney U test was used to compare tumor size and DOI between age and sex groups. The Kruskal-Wallis test was used for comparisons among the four groups (young men, young women, old men, and old women). Other clinicopathological parameters and IHC results were compared using Pearson's chi-square test and the Fisher's exact test. OS and DFS were analyzed according to the Kaplan-Meier method with univariate analysis (log-rank test). All calculated p-values were 2-sided, and values less than 0.05 were considered statistically significant.

Ethics statement

All procedures performed for the current study were approved by the Institutional Review Board (IRB) of Asan Medical Center (approval No. 2018-0395) in accordance with the 1964 Helsinki declaration and its later amendments. Formal written informed consent was waived by the IRB.

RESULTS

Patients were divided into four groups according to age and sex;

young men, young women, old men, and old women. Clinical characteristics are listed in Table 2, and histopathological data are listed in Table 3. We also compared patients between age and sex groups. Clinicopathological data therein are included in the Supplementary Materials (Supplementary Tables S1–4).

Age at diagnosis ranged from 20.7 to 88.0 years (median, 56.1 years; 95% confidence interval, 52.88 to 57.26). Young patients accounted for 27.0% (51/189). Smoking and drinking status were markedly different between sexes, but not age groups (Tables 2, Supplementary Tables S1, 2). Most smokers (61/69, 88.4%) and regular drinkers (86/99, 86.9%) were men. Proportions of heavy smokers and drinkers were slightly lower in young patients, but these differences were not statistically significant. Women comprised 40.2% (72 of 189) of all patients. More women were in the young patient group (25 of 51, 49%), and more likely to be young non- or ex-smokers (21 of 30, 70%). OS and DFS were not significantly different by age (young or old) or sex (Fig. 1). Young women presented with relatively lower mortality rates (28.0%) than the other groups combined (48.2%), but this difference was not statistically significant ($p=.082$). Relatively poor survival among young men (50.0% vs 44.8% of others) was also observed but not statistically significant ($p=.678$).

Histologic grade tended to be higher in young patients ($p=.021$) but did not vary between sexes (Supplementary Tables S3, 4). When we compared the four groups divided by sex and age, none of the histopathological parameters including tumor size,

Table 2. Demographics and clinical information

Characteristic	Young (<45 yr, n=51)		Old (≥45 yr, n=138)		p-value
	Men (n=26)	Women (n=25)	Men (n=87)	Women (n=51)	
Age (yr)					<.001
Mean (95% CI)	35.5 (32.8–38.2)	34.8 (32.0–37.6)	61.5 (59.6–63.5)	64.0 (60.8–67.2)	
Smoking status					<.001
Non- or ex-smoker	9 (34.6)	21 (84.0)	43 (49.4)	47 (92.2)	
Light smoker	7 (26.9)	3 (12.0)	10 (11.5)	1 (2.0)	
Heavy smoker	10 (38.5)	1 (4.0)	34 (39.1)	3 (5.9)	
Alcohol use					<.001
Abstain	6 (23.1)	20 (80.0)	24 (27.6)	45 (88.2)	
Light drinker	15 (57.7)	3 (12.0)	35 (40.2)	6 (11.8)	
Heavy drinker	5 (19.2)	2 (8.0)	28 (32.2)	0	
Adjuvant treatment					.550
None	9 (34.6)	11 (44.0)	42 (48.3)	25 (49.0)	
Radiotherapy	12 (46.2)	8 (32.0)	26 (29.9)	20 (39.2)	
Chemotherapy	0	0	5 (5.7)	1 (2.0)	
Chemo + radiotherapy	5 (19.2)	6 (24.0)	14 (16.1)	5 (9.8)	
Recurrence (%)	11 (42.3)	9 (36.0)	25 (28.7)	18 (35.3)	.597
Deceased (%)	13 (50.0)	7 (28.0)	42 (48.3)	24 (47.1)	.309

Values are presented as number (%) unless otherwise indicated. CI, confidence interval.

Table 3. Histopathologic data and stage

Characteristic	Young (<45, n=51)		Old (≥45, n=138)		p-value
	Men (n=26)	Women (n=25)	Men (n=87)	Women (n=51)	
Tumor size (cm)					.868
Mean (95% CI)	2.7 (2.1–3.3)	2.6 (2.0–3.1)	2.5 (2.2–2.8)	3.0 (2.1–3.8)	
Depth of invasion (mm)					.479
Mean (95% CI)	11.9 (9.0–14.8)	11.9 (8.4–15.3)	10.1 (8.5–11.6)	10.7 (9.0–12.4)	
Histological grade					.102
Well differentiated	11 (42.3)	7 (28.0)	45 (51.7)	26 (51.0)	
Moderately differentiated	8 (30.8)	13 (52.0)	35 (40.2)	19 (37.3)	
Poorly differentiated	7 (26.9)	5 (20.0)	7 (8.0)	6 (11.8)	
Lymphovascular invasion					.625
Present	6 (23.1)	6 (24.0)	63 (72.4)	42 (82.4)	
Absent	20 (76.9)	19 (76.0)	24 (27.6)	9 (17.6)	
Perineural invasion					.661
Present	11 (42.3)	10 (40.0)	29 (33.3)	22 (43.1)	
Absent	15 (57.7)	15 (60.0)	58 (66.7)	29 (56.9)	
Tumor-infiltrating lymphocyte					.335
Low	13 (50.0)	14 (56.0)	53 (60.9)	28 (54.9)	
Intermediate	10 (38.5)	7 (28.0)	24 (27.6)	10 (19.6)	
High	3 (11.5)	4 (16.0)	10 (11.5)	13 (25.5)	
T category					.569
T1	4 (15.4)	2 (8.0)	23 (26.4)	26.4 (10.0)	
T2	9 (34.6)	13 (52.0)	30 (34.5)	34.5 (17.0)	
T3	13 (50.0)	10 (40.0)	33 (37.9)	37.9 (24.0)	
T4	0	0	1 (1.1)	0	
N category					.849
N0	11 (42.3)	13 (52.0)	47 (54.0)	29 (56.9)	
N1	5 (19.2)	4 (16.0)	12 (13.8)	9 (17.6)	
N2	6 (23.1)	3 (12.0)	18 (20.7)	9 (17.6)	
N3	4 (15.4)	5 (20.0)	10 (11.5)	4 (7.8)	

Values are presented as number (%) unless otherwise indicated. CI, confidence interval.

DOI, histologic grade, LVI, PNI, TIL group, T and N category were significantly different for any group (Table 3). Notably, higher TIL was correlated to better OS ($p=.002$) and DFS ($p=.017$) rates (Fig. 2).

IHC stains for sex hormone receptors were positive in a small number of patients. Only a single case presented with nuclear expression of ER (51.1-year-old male, non-smoker) and two cases presented with expression of AR (case 1, 40.2-year-old female, non-smoker; case 2, 56.7-year-old, male, non-smoker). PR was not expressed in any of the study participant samples. Expression levels as determined by IHC stainings of p16, p53, mdm2, GSTP1, and cyclin D1 were compared between patients grouped by age, sex, and smoking and drinking status, and no significant differences were found for any cohort (Table 4). Among immunomarkers, cyclin D1 expression was correlated to OS ($p=.009$) and DFS ($p=.011$) (Fig. 3). Other markers (p53, mdm2, p16, and GSTP1) were not correlated to any clinicopathological parameters.

DISCUSSION

SCCOT in young and non-smoking patients has been reported since the 1980s but became a substantial issue after 2000 when epidemiologic evidence demonstrated an increasing incidence in this group. Previously, physicians thought that young SCCOT patients had poorer prognoses, and more aggressive treatments were used in this population. However, this notion has yet to be empirically substantiated.⁷ Many studies attempted to find biological factors unique to young patients with SCCOT, but distinctive features were not found.^{11,32,33} Indeed, SCCOT in young and old patients has not been found to exhibit relevant difference at the molecular level.³⁴ Pickering et al.¹⁰ found certain genomic similarities between SCCOT in young patients and older smokers by whole-exome sequencing. However, these studies were mainly conducted by Western countries so data from Asian populations are insufficient. Recently, Sun et al.³⁵ reported that prognoses for young Chinese patients with oral SCC were similar to those for

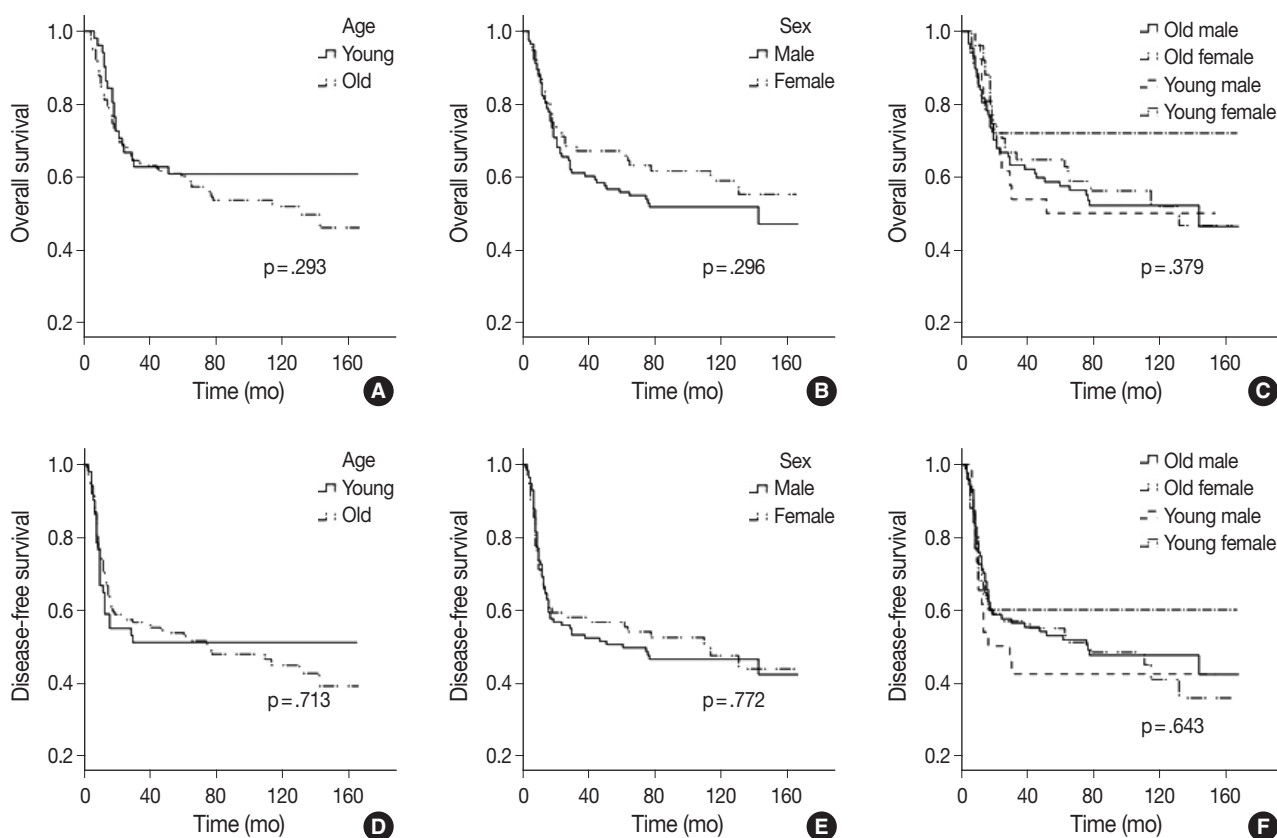


Fig. 1. Kaplan-Meier estimation of overall survival and disease-free survival curves for age and sex. Neither overall survival (A–C) nor disease-free survival (D–F) was significantly associated with age or sex.

older patients. In this study, we also found equivalent results for old and young patients from Korea.

Briefly, the only clinicopathological parameter that differed between young and old patients was histological grade (Table 3), which was found to be worse in the young group. Male-to-female ratios were also not statistically different by age, although a relatively higher proportion of women was observed in young patients. This tendency became more significant in the young, non-smoking group where women were predominant (21 of 27, 77.8%). This finding recapitulated those from previous studies reporting that young women with no history of tobacco or alcohol use were more vulnerable to SCCOT than their male counterparts.⁴ This epidemiologic peculiarity aroused our interest in a potential relationship between SCCOT and sex hormone receptor expression.

Previous studies reported ER expression in 11% to 50% of SCCOT cases.^{13,14,36} In this study, however, we only observed focal ER expression in a single patient, despite the use of automated IHC staining with a well-established primary antibody and staining protocol. The only ER-expressing tumor found was that of an older male with no history of smoking. Interestingly,

in other reports, most patients presenting with ER-positive head and neck cancer were also older males.^{13,14} These results suggest that ER involvement might be primarily related to the original patient group of older men. PR was negative in all cases; this is also consistent with a previous report.¹⁴ Immunoreactivity with nuclear expression for AR was seen in two cases, in contrast to previous reports reporting AR positivity in up to 67% of patients, most of them expressing AR in the cytoplasm.³⁷ Since true positivity for AR requires nuclear expression, the importance of AR expression in young SCCOT patients seems to be limited.

Inter-individual variation in metabolic capacity for toxins could influence the carcinogenesis of SCCOT in young patients. GSTP1 is an important detoxifying enzyme, but a relationship between GSTP1 and oral carcinogenesis remains unclear. Genetic polymorphisms in the *GSTP1* gene has been reported to be associated with impaired metabolism of carcinogens, thereby elevating the risk of several tumors, including head and neck cancer.^{21,38} Soares et al.¹⁷ observed increased GSTP1 expression in non-tumor margins in both smoking and drinking patients and suggested that this result could be a reaction to carcinogen exposure. In the current study, all tumors presented with diffuse GSTP1 expres-

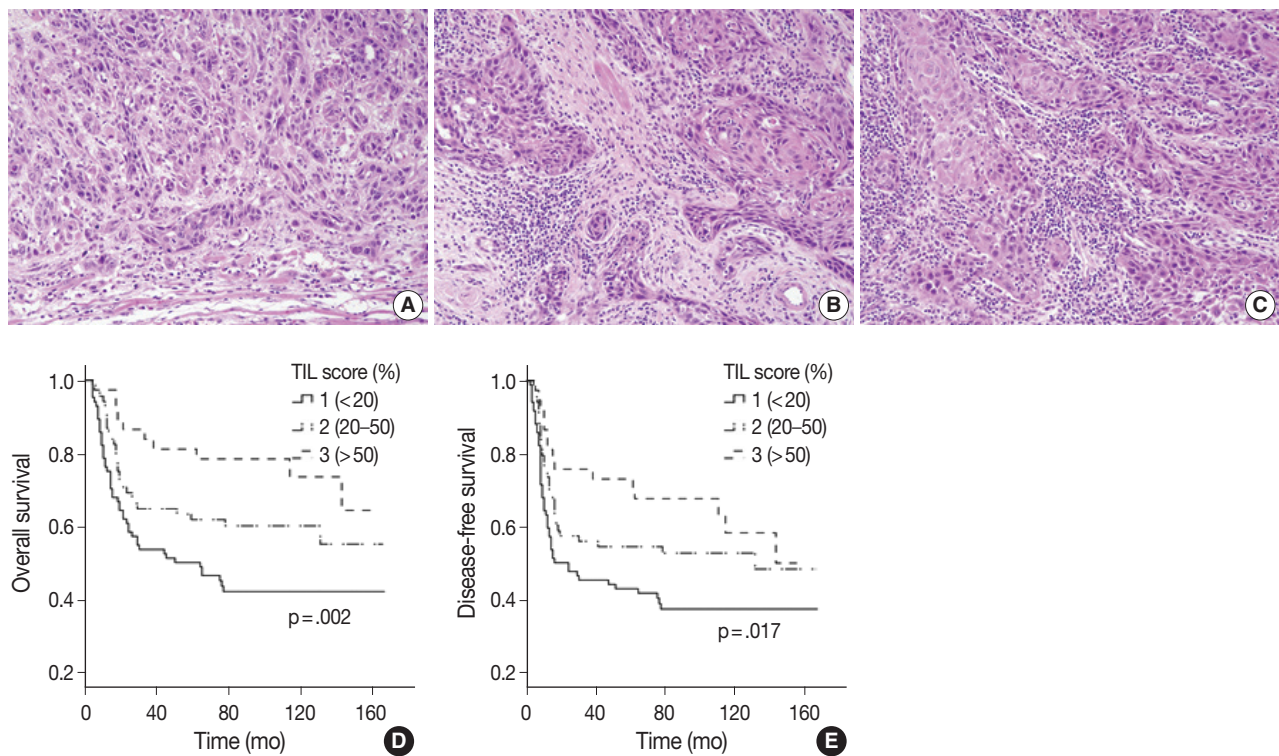


Fig. 2. Examples of tumor-infiltrating lymphocyte (TIL) scores and Kaplan-Meier survival curves. Each tumor was given a TIL group depending upon the amount of stromal lymphocytic infiltration. Images represent low (A), intermediate (B), and high (C) group. Higher TIL groups were associated with better overall survival (D) and disease-free survival (E).

Table 4. Expression profiles of immunomarkers by age, sex, smoking, and alcohol use

	Age		p-value	Sex		p-value	Smoking			p-value	Alcohol use			p-value
	Young (<45 yr)	Old (≥45 yr)		Male	Female		Non- or ex-smoker	Light smoker	Heavy smoker		Abstain	Light drinker	Heavy drinker	
p16			.072			.893				.465				.307
0	27 (52.9)	77 (55.8)		60 (53.1)	44 (57.9)		61 (50.8)	12 (57.1)	31 (64.6)		52 (54.7)	29 (49.2)	23 (65.7)	
1+	8 (15.7)	39 (28.3)		29 (25.7)	18 (23.7)		34 (28.3)	4 (19.0)	9 (18.8)		21 (22.1)	21 (35.6)	5 (14.3)	
2+	7 (13.7)	11 (8.0)		12 (10.6)	6 (7.9)		12 (10.0)	1 (4.8)	5 (10.4)		10 (10.5)	4 (6.8)	4 (11.4)	
3+	9 (17.6)	11 (8.0)		12 (10.6)	8 (10.5)		13 (10.8)	4 (19.0)	3 (6.3)		12 (12.6)	5 (8.5)	3 (8.6)	
p53			.443			.596				.739				.676
0	9 (17.6)	20 (14.5)		18 (15.9)	11 (14.5)		19 (15.8)	5 (23.8)	5 (10.4)		13 (13.7)	11 (18.6)	5 (14.3)	
1+	15 (29.4)	28 (20.3)		25 (22.1)	18 (23.7)		26 (21.7)	5 (23.8)	12 (25.0)		18 (18.9)	14 (23.7)	11 (31.4)	
2+	3 (5.9)	13 (9.4)		12 (10.6)	4 (5.3)		9 (7.5)	1 (4.8)	6 (12.5)		8 (8.4)	6 (10.2)	2 (5.7)	
3+	24 (47.1)	77 (55.8)		58 (51.3)	43 (56.6)		66 (55.0)	10 (47.6)	25 (52.1)		56 (58.9)	28 (47.5)	17 (48.6)	
mdm2			.442			.403				.464				.877
0	31 (60.8)	72 (52.2)		57 (50.4)	46 (60.5)		69 (57.5)	9 (42.9)	25 (52.1)		55 (57.9)	30 (50.8)	18 (51.4)	
1+	19 (37.3)	59 (42.8)		51 (45.1)	27 (35.5)		45 (37.5)	12 (57.1)	21 (43.8)		36 (37.9)	26 (44.1)	16 (45.7)	
2+	1 (2.0)	7 (5.1)		5 (4.4)	3 (3.9)		6 (5.0)	0	2 (4.2)		4 (4.2)	3 (5.1)	1 (2.9)	
3+	0	0		0	0		0	0	0		0	0	0	
Cyclin D1			.247			.771				.883				.662
Low	16 (31.4)	56 (40.6)		44 (38.9)	28 (36.8)		46 (38.3)	7 (33.3)	19 (39.6)		38 (40.0)	23 (39.0)	11 (31.4)	
High	35 (68.6)	82 (59.4)		69 (61.1)	48 (63.2)		74 (61.7)	14 (66.7)	29 (60.4)		57 (60.0)	36 (61.0)	24 (68.6)	
GSTP1			.082			.952				.599				.266
Weak	11 (21.6)	16 (11.6)		16 (14.2)	11 (14.5)		18 (15.0)	4 (19.0)	5 (10.4)		16 (16.8)	9 (15.3)	2 (5.7)	
Strong	40 (78.4)	122 (88.0)		97 (85.8)	65 (85.5)		102 (85.0)	17 (81.0)	43 (89.6)		79 (83.2)	50 (84.7)	33 (94.3)	

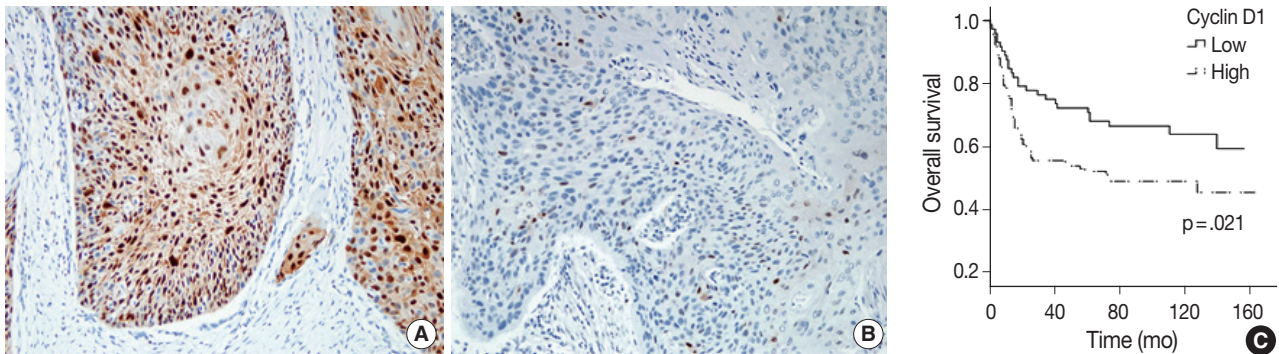


Fig. 3. Immunohistochemistry for cyclin D1 and Kaplan-Meier survival curve. Tumor cells showing strong (A) or weak (B) nuclear expression of cyclin D1. Strong expression of cyclin D1 correlated with poor overall survival (C).

sion and heterogeneous staining intensities. Overall intensity scores did not vary by age, sex or smoking or drinking status. We also found that strong GSTP1 expression was not related to prognosis. Epithelial tissues in non-tumor margins showed similar or slightly weaker intensities than those of matched tumor cells. These results suggest that expression of GSTP1 is not a suitable marker for individual cancer susceptibility or toxin exposure related to SCCOT.

Other IHC markers, p53, cyclin D1, mdm2, and p16, were variably positive in a significant proportion of cases but their expression levels were not statistically different by age, sex or smoking or drinking status. Strong expression of cyclin D1 was associated with poor prognosis, a finding that is consistent with previous reports.^{15,19,39} However, the lack of standardized interpretation criteria of cyclin D1 expression parameters compromises the reliability and integrity of these results. The relationship between cyclin D1 and SCCOT is worthy of further investigation, particularly with respect to standardizing the interpretation criteria. No standardized TIL assessment guideline for oral SCC exists, either. Several reports suggest a prognostic impact of TIL on oral SCC^{40,41} but they used different assessment methods and demonstrated conflicting results. We applied the TIL assessment method used in breast cancer²⁹ and found a significant correlation between TIL and OS, implying that this method might be a candidate for standardized assessment.

This study evaluated the clinicopathological parameters and expression profiles of several tumorigenic candidate proteins of SCCOT and found no significant difference between young and old patients nor between male and female patients. Despite epidemiologic idiosyncrasy, SCCOT in young women appears to be similar to that in older men. Previous studies reported similar data and came to similar conclusions.^{6-8,10,11,42} These results, combined with epidemiological data, suggest the presence of unknown carcinogenic factors contributing to an emerging incidence of

SCCOT in young women via a similar pathogenetic sequence to that associated with known risk factors. We investigated two candidates for these factors, hormone receptors and GSTP1, but significant findings were not observed. Considering that known risk factors are primarily associated with toxin exposure (tobacco, betel quid, or alcohol), extrinsic factors appear to be more important than individual factors of age, sex, or intrinsic metabolic activity in the pathogenesis of SCCOT. Possible exposure to toxic materials associated with altered lifestyles or new environmental pollutants should thereby be investigated in the young female SCCOT population.

Electronic Supplementary Material

Supplementary materials are available at Journal of Pathology and Translational Medicine (<https://jpatholtm.org>).

ORCID

Gyuheon Choi: <https://orcid.org/0000-0002-2825-987X>
 Joon Seon Song: <https://orcid.org/0000-0002-7429-4254>
 Seung-Ho Choi: <https://orcid.org/0000-0001-9109-9621>
 Soon Yuhl Nam: <https://orcid.org/0000-0002-8299-3573>
 Sang Yoon Kim: <https://orcid.org/0000-0002-2162-7983>
 Jong-Lyel Roh: <https://orcid.org/0000-0002-1537-1977>
 Bu-Kyu Lee: <https://orcid.org/0000-0001-8483-937X>
 Kyung-Ja Cho: <https://orcid.org/0000-0002-4911-7774>

Author Contributions

Conceptualization: KJC.
 Data curation: KJC, GC.
 Formal analysis: GC.
 Funding acquisition: KJC.
 Investigation: GC.
 Methodology: KJC.

Project administration: GC.
 Resources: SHC, SYN, SYK, JLR, BKL.
 Supervision: KJC.
 Validation: KJC, JSS.
 Visualization: GC.
 Writing – original draft preparation: GC.
 Writing – review & editing: KJC, JSS.

Conflicts of Interest

The authors declare that they have no potential conflicts of interest.

Funding

No funding to declare.

REFERENCES

- Scully C, Bagan J. Oral squamous cell carcinoma: overview of current understanding of aetiopathogenesis and clinical implications. *Oral Dis* 2009; 15: 388-99.
- Ng JH, Iyer NG, Tan MH, Edgren G. Changing epidemiology of oral squamous cell carcinoma of the tongue: a global study. *Head Neck* 2017; 39: 297-304.
- Patel SC, Carpenter WR, Tyree S, et al. Increasing incidence of oral tongue squamous cell carcinoma in young white women, age 18 to 44 years. *J Clin Oncol* 2011; 29: 1488-94.
- Harris SL, Kimple RJ, Hayes DN, Couch ME, Rosenman JG. Never-smokers, never-drinkers: unique clinical subgroup of young patients with head and neck squamous cell cancers. *Head Neck* 2010; 32: 499-503.
- Choi SW, Moon EK, Park JY, et al. Trends in the incidence of and survival rates for oral cavity cancer in the Korean population. *Oral Dis* 2014; 20: 773-9.
- Blanchard P, Belkhir F, Temam S, et al. Outcomes and prognostic factors for squamous cell carcinoma of the oral tongue in young adults: a single-institution case-matched analysis. *Eur Arch Otorhinolaryngol* 2017; 274: 1683-90.
- Goepfert RP, Kezirian EJ, Wang SJ. Oral tongue squamous cell carcinoma in young women: a matched comparison-do outcomes justify treatment intensity? *ISRN Otolaryngol* 2014; 2014: 529395.
- Majchrzak E, Szybiak B, Wegner A, et al. Oral cavity and oropharyngeal squamous cell carcinoma in young adults: a review of the literature. *Radiol Oncol* 2014; 48: 1-10.
- van Monsjou HS, Wreesmann VB, van den Brekel MW, Balm AJ. Head and neck squamous cell carcinoma in young patients. *Oral Oncol* 2013; 49: 1097-102.
- Pickering CR, Zhang J, Neskey DM, et al. Squamous cell carcinoma of the oral tongue in young non-smokers is genomically similar to tumors in older smokers. *Clin Cancer Res* 2014; 20: 3842-8.
- Santos HB, dos Santos TK, Paz AR, et al. Clinical findings and risk factors to oral squamous cell carcinoma in young patients: a 12-year retrospective analysis. *Med Oral Patol Oral Cir Bucal* 2016; 21: e151-6.
- Lingen MW, Chang KW, McMurray SJ, et al. Overexpression of p53 in squamous cell carcinoma of the tongue in young patients with no known risk factors is not associated with mutations in exons 5-9. *Head Neck* 2000; 22: 328-35.
- Grimm M, Biegner T, Teriete P, et al. Estrogen and progesterone hormone receptor expression in oral cavity cancer. *Med Oral Patol Oral Cir Bucal* 2016; 21: e554-8.
- Colella G, Izzo G, Carinci F, et al. Expression of sexual hormones receptors in oral squamous cell carcinoma. *Int J Immunopathol Pharmacol* 2011; 24(2 Suppl): 129-32.
- Kaminagakura E, Werneck da Cunha I, Soares FA, Nishimoto IN, Kowalski LP. CCND1 amplification and protein overexpression in oral squamous cell carcinoma of young patients. *Head Neck* 2011; 33: 1413-9.
- Lang J, Song X, Cheng J, Zhao S, Fan J. Association of GSTP1 I105Val polymorphism and risk of head and neck cancers: a meta-analysis of 28 case-control studies. *PLoS One* 2012; 7: e48132.
- Soares PO, Maluf Cury P, Mendoza Lopez RV, et al. GSTP1 expression in non-smoker and non-drinker patients with squamous cell carcinoma of the head and neck. *PLoS One* 2017; 12: e0182600.
- Yanamoto S, Kawasaki G, Yoshitomi I, Mizuno A. p53, mdm2, and p21 expression in oral squamous cell carcinomas: relationship with clinicopathologic factors. *Oral Surg Oral Med Oral Pathol Oral Radiol Endod* 2002; 94: 593-600.
- Mineta H, Miura K, Takebayashi S, et al. Cyclin D1 overexpression correlates with poor prognosis in patients with tongue squamous cell carcinoma. *Oral Oncol* 2000; 36: 194-8.
- Harris SL, Thorne LB, Seaman WT, Hayes DN, Couch ME, Kimple RJ. Association of p16(INK4a) overexpression with improved outcomes in young patients with squamous cell cancers of the oral tongue. *Head Neck* 2011; 33: 1622-7.
- Karen-Ng LP, Marhazlinda J, Rahman ZA, et al. Combined effects of isothiocyanate intake, glutathione S-transferase polymorphisms and risk habits for age of oral squamous cell carcinoma development. *Asian Pac J Cancer Prev* 2011; 12: 1161-6.
- Koenigs MB, Lefranc-Torres A, Bonilla-Velez J, et al. Association of estrogen receptor alpha expression with survival in oropharyngeal cancer following chemoradiation therapy. *J Natl Cancer Inst* 2019; 111: 933-42.

23. Mohamed H, Aro K, Jouhi L, et al. Expression of hormone receptors in oropharyngeal squamous cell carcinoma. *Eur Arch Otorhinolaryngol* 2018; 275: 1289-300.
24. Morse DE, Katz RV, Pendry DG, et al. Smoking and drinking in relation to oral epithelial dysplasia. *Cancer Epidemiol Biomarkers Prev* 1996; 5: 769-77.
25. Blot WJ, McLaughlin JK, Winn DM, et al. Smoking and drinking in relation to oral and pharyngeal cancer. *Cancer Res* 1988; 48: 3282-7.
26. Morse DE, Psoter WJ, Cleveland D, et al. Smoking and drinking in relation to oral cancer and oral epithelial dysplasia. *Cancer Causes Control* 2007; 18: 919-29.
27. Amin MB, Edge S, Greene F, et al. *AJCC cancer staging manual*. 8th ed. New York: Springer, 2017.
28. Hendry S, Salgado R, Gevaert T, et al. Assessing tumor-infiltrating lymphocytes in solid tumors: a practical review for pathologists and proposal for a standardized method from the International Immunooncology Biomarkers Working Group: Part 1: assessing the host immune response, TILs in invasive breast carcinoma and ductal carcinoma in situ, metastatic tumor deposits and areas for further research. *Adv Anat Pathol* 2017; 24: 235-51.
29. Hendry S, Salgado R, Gevaert T, et al. Assessing tumor-infiltrating lymphocytes in solid tumors: a practical review for pathologists and proposal for a standardized method from the International Immuno-Oncology Biomarkers Working Group: Part 2: TILs in melanoma, gastrointestinal tract carcinomas, non-small cell lung carcinoma and mesothelioma, endometrial and ovarian carcinomas, squamous cell carcinoma of the head and neck, genitourinary carcinomas, and primary brain tumors. *Adv Anat Pathol* 2017; 24: 311-35.
30. Ofner D, Maier H, Riedmann B, et al. Immunohistochemically detectable p53 and mdm-2 oncoprotein expression in colorectal carcinoma: prognostic significance. *Clin Mol Pathol* 1995; 48: M12-6.
31. Klaes R, Friedrich T, Spitkovsky D, et al. Overexpression of p16(INK4A) as a specific marker for dysplastic and neoplastic epithelial cells of the cervix uteri. *Int J Cancer* 2001; 92: 276-84.
32. Zhang YY, Wang DC, Su JZ, Jia LF, Peng X, Yu GY. Clinicopathological characteristics and outcomes of squamous cell carcinoma of the tongue in different age groups. *Head Neck* 2017; 39: 2276-82.
33. Dediol E, Sabol I, Virag M, Grce M, Muller D, Manojlovic S. HPV prevalence and p16INKa overexpression in non-smoking non-drinking oral cavity cancer patients. *Oral Dis* 2016; 22: 517-22.
34. Dos Santos Costa SF, Brennan PA, Gomez RS, et al. Molecular basis of oral squamous cell carcinoma in young patients: is it any different from older patients? *J Oral Pathol Med* 2018; 47: 541-6.
35. Sun Q, Fang Q, Guo S. A comparison of oral squamous cell carcinoma between young and old patients in a single medical center in China. *Int J Clin Exp Med* 2015; 8: 12418-23.
36. Chang YL, Hsu YK, Wu TF, et al. Regulation of estrogen receptor alpha function in oral squamous cell carcinoma cells by FAK signaling. *Endocr Relat Cancer* 2014; 21: 555-65.
37. Wu TF, Luo FJ, Chang YL, et al. The oncogenic role of androgen receptors in promoting the growth of oral squamous cell carcinoma cells. *Oral Dis* 2015; 21: 320-7.
38. Mutallip M, Nohata N, Hanazawa T, et al. Glutathione S-transferase P1 (GSTP1) suppresses cell apoptosis and its regulation by miR-133alpha in head and neck squamous cell carcinoma (HNSCC). *Int J Mol Med* 2011; 27: 345-52.
39. Zhao Y, Yu D, Li H, et al. Cyclin D1 overexpression is associated with poor clinicopathological outcome and survival in oral squamous cell carcinoma in Asian populations: insights from a meta-analysis. *PLoS One* 2014; 9: e93210.
40. Brandwein-Gensler M, Teixeira MS, Lewis CM, et al. Oral squamous cell carcinoma: histologic risk assessment, but not margin status, is strongly predictive of local disease-free and overall survival. *Am J Surg Pathol* 2005; 29: 167-78.
41. Cho YA, Yoon HJ, Lee JI, Hong SP, Hong SD. Relationship between the expressions of PD-L1 and tumor-infiltrating lymphocytes in oral squamous cell carcinoma. *Oral Oncol* 2011; 47: 1148-53.
42. Chang TS, Chang CM, Ho HC, et al. Impact of young age on the prognosis for oral cancer: a population-based study in Taiwan. *PLoS One* 2013; 8: e75855.

A Multi-institutional Study of Prevalence and Clinicopathologic Features of Non-invasive Follicular Thyroid Neoplasm with Papillary-like Nuclear Features (NIFTP) in Korea

Ja Yeong Seo, Ji Hyun Park, Ju Yeon Pyo, Yoon Jin Cha, Chan Kwon Jung¹, Dong Eun Song², Jeong Ja Kwak³, So Yeon Park⁴, Hee Young Na⁴, Jang-Hee Kim⁵, Jae Yeon Seok⁶, Hee Sung Kim⁷, Soon Won Hong

Department of Pathology, Gangnam Severance Hospital, Yonsei University College of Medicine, Seoul;

¹Department of Hospital Pathology, Seoul St. Mary's Hospital, College of Medicine, The Catholic University of Korea, Seoul;

²Department of Pathology, Asan Medical Center, University of Ulsan College of Medicine, Seoul;

³Department of Pathology, Soonchunhyang University Bucheon Hospital, Soonchunhyang University College of Medicine, Bucheon;

⁴Department of Pathology, Seoul National University Bundang Hospital, Seoul National University College of Medicine, Seongnam;

⁵Department of Pathology, Ajou University School of Medicine, Suwon;

⁶Department of Pathology, Gil Medical Center, Gachon University College of Medicine, Incheon;

⁷Department of Pathology, Chung-Ang University Hospital, Chung-Ang University College of Medicine, Seoul, Korea

Background: In the present multi-institutional study, the prevalence and clinicopathologic characteristics of non-invasive follicular thyroid neoplasm with papillary-like nuclear features (NIFTP) were evaluated among Korean patients who underwent thyroidectomy for papillary thyroid carcinoma (PTC). **Methods:** Data from 18,819 patients with PTC from eight university hospitals between January 2012 and February 2018 were retrospectively evaluated. Pathology reports of all PTCs and slides of potential NIFTP cases were reviewed. The strict criterion of no papillae was applied for the diagnosis of NIFTP. Due to assumptions regarding misclassification of NIFTP as non-PTC tumors, the lower boundary of NIFTP prevalence among PTCs was estimated. Mutational analysis for *BRAF* and three *RAS* isoforms was performed in 27 randomly selected NIFTP cases. **Results:** The prevalence of NIFTP was 1.3% (238/18,819) of all PTCs when the same histologic criteria were applied for NIFTP regardless of the tumor size but decreased to 0.8% (152/18,819) when tumors ≥ 1 cm in size were included. The mean follow-up was 37.7 months and no patient with NIFTP had evidence of lymph node metastasis, distant metastasis, or disease recurrence during the follow-up period. A difference in prevalence of NIFTP before and after NIFTP introduction was not observed. *BRAF*^{V600E} mutation was not found in NIFTP. The mutation rate for the three *RAS* genes was 55.6% (15/27). **Conclusions:** The low prevalence and indolent clinical outcome of NIFTP in Korea was confirmed using the largest number of cases to date. The introduction of NIFTP may have a small overall impact in Korean practice.

Key Words: Thyroid carcinoma; Follicular variant; Papillary carcinoma; Non-invasive follicular thyroid neoplasm with papillary-like nuclear features

Received: July 19, 2019 **Revised:** September 9, 2019 **Accepted:** September 18, 2019

Corresponding Author: Chan Kwon Jung, MD, PhD, Department of Hospital Pathology, Seoul St. Mary's Hospital, College of Medicine, The Catholic University of Korea, 222 Banpo-daero, Seocho-gu, Seoul 06591, Korea

Tel: +82-2-2258-1622, Fax: +82-2-2258-1627, E-mail: ckjung@catholic.ac.kr

Corresponding Author: Soon Won Hong, MD, PhD, Department of Pathology, Gangnam Severance Hospital, Yonsei University College of Medicine, 211 Eonju-ro, Gangnam-gu, Seoul 06273, Korea

Tel: +82-2-2019-3540, Fax: +82-2-2019-3540, E-mail: SOONWONH@yuhs.ac

The follicular variant of papillary thyroid carcinoma (FVPTC) is the second most common type of papillary thyroid carcinoma (PTC) and accounts for 5%–41% of all PTC subtypes.¹⁻⁴ FVPTC comprises two major subtypes: infiltrative FVPTC and encapsulated FVPTC (EFVPTC).⁵ The incidence of EFVPTC has gradually increased over the past two decades and constitutes more

than 10% of all thyroid malignancies diagnosed in North America and Europe.⁶ EFVPTC can be further classified into two subtypes: invasive EFVPTC and non-invasive EFVPTC based on the status of capsular or vascular tumor invasion.⁷ The majority of non-invasive EFVPTCs behave as indolent non-malignant tumors and have been renamed as non-invasive follicular thyroid

neoplasm with papillary-like nuclear features (NIFTP).⁸ This introduction of NIFTP concept has significantly affected clinical practice by reducing the therapeutic intensity for patients with EFVPTCs.

Differentiating NIFTP from invasive EFVPTC solely based on cytomorphologic findings is impossible when using thyroid fine needle aspiration cytology. NIFTPs are mostly interpreted as indeterminate categories.⁹ The two most common genetic mutations found in thyroid tumors are *BRAF* and *RAS* point mutations.¹⁰ *RAS* mutations occur in 30%–40% of EFVPTCs.^{11–14} The *BRAF*^{V600E} mutation is absent in NIFTPs but can occur in up to 30% of invasive EFVPTCs.^{14,15}

In Korea, a low rate of NIFTP has been reported in several studies.^{16–18} However, the studies were limited by small sample size and single institution, and the results might not represent the general population. Therefore, in the present study, the prevalence of NIFTP among Korean patients was evaluated by reviewing multicenter-based data using the largest cohort size to date in Korea.

MATERIALS AND METHODS

Study cohort

Data from 18,819 patients with PTC from eight university hospitals were retrospectively analyzed. The tumors were diagnosed from surgically resected specimens between January 2012 and February 2018. The slides of all cases initially diagnosed as EFVPTC on pathology reports were reviewed and reclassified into NIFTP, invasive EFVPTC, and other PTC subtypes. The NIFTP was diagnosed according to the criteria of *World Health Organization (WHO) Classification of Tumours of Endocrine*¹⁹ and recently revised diagnostic criteria:²⁰ (1) encapsulation or clear demarcation of the tumors (thick, thin, or partial capsule, or well circumscribed with a clear demarcation from adjacent thyroid tissues), (2) follicular growth pattern with no papillae (including microfollicular, normofollicular, or macrofollicular architecture with abundant colloid) with no psammoma bodies and < 30% solid/trabecular/insular growth pattern, (3) nuclear score 2–3, (4) no capsular or vascular invasion (requires adequate microscopic examination of the tumor capsule interface), (5) no tumor necrosis, (6) no high mitotic activity (high mitotic activity defined as at least 3 mitoses per 10 high-power fields (400×) (Fig. 1). A nuclear score of 2–3 is diagnostic of NIFTP. However, if florid nuclear features (nuclear score 3) of PTC are present, a meticulous histopathologic examination of the entire tumor is required for the detection of any true papillae, psam-

oma bodies, aggressive histology, or invasion into tumor capsule or vessels.

Molecular analysis of *NRAS* and *HRAS* genes

Molecular analysis of 27 NIFTP cases obtained from a single institution was performed. Genomic DNA was extracted from paraffin-embedded thyroid specimen blocks. The representative slides were selected and the tumor tissues were manually dissected under a stereomicroscope and stored in a 1.5 mL tube. Genomic DNAs were extracted from 5–10- μ m-thick tissue sections using the QIAamp DNA Mini Kit (Qiagen, Hilden, Germany) according to the manufacturer's instructions. Exon 3 of *NRAS* and *HRAS* genes was amplified using polymerase chain reaction (PCR) with the following primers: (1) *NRAS*-exon 3–197 bp, forward (5'-CCCCTTACCCTCCACACC-3') and reverse (5'-GAGGTAAATATCCGCAAATGACTT-3'); (2) *HRAS*-exon 3–201 bp, forward (5'-GTCCTCCTGCAGGATTCCTA-3') and reverse (5'-CGGGGTTACCTGTACT-3'). The PCR cycling conditions for *NRAS* and *HRAS* mutations were as follows: initial activation at 94°C for 15 minutes; 35 cycles at 94°C for 30 seconds, 51°C–57°C for 30 seconds, 72°C for 30 seconds, final extension at 72°C for 10 minutes. The amplicons were analyzed using 2% agarose gel electrophoresis and purified using QIAquick PCR purification kit (Qiagen). The amplified PCR products were sequenced using Sanger sequencing. The amplicons were evaluated on 2% agarose gel electrophoresis and purified using the QIAquick PCR purification kit (Qiagen). The amplified PCR products were analyzed using the automated sequencing machine ABI 3730 (Applied Biosystems, Foster City, CA, USA), which performed Sanger sequencing using the same PCR primers.¹⁷

Molecular analysis of *KRAS* gene

For detection of the *KRAS* mutation, a PNAclap *KRAS* mutation detection kit (Panagene, Daejeon, Korea) was used. The following reagents were used in all PCR reactions (total volume, 20 μ L): 10 ng template DNA, primer, peptide nucleic acid (PNA) probe set, and SYBR Green PCR Master Mix. A CFX 96 (Bio-Rad, Hercules, CA, USA) was used for the real-time PCR of PNA-mediated clamping. PCR cycling conditions consisted of the following sequential steps: 5-minute hold at 94°C followed by 40 cycles at 94°C for 30 seconds, 70°C for 20 seconds, 63°C for 30 seconds, and 72°C for 30 seconds. All seven mutations in the *KRAS* gene were detected using one-step PNA-mediated real-time PCR clamping. PNA probes and DNA primers were used for the corresponding clamping reaction. SYBR Green flu-

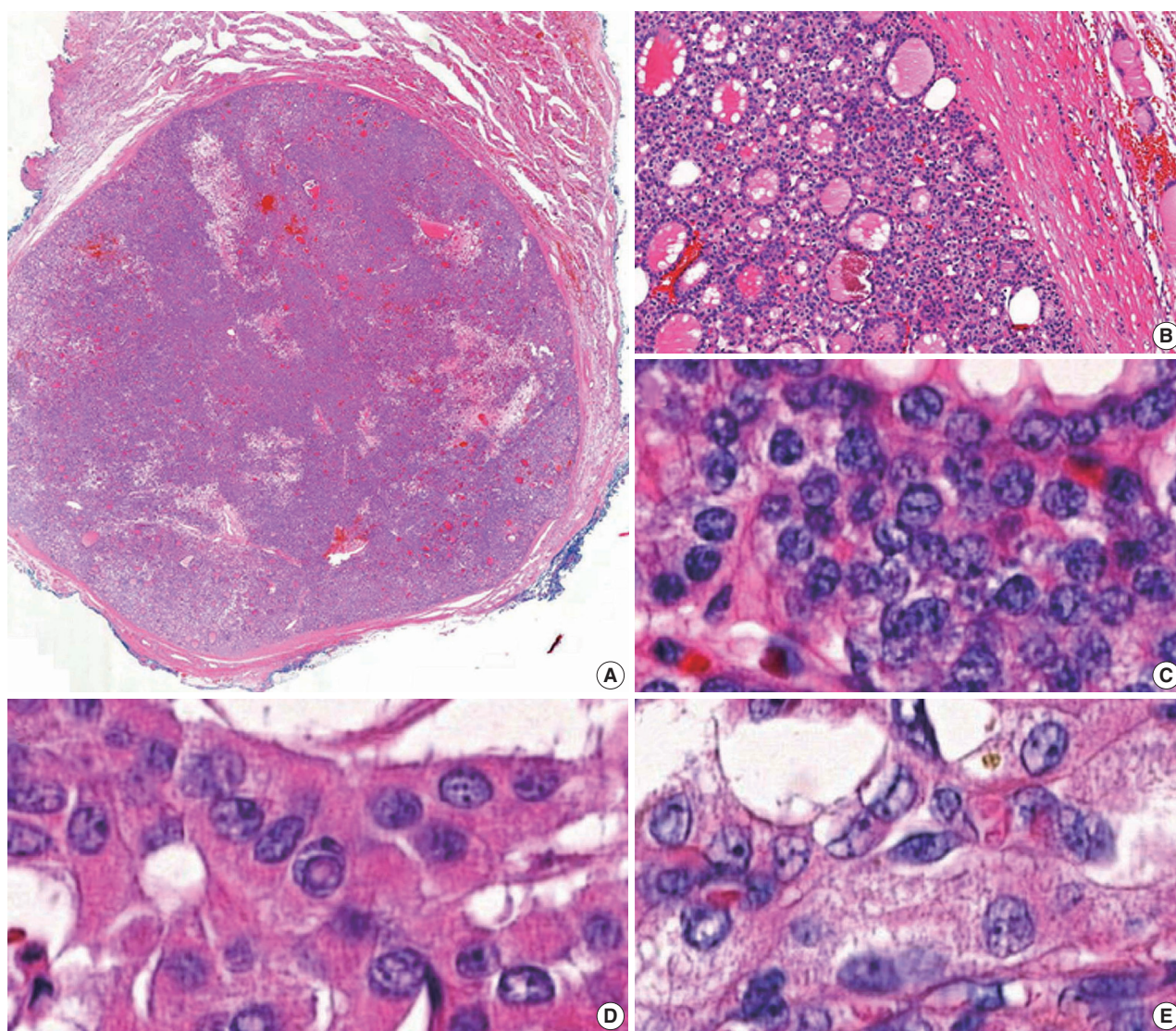


Fig. 1. (A) A case of non-invasive follicular thyroid neoplasm with papillary-like nuclear features (NIFTP): low power view, NIFTP composed entirely of a follicular growth pattern with complete encapsulation (scan view). (B) NIFTP shows a thick fibrous capsule without capsular and vascular invasion. (C) NIFTP with nuclear score 2. (D, E) Papillary thyroid carcinoma showing nuclear score 3.

orescent dye was applied for the detection of positive reaction signals. The amplification of the wild-type target was suppressed by the PNA probe sequence complementary to wild-type DNA. Due to this suppression, the amplification of mutant sequences was specifically preferred by competitive inhibition of DNA primers binding to wild-type DNA. The threshold cycle (Ct) value was used to evaluate PCR efficiency. The SYBR Green amplification plots were generated to analyze Ct values for the control and mutation assays. Mutation status was determined by Ct value differences ≥ 2 , which were obtained between the control and samples.

Molecular analysis of *BRAF* gene

Mutational analysis of *BRAF* was performed using two different methods. The PNA-Clamp *BRAF* mutation detection kit (Panagene) was used to detect the *BRAF*^{V600E} mutation. Each reaction tube had a total volume of 20 μ L and included a mixture of template DNA, primers, PNA probe, and SYBR Green PCR Master Mix. Real-time PCR of PNA-clamping PCR was performed using a CFX96 real-time PCR system (Bio-Rad, Pleasanton, CA, USA). The PNA probe was complementary to wild-type (V600). PCR was performed under the following conditions: 5-minute hold at 94°C, 40 cycles of 30 seconds at 94°C, 20 seconds at 70°C, 30 seconds at 63°C, and 30 seconds at 72°C.

The PNA probe and primers incorporated in the assay were separate oligonucleotides, and the PNA probe location was placed between forward and reverse primers within the template. Intercalation of SYBR Green fluorescent dye was used to detect positive signals.

Pyrosequencing for the *BRAF* mutation analysis was performed as described in detail elsewhere.²¹ The primers used for PCR were the following: forward primer (5'-GAAGACCTCA-CAGTAAAATAG-3') and reverse primer (5'-biotin-ATAGCCT-CAATTCTTACCATCC-3'). The pyrosequencing reaction was performed with a sequencing primer (5'-biotin-ATAGCCT-CAATTCTTACCATCC-3') on a Pyromark Q24 instrument (Qiagen). The PyroMark Q24 software (Qiagen) was used for analysis of the pyrogram results.

Statistical analysis

Clinicopathological parameters of NIFTP before and after NIFTP introduction were analyzed using the chi-square test or Fisher's exact test for categorical variables and the t-test for continuous variables. All statistical analyses were performed using SPSS ver. 22.0 (IBM Corp., Armonk, NY, USA). A p-value of <0.05 was considered statistically significant.

Ethics statement

The current study was approved by the Institutional Review Boards (IRBs) of eight institutions. Ethics approval for all procedures performed in the current study was obtained from the IRB (approval No. 3-2018-0271). Formal written informed consent was waived by the IRB.

RESULTS

The prevalence of NIFTP in PTC cases

To evaluate the incidence of NIFTP in the Korean population, data were retrospectively collected from the eight university hospitals in Korea. The incidence of NIFTP in each institution is shown in Table 1. After reviewing pathology reports of 18,819 patients with PTC, 378 patients (2.0%) were initially diagnosed with non-invasive EFVPTC as potential NIFTP cases; 140 cases were excluded from NIFTP diagnosis after review of pathology slides acquired from 378 cases. The most common reason for exclusion was the presence of small, but true papillae that were reclassified as conventional PTC. Other reasons for exclusion were reclassification as infiltrative FVPTC or unavailability for slide review. Finally, 238 (1.3%) of all PTCs were eligible for the diagnosis of NIFTP after slide review.

Among 238 cases of NIFTP, 174 cases (73.3%) had only NIFTP; in the remaining 64 cases (26.7%), NIFTP coexisted with other malignancies, such as conventional PTC, infiltrative FVPTC, tall cell variant PTC, oncocytic variant PTC, follicular carcinoma, or poorly differentiated carcinoma (Table 2).

Because not all cases were available for slide review and NIFTP can be misclassified as non-PTC tumors, the lower boundary for the prevalence of NIFTP among PTCs was estimated. When the same histologic criteria was applied for the diagnosis of NIFTP regardless of the tumor size, the prevalence of NIFTP was 238 (1.3%) among all PTCs. Among the reclassified 238 NIFTP cases, 86 had a tumor <1.0 cm and 152 had a tumor ≥1.0 cm (Table 2). Therefore, the expected lower boundary for the prevalence of NIFTP was 0.8% (152/18,819) when tumors ≥1.0 cm were included for the diagnosis of NIFTP.

Clinicopathologic characteristics of patients with NIFTP

Among 152 patients with NIFTP ≥1.0 cm in size, 125 (82.2%) patients had only NIFTP and the remaining 27 patients (17.8%) had NIFTP coexisting with thyroid cancer. The clinicopathologic characteristics were evaluated in patients with only NIFTP. The demographics of 125 NIFTP patients are shown in Table 3. The mean age was 46.7 years (range, 23 to 73 years). The NIF-

Table 1. The prevalence of NIFTP in eight university hospitals

Institution	Period	PTC	Invasive EFVPTC	NIFTP
A	2012–2017	1,427	44 (3.1)	26 (1.8)
B	2013–2016	1,342	35 (2.6)	35 (2.6)
C	2013–2017	3,927	192 (4.9)	100 (2.5)
D	2013–2017	6,200	134 (2.2)	24 (0.4)
E	2013–2017	3,083	37 (1.2)	23 (0.7)
F	2014–2017	734	9 (1.2)	5 (0.7)
G	2015–2017	1,077	2 (0.2)	20 (1.9)
H	2015–2018	1,029	14 (1.4)	5 (0.5)
Total		18,819	467 (2.5)	238 (1.3)

Values are presented as number (%).

NIFTP, non-invasive follicular thyroid neoplasm with papillary-like nuclear features; PTC, papillary thyroid carcinoma; EFVPTC, encapsulated follicular variant of PTC.

Table 2. Prevalence of NIFTP according to the tumor size among 18,819 patients with initial diagnosis of papillary thyroid carcinoma

	Total	≥1.0 cm	<1.0 cm
All cases of NIFTP	238 (1.3)	152 (0.8)	86 (0.5)
NIFTP alone	174 (73.3)	125 (82.2)	49 (57.0)
NIFTP coexisting with malignancy	64 (26.7)	27 (17.8)	37 (43.0)

Values are presented as number (%).

NIFTP, non-invasive follicular thyroid neoplasm with papillary-like nuclear features.

TP patients included 93 females (74.4%) and 32 males (25.6%). The median primary tumor size was 26.2 mm (range, 10 to 80 mm). Among 125 patients, 101 (80.8%) underwent cervical lymph node dissection and lymph node metastasis was not found. In addition, no patient had lymphatic/vascular invasion or distant metastases. Regarding surgical methods, a total of 44 patients (35.2%) underwent total thyroidectomy and 81 patients (64.8%) received lobectomy or isthmectomy. Furthermore, 29 patients (23.2%) underwent radioactive iodine (RAI) remnant ablation therapy based on the initial tumor size. Disease recurrence was not observed in any NIFTP patient during a median follow-up period of 25.1 months.

Impact of NIFTP on pathologic examination and clinical practice

A difference in the prevalence of NIFTP before and after NIFTP introduction was not observed (Table 3). The number of paraffin blocks for diagnosis of NIFTP did not increase after the introduction of NIFTP (average 5.2 per tumor before April 2016 and average 5.5 per tumor after April 2016).

The rate of lymph node dissection increased from 72.7% before April 2016 to 89.8% after April 2016. The rate of total thyroidectomy decreased from 43.9% before April 2016 to 25.4% after April 2016. The number of patients undergoing postoperative RAI therapy was significantly reduced from 25.8% before April 2016 to 20.3% after April 2016 (Table 3). RAI treatment was performed due to coexisting thyroid cancers in most cases.

Table 3. Demographic and clinicopathologic features of 125 patients with NIFTP alone before and after NIFTP introduction

	Overall	Before NIFTP introduction ^a	After NIFTP introduction	p-value
Prevalence of NIFTP	125/18,819 (0.7)	66/9,656 (0.6)	59/9,163 (0.7)	.739
Sex				.004
Male	32 (25.6)	24 (36.4)	8 (13.6)	
Female	93 (74.4)	42 (63.6)	51 (86.4)	
Age, mean ± SD (range, yr)	46.7 ± 12.5 (23–73)	47.9 ± 13.1 (23–73)	45.3 ± 11.9 (25–73)	.238
Tumor size, median (range, mm)	26.2 (10–80)	24.5 (10–61)	28.0 (10–80)	.195
No. of paraffin blocks, median (range)	5.3 (1–26)	5.2 (2–26)	5.5 (1–18)	.398
Lymph node dissection				.385
Performed	101 (80.8)	48 (72.7)	53 (89.8)	
Not performed	24 (19.2)	18 (27.3)	6 (10.2)	
Lymph node metastases				>.99
Positive	0	0	0	
Negative ^b	125 (100)	66 (100)	59 (100)	
Surgical procedure				.021
Lobectomy or isthmectomy	81 (64.8)	37 (56.1)	44 (74.6)	
Total thyroidectomy	44 (35.2)	29 (43.9)	15 (25.4)	
Lymphatic invasion				1.000
Positive	0	0	0	
Negative	125 (100)	66 (100)	59 (100)	
Vascular invasion				1.000
Positive	0	0	0	
Negative	125 (100)	66 (100)	59 (100)	
Distant metastasis				1.000
Positive	0	0	0	
Negative	125 (100)	66 (100)	59 (100)	
Postoperative radioactive iodine therapy				.365
Performed	29 (23.2)	17 (25.8)	12 (20.3)	
Not performed	96 (76.8)	49 (74.2)	47 (79.7)	
Follow-up, median ± SD (range, mo)	25.1 ± 19.1 (0–60)	36.2 ± 14.5 (0–60)	10.7 ± 6.6 (1–24)	
Recurrence of disease				1.000
Positive	0	0	0	
Negative	125 (100)	66 (100)	59 (100)	

Values are presented as number (%) unless otherwise indicated.

NIFTP, non-invasive follicular thyroid neoplasm with papillary-like nuclear features; SD, standard deviation.

^aBefore April, 2016; ^bIncludes pN0 and pNx stages.

BRAF and RAS mutations in NIFTPs

Twenty-seven patients diagnosed with NIFTP at the Gangnam Severance Hospital after April 2016 were randomly selected for gene analysis; *BRAF*^{V600E} mutation was not observed. As shown in Table 4, the overall frequency of three *RAS* gene mutations was 55.6% (15/27). The mutation rates of *NRAS*, *HRAS*, and *KRAS* were 22.2%, 22.2%, and 11.1%, respectively.

DISCUSSION

The overall prevalence of NIFTP was 1.3% (range, 0.4% to 2.6%) of all PTCs in the present study, which included the largest cohort size researched to date among the Korean population (Table 1). According to the recent study by Nikiforov et al.,⁸ any masses < 1.0 cm were not included in the diagnosis of NIFTP. Moreover, in another recent NIFTP study, data on the sub-centimeter NIFTP were limited.²² Thus, the expected lower boundary for the prevalence of NIFTP was 0.8% when tumors ≥ 1 cm in size were included in the diagnosis of NIFTP.

Table 4. Molecular profiles of noninvasive follicular thyroid neoplasm with papillary-like nuclear features (n=27)

Mutation	No. (%)
<i>BRAF</i> ^{V600E}	
Present	0
Absent	27 (100)
All <i>RAS</i> mutation	
Present	15 (55.6)
<i>NRAS</i>	
c.181C>A (p.Gln61Lys)	3 (50.0)
c.182A>G (p.Gln61Arg)	3 (50.0)
<i>HRAS</i>	
c.182A>G (p.Gln61Arg)	6 (100)
<i>KRAS</i> codon 61 mutation ^a	
	3 (11.1)

^a*KRAS* mutation was analyzed by PNAclamp *KRAS* mutation detection kit. The assay cannot identify specific mutation types.

These results are consistent with the findings from a previous study in which the mean prevalence of NIFTP was 1.5% (range, 0% to 4.7%) in nine institutions from six Asian countries, including Korea.²³ The prevalence of NIFTP is constantly lower in Asian studies than in Western population-based studies.^{22,24-27}

NIFTPs frequently have *RAS* mutations but no *BRAF*^{V600E} mutation.¹¹⁻¹⁴ However, the *BRAF*^{V600E} mutation was found in some NIFTP cases in several studies immediately performed after the initial publication of NIFTP.^{17,18,28,29} Table 5 summarizes the results of *BRAF* mutation in NIFTP reported in previous studies from six Korean institutions.^{17,18,28-31} When the strict criterion of “0% papillae” was applied in the present study, no *BRAF* mutation was found in NIFTPs. In the present case series, a case of *BRAF*^{V600E}-positive tumor originally diagnosed as non-invasive EFVPTC was found. The pathology slides were re-examined after cutting deeper sections and a true papillary structure was found in a focal area. Therefore, the case was reclassified as encapsulated classic PTC with predominant follicular growth pattern. This finding reconfirms the strict diagnostic criteria for NIFTP are helpful for excluding true PTC. Because the diagnostic criteria for NIFTP have been updated, NIFTP should no longer include any follicular patterned tumors with well-formed papillae or high-risk gene mutations such as *BRAF*^{V600E}, *TERT* promoter, or *TP53*.²⁰

The present study had several technical limitations. First, due to the retrospective multicenter-based nature of this study, inter-observer variability in the diagnosis of NIFTP based on histology was not considered. Second, since only the cases diagnosed with PTC were included, the possibility that NIFTP was diagnosed as benign, such as nodular hyperplasia or follicular adenoma, may result in differences in actual prevalence. However, the prevalence of NIFTP did not change significantly even after the introduction of NIFTP. Third, although the overall study cohort size was relatively large, genetic analysis of *BRAF* and *RAS* mutations

Table 5. Characteristics of NIFTP in Korean population reported in literature

Study	Period	Diagnostic criteria	PTC	NIFTP	No. (%)			
					<i>BRAF</i> ^{V600E} mutation	<i>RAS</i> mutation	Lymph node metastasis	Distant metastasis
Cho et al. (2017) ¹⁷	2008–2014	<1% papillae	6,269	105	10 (10.0)	-	3 (2.9)	1 (1.0)
		0% papillae	6,269	95	0	48/89 (53.9)	2 (2.1)	0
Kim et al. (2017) ²⁸	2009–2014	<1% papillae	6,548	43	3 (7.0)	-	1 (2.3)	0
Lee et al. (2017) ¹⁸	2010–2014	<1% papillae	769	21	5 (23.8)	12 (57.1)	1 (4.7)	0
Kim et al. (2018) ³⁰	2011–2012	<1% papillae	1,411	2	0	-	0	0
Kim et al. (2018) ³¹	2013–2016	0% papillae	-	32	0	15 (46.9)	0	0
Kim et al. (2018) ²⁹	2014–2016	<1% papillae	2,853	73	9 (12.3)	36 (49.3)	9 (12.3)	0

NIFTP, noninvasive follicular thyroid neoplasm with papillary-like nuclear features; PTC, papillary thyroid carcinoma.

were performed in only a limited number of NIFTP cases. Nevertheless, the results were consistent with previous study results showing NIFTP has no *BRAF*^{V600E} mutation and frequent *RAS* mutations.^{8,15,20}

The results from this study has shown the low prevalence of NIFTP among PTCs in Korea using the largest number of cases to date. Adverse outcomes were not experienced by any patient with NIFTP during the follow-up period. The introduction of NIFTP may have a small overall impact in Korean practice.

ORCID

Ja Yeong Seo: <https://orcid.org/0000-0003-4859-3864>
 Ji Hyun Park: <https://orcid.org/0000-0002-3002-6856>
 Ju Yeon Pyo: <https://orcid.org/0000-0002-9198-5065>
 Yoon Jin Cha: <https://orcid.org/0000-0002-5967-4064>
 Chan Kwon Jung: <https://orcid.org/0000-0001-6843-3708>
 Dong Eun Song: <https://orcid.org/0000-0002-9583-9794>
 Jeong Ja Kwak: <https://orcid.org/0000-0003-3477-3442>
 So Yeon Park: <https://orcid.org/0000-0002-0299-7268>
 Hee Young Na: <https://orcid.org/0000-0002-2464-0665>
 Jang-Hee Kim: <https://orcid.org/0000-0001-5825-1361>
 Jae Yeon Seok: <https://orcid.org/0000-0002-9567-6796>
 Hee Seung Kim: <https://orcid.org/0000-0002-5421-1108>
 Soon Won Hong: <https://orcid.org/0000-0002-0324-2414>

Author Contributions

Conceptualization: SWH, CKJ.
 Data curation: JYS, JHP, JYP, YJC, CKJ.
 Formal analysis: JYS, JHP, JYP.
 Funding acquisition: SWH.
 Investigation: JYS, JHP, JYP, YJC, CKJ, DES, JJK, SYP, HYN, JHK, JYS, HSK, SWH.
 Methodology: JYS, JYP, YJC, CKJ, SWH.
 Project administration: CKJ, SWH.
 Resources: JYS, JYP, YJC, CKJ, DES, JJK, SYP, HYN, JHK, JYS, HSK, SWH.
 Supervision: CKJ, SWH.
 Validation: JYS, JYP, YJC, CKJ, SWH.
 Visualization: JYS.
 Writing—original draft: JYS, CKJ, SWH.
 Writing—review & editing: JYS, CKJ, SWH.

Conflicts of Interest

CKJ and SYP, editors-in-chief of the Journal of Pathology and Translational Medicine and SWH, an editorial board member of

the Journal of Pathology and Translational Medicine, were not involved in the editorial evaluation or decision to publish this article. All remaining authors have declared no conflicts of interest.

Funding

This research was supported and funded by the Korean Society of Pathologists (grant number: 2017-05-001).

REFERENCES

- Lang BH, Lo CY, Chan WF, Lam AK, Wan KY. Classical and follicular variant of papillary thyroid carcinoma: a comparative study on clinicopathologic features and long-term outcome. *World J Surg* 2006; 30: 752-8.
- Baloch ZW, Shafique K, Flannagan M, Livolsi VA. Encapsulated classic and follicular variants of papillary thyroid carcinoma: comparative clinicopathologic study. *Endocr Pract* 2010; 16: 952-9.
- Zidan J, Karen D, Stein M, Rosenblatt E, Basher W, Kuten A. Pure versus follicular variant of papillary thyroid carcinoma: clinical features, prognostic factors, treatment, and survival. *Cancer* 2003; 97: 1181-5.
- Yu XM, Schneider DF, Levenson G, Chen H, Sippel RS. Follicular variant of papillary thyroid carcinoma is a unique clinical entity: a population-based study of 10,740 cases. *Thyroid* 2013; 23: 1263-8.
- Liu J, Singh B, Tallini G, et al. Follicular variant of papillary thyroid carcinoma: a clinicopathologic study of a problematic entity. *Cancer* 2006; 107: 1255-64.
- Jung CK, Little MP, Lubin JH, et al. The increase in thyroid cancer incidence during the last four decades is accompanied by a high frequency of *BRAF* mutations and a sharp increase in *RAS* mutations. *J Clin Endocrinol Metab* 2014; 99: E276-85.
- Hirokawa M, Carney JA, Goellner JR, et al. Observer variation of encapsulated follicular lesions of the thyroid gland. *Am J Surg Pathol* 2002; 26: 1508-14.
- Nikiforov YE, Seethala RR, Tallini G, et al. Nomenclature revision for encapsulated follicular variant of papillary thyroid carcinoma: a paradigm shift to reduce overtreatment of indolent tumors. *JAMA Oncol* 2016; 2: 1023-9.
- Baloch ZW, Seethala RR, Faquin WC, et al. Noninvasive follicular thyroid neoplasm with papillary-like nuclear features (NIFTP): a changing paradigm in thyroid surgical pathology and implications for thyroid cytopathology. *Cancer Cytopathol* 2016; 124: 616-20.
- Nikiforov YE, Nikiforova MN. Molecular genetics and diagnosis of thyroid cancer. *Nat Rev Endocrinol* 2011; 7: 569-80.
- Zhu Z, Gandhi M, Nikiforova MN, Fischer AH, Nikiforov YE. Molecular profile and clinical-pathologic features of the follicular variant

- of papillary thyroid carcinoma: an unusually high prevalence of *RAS* mutations. *Am J Clin Pathol* 2003; 120: 71-7.
12. Adeniran AJ, Zhu Z, Gandhi M, et al. Correlation between genetic alterations and microscopic features, clinical manifestations, and prognostic characteristics of thyroid papillary carcinomas. *Am J Surg Pathol* 2006; 30: 216-22.
 13. Zhao L, Dias-Santagata D, Sadow PM, Faquin WC. Cytological, molecular, and clinical features of noninvasive follicular thyroid neoplasm with papillary-like nuclear features versus invasive forms of follicular variant of papillary thyroid carcinoma. *Cancer Cytopathol* 2017; 125: 323-31.
 14. McFadden DG, Dias-Santagata D, Sadow PM, et al. Identification of oncogenic mutations and gene fusions in the follicular variant of papillary thyroid carcinoma. *J Clin Endocrinol Metab* 2014; 99: E2457-62.
 15. Howitt BE, Paulson VA, Barletta JA. Absence of *BRAF* V600E in non-infiltrative, non-invasive follicular variant of papillary thyroid carcinoma. *Histopathology* 2015; 67: 579-82.
 16. Song RY, Kang KH, Kim HS, Park SJ. Significance of follicular variant of papillary thyroid carcinoma: study from a thyroid cancer center. *Int J Thyroidol* 2017; 10: S162.
 17. Cho U, Mete O, Kim MH, Bae JS, Jung CK. Molecular correlates and rate of lymph node metastasis of non-invasive follicular thyroid neoplasm with papillary-like nuclear features and invasive follicular variant papillary thyroid carcinoma: the impact of rigid criteria to distinguish non-invasive follicular thyroid neoplasm with papillary-like nuclear features. *Mod Pathol* 2017; 30: 810-25.
 18. Lee SE, Hwang TS, Choi YL, et al. Molecular profiling of papillary thyroid carcinoma in Korea with a high prevalence of *BRAF*^{V600E} mutation. *Thyroid* 2017; 27: 802-10.
 19. Nikiforov YE, Ghossein RA, Kakudo K. Non-invasive follicular thyroid neoplasm with papillary-like nuclear features. In: Lloyd RV, Osamura RY, Klöppel G, Rosai J, eds. *WHO classification of tumours of endocrine organs*. 4th ed. Lyon: IARC Press, 2017; 78-80.
 20. Nikiforov YE, Baloch ZW, Hodak SP, et al. Change in diagnostic criteria for noninvasive follicular thyroid neoplasm with papillary-like nuclear features. *JAMA Oncol* 2018; 4: 1125-6.
 21. Kang SH, Pyo JY, Yang SW, Hong SW. Detection of *BRAF* V600E mutation with thyroid tissue using pyrosequencing: comparison with PNA-clamping and real-time PCR. *Am J Clin Pathol* 2013; 139: 759-64.
 22. Bychkov A, Jung CK, Liu Z, Kakudo K. Noninvasive follicular thyroid neoplasm with papillary-like nuclear features in Asian practice: perspectives for surgical pathology and cytopathology. *Endocr Pathol* 2018; 29: 276-88.
 23. Bychkov A, Hirokawa M, Jung CK, et al. Low rate of noninvasive follicular thyroid neoplasm with papillary-like nuclear features in Asian practice. *Thyroid* 2017; 27: 983-4.
 24. Satoh S, Yamashita H, Kakudo K. Thyroid cytology: the Japanese system and experience at Yamashita Thyroid Hospital. *J Pathol Transl Med* 2017; 51: 548-54.
 25. Liu Z, Song Y, Han B, Zhang X, Su P, Cui X. Non-invasive follicular thyroid neoplasm with papillary-like nuclear features and the practice in Qilu Hospital of Shandong University, China. *J Basic Clin Med* 2017; 6: 22-5.
 26. Paulson VA, Shivdasani P, Angell TE, et al. Noninvasive follicular thyroid neoplasm with papillary-like nuclear features accounts for more than half of "carcinomas" harboring *RAS* mutations. *Thyroid* 2017; 27: 506-11.
 27. Jung CK, Kim C. Effect of lowering the diagnostic threshold for encapsulated follicular variant of papillary thyroid carcinoma on the prevalence of non-invasive follicular thyroid neoplasm with papillary-like nuclear features: a single-institution experience in Korea. *J Basic Clin Med* 2017; 6: 26-8.
 28. Kim MJ, Won JK, Jung KC, et al. Clinical characteristics of subtypes of follicular variant papillary thyroid carcinoma. *Thyroid* 2018; 28: 311-8.
 29. Kim TH, Lee M, Kwon AY, et al. Molecular genotyping of the non-invasive encapsulated follicular variant of papillary thyroid carcinoma. *Histopathology* 2018; 72: 648-61.
 30. Kim H, Kim BH, Kim YK, et al. Prevalence of *BRAF*^{V600E} mutation in follicular variant of papillary thyroid carcinoma and non-invasive follicular tumor with papillary-like nuclear features (NIFTP) in a *BRAF*^{V600E} prevalent area. *J Korean Med Sci* 2018; 33: e75.
 31. Kim M, Jeon MJ, Oh HS, et al. *BRAF* and *RAS* mutational status in noninvasive follicular thyroid neoplasm with papillary-like nuclear features and invasive subtype of encapsulated follicular variant of papillary thyroid carcinoma in Korea. *Thyroid* 2018; 28: 504-10.

Clinical Utility of a Fully Automated Microsatellite Instability Test with Minimal Hands-on Time

Miseon Lee¹, Sung-Min Chun^{1,2}, Chang Ohk Sung^{1,2}, Sun Y. Kim³, Tae W. Kim³, Se Jin Jang^{1,2}, Jihun Kim^{1,2}

¹Department of Pathology, ²Asan Center for Cancer Genome Discovery, ³Department of Oncology, Asan Medical Center, University of Ulsan College of Medicine, Seoul, Korea

Background: Microsatellite instability (MSI) analysis is becoming increasingly important in many types of tumor including colorectal cancer (CRC). The commonly used MSI tests are either time-consuming or labor-intensive. A fully automated MSI test, the Idylla MSI assay, has recently been introduced. However, its diagnostic performance has not been extensively validated in clinical CRC samples. **Methods:** We evaluated 133 samples whose MSI status had been rigorously validated by standard polymerase chain reaction (PCR), clinical next-generation sequencing (NGS) cancer panel test, or both. We evaluated the diagnostic performance of the Idylla MSI assay in terms of sensitivity, specificity, and positive and negative predictive values, as well as various sample requirements, such as minimum tumor purity and the quality of paraffin blocks. **Results:** Compared with the gold standard results confirmed through both PCR MSI test and NGS, the Idylla MSI assay showed 99.05% accuracy (104/105), 100% sensitivity (11/11), 98.94% specificity (93/94), 91.67% positive predictive value (11/12), and 100% negative predictive value (93/93). In addition, the Idylla MSI assay did not require macro-dissection in most samples and reliably detected MSI-high in samples with approximately 10% tumor purity. The total turnaround time was about 150 minutes and the hands-on time was less than 2 minutes. **Conclusions:** The Idylla MSI assay shows good diagnostic performance that is sufficient for its implementation in the clinic to determine the MSI status of at least the CRC samples. In addition, the fully automated procedure requires only a few slices of formalin-fixed paraffin-embedded tissue and might greatly save time and labor.

Key Words: Microsatellite instability; Polymerase chain reaction; Idylla MSI test; Diagnostic performance; Tumor purity

Received: August 5, 2019 **Revised:** September 12, 2019 **Accepted:** September 25, 2019

Corresponding Author: Jihun Kim, MD, Department of Pathology, Asan Medical Center, University of Ulsan College of Medicine, 88 Olympic-ro 43-gil, Songpa-gu, Seoul 05505, Korea

Tel: +82-2-3010-4556, Fax: +82-2-472-7898, E-mail: jihunkim@amc.seoul.kr

Microsatellites, also known as short tandem repeats, are repetitive sequences usually composed of one to six base pairs, repeating from 5 to 50 times and accounting for about 3% of the whole human genome. Due to this repeated structure, DNA sequence mismatches are likely to occur during DNA replication. Mismatch repair (MMR) is a DNA repair system that can correct the errors. Failure to correct these errors during DNA replication results in a variation in the length of the repeat region, which is called microsatellite instability (MSI).¹ MSI has been identified in about 15%–20% of colorectal cancer (CRC) which may be sporadic (12%–14%) or Lynch syndrome-associated (1%–3%).² In sporadic colorectal cases, the tumors are mainly caused by epigenetic silencing of the *MLH1* gene³ promoter by acquired hypermethylation, which is in association with a high CpG island methylation phenotype.⁴ It accounts for approximately 70%–90% of CRC with MSI.^{1,5} In Lynch syndrome, the tumors with

MSI are frequently caused by autosomal dominant germline mutations in the MMR genes.¹

Currently, it is becoming increasingly important to determine the MSI status in patients with CRC because MSI-high (MSI-H) CRC is often associated with Lynch syndrome and MMR deficient CRCs can clinically benefit from immune checkpoint inhibitors.⁶ The MSI status can be detected by immunohistochemistry (IHC) for MMR proteins or polymerase chain reaction (PCR)-based MSI tests, which are currently considered the gold standard method. However, this method requires normal tissues, and it is time-consuming and labor-intensive. Recently, next-generation sequencing (NGS) has been reported to successfully detect the MSI status.^{7,8} This can be done by either direct sequencing of the microsatellite loci or analysis of the total mutation burden or proportion of insertion/deletion mutations. However, NGS experiments are expensive and only available in

specialized laboratories.

In this study, we tested Idylla MSI assay in terms of its diagnostic performance, the minimum requirements for tumor purity, and turnaround time through the examination of the surgically resected samples or colonoscopic biopsy CRC samples, the MSI status of which were rigorously confirmed through either standard PCR fragment analysis or clinical NGS test.

MATERIALS AND METHODS

Sample selection

Formalin-fixed paraffin-embedded (FFPE) tumor tissues from 115 pathologically confirmed CRC patients who underwent surgical resection ($n = 109$) or colonoscopic biopsy ($n = 3$) at Asan Medical Center from 2010 to 2016 were used. All samples had MSI results that were confirmed by standard PCR analysis, NGS test, or both. We used five markers (BAT25, BAT26, D2S123, D5S346, and D17S250) recommended by the National Cancer Institute (NCI) for the standard PCR MSI analysis. Diagnosis of the MSI status through NGS was carried out as described previously.⁷ Hematoxylin and eosin-stained slides from FFPE were reviewed by two pathologists (M.L and J.K.) for tumor distribution and cellularity. The areas of the slide presenting the highest tumor cellularity were marked, and tumor cellularity was evaluated by rough estimation of the proportion of tumor cell nuclei relative to non-neoplastic cell nuclei. In order to determine the minimum required tumor purity, the tumor area was marked in various ways so that various proportions of tumor nuclei could be included in the analytes in two cases.

Tissue handling was done according to the instructions provided by the manufacturers (Fig. 1). Briefly, macro-dissection was done if the tumor cellularity was less than 20%, and whole cut sections were used if it was more than 20% (Fig. 1). We obtained 5- μ m FFPE tissue sections: 1 section when the tumor area is equal

to or greater than 50 mm² and 2–5 sections when the tumor area is less than 50 mm² depending on the tumor surface area (Fig. 1). In most cases, macro-dissection was not required. The scraped FFPE tissue fragments were directly put into the cartridge.

The Idylla MSI assay

The Idylla MSI assay (Biocartis NV, Mechelen, Belgium) was performed as described previously.⁹ Briefly, the scraped FFPE tissue fragments were loaded directly onto a designated cartridge and the device was run for approximately 150 minutes. Detection of these specific targets was performed using fluorescently labeled molecular beacons after PCR amplification. These beacons melt differentially from the wild type or mutated amplicons with increasing temperature. The MSI test-specific software, namely, Test Type Package, automatically checked the validity of the measured fluorescence profiles: the presence of specific PCR amplicons resulted in biomarker-specific fluorescence profiles. Next, a powerful pattern-recognition algorithm trained on several thousands of profiles calculated a probability score (MSI score) for any given valid biomarker-specific profile. This MSI score per biomarker expressed the probability of a pattern being wild type or mutant. As such, MSI biomarkers were scored individually and reported as “No mutation detected,” “Mutation detected” or “Invalid.” The Idylla MSI assay uses seven biomarkers, namely *ACVR2A*, *BTBD7*, *DID01*, *MRE11*, *RYR3*, *SEC31A*, and *SULF2*. Those biomarkers were chosen based on their short length that is advantageous for probe-based PCR, stability over different cancer types and ethnicities, minimized false positives and negatives, and diagnostic performance optimized for the test platform. A test result was considered valid if ≥ 5 out of 7 MSI biomarkers show valid amplified signals. The tumors were classified into two categories. High frequency of MSI (MSI-H) was defined if two or more of the seven markers were positive, and microsatellite stable (MSS) if less than two of seven markers

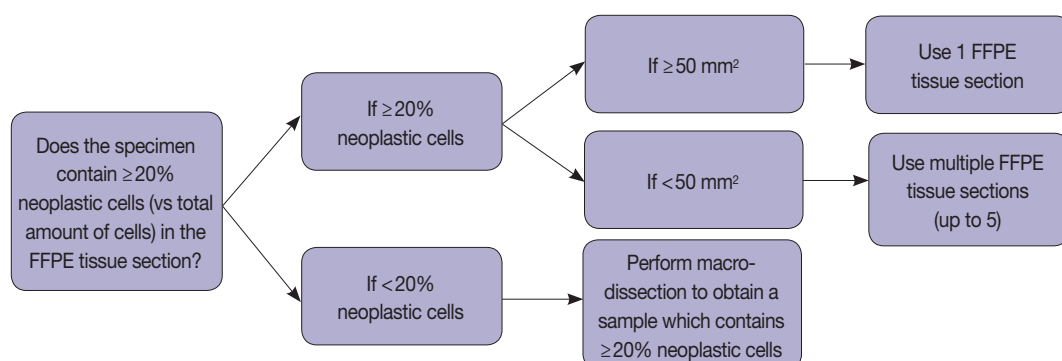


Fig. 1. Sample processing protocol depending on the tumor purity and tissue surface area. FFPE, formalin-fixed paraffin-embedded.

were positive.

Determination of limit of detection

We randomly selected four cases that were confirmed as MSI-H by standard PCR analysis and determined the limit of detection through stepwise tumor marking that results in varying degrees of tumor cellularity. As shown in Supplementary Fig. S1, we designated the tumor areas with varying degrees of non-neoplastic cells so that the approximate tumor cellularity is 80%, 60%, 40%, 20%, or 10%, respectively. In three cases, samples with approximately 5% and/or 2% tumor purity were also analyzed (Supplementary Fig. S1).

Statistical analysis

We compared the results of Idylla MSI assay with the combined gold standard MSI results for the 105 cases. The sensitivity, specificity, positive predictive value, negative predictive value, and accuracy of Idylla MSI assay were calculated for each test in comparison with the combined gold standard.

Ethics statement

Written informed consent was obtained from all patients and this study was approved by the Institutional Review Board (protocol number: 2018-1518).

RESULTS

Idylla MSI assay

All 115 cases showed “valid” results. Thirteen out of 115 cases (11.3%) were classified as MSI-H (Table 1). Mutations

were detected in at least four of seven marker genes in these 13 MSI-H cases (Table 1). Among the MSS samples, most cases did not reveal any mutation in the seven markers; however, a particular case (case No. 71) showed *MRE11* mutation on Idylla MSI assay but the assay categorized it as MSS because the probability score was below the threshold.

Validation of the MSI status through standard PCR analysis, NGS, or both

Standard PCR analysis for MSI using the five markers recommended by NCI were carried out in the 108 cases except for the seven cases that were not available for tissue analysis. Of the 108 cases, 89 cases were MSS, five cases were low frequency of MSI (MSI-L), and 14 cases were MSI-H. The NGS test for MSI was performed on all 115 cases, and three of them failed during the library preparation step of NGS analysis. Of the 112 cases with valid NGS results, 101 cases were MSS while 11 cases were MSI-H. The results of standard PCR analysis and the results of NGS test results for MSI were completely concordant in all 105 cases with both test results, except for the cases without available tissue material for standard PCR analysis and those that failed the NGS test (Table 2). We combined the results of standard PCR analysis and NGS test and thereafter used the combined results as a gold standard. For standard PCR results, MSI-L results were considered MSS.

Comparison between Idylla MSI assay and the gold standard MSI results

We compared the results of Idylla MSI assay with the combined gold standard MSI results for the 105 cases with both results of

Table 1. A detailed list of the mutated marker genes in the MSI-H cases that were determined by the Idylla MSI assay

Case No.	Biomarker							Mutant marker/Total makers
	<i>ACVR2A</i>	<i>BTBD7</i>	<i>DIDO1</i>	<i>MRE11</i>	<i>RYR3</i>	<i>SEC31A</i>	<i>SULF2</i>	
4	Mut	Mut	Mut	Mut	Mut	No	Mut	6/7
28	Mut	Mut	No	Mut	No	No	Mut	4/7
52	Mut	Mut	Mut	No	Mut	Mut	Mut	6/7
54	Mut	Mut	Mut	No	Mut	Mut	Mut	6/7
57	Mut	Mut	Mut	Mut	No	Mut	Mut	6/7
65	Mut	Mut	Mut	Mut	Mut	Mut	No	6/7
104	No	No	Mut	Mut	Mut	No	Mut	4/7
113	Mut	Mut	Mut	Mut	Mut	Mut	Mut	7/7
117	Mut	Mut	Mut	Mut	Mut	Mut	Mut	7/7
118	Mut	Mut	Mut	Mut	Mut	Mut	Mut	7/7
120	Mut	Mut	Mut	Mut	No	Mut	No	5/7
124	Mut	Mut	Mut	No	No	Mut	Mut	5/7
132	Mut	No	Mut	Mut	Mut	Mut	Mut	6/7

MSI-H, microsatellite instability-high; MSI, microsatellite instability; Mut, mutation detected; No, no mutation detected.

standard PCR analysis and NGS test. Idylla MSI assay achieved 99.05% accuracy (104 of 105), 100% sensitivity (11 of 11), 98.94% specificity (93 of 94), 91.67% positive predictive value (11 of 12), and 100% negative predictive value (93/93) for the detection for MSI (Table 3). Only one case (case No. 28) showed discordant result between the Idylla MSI assay and the gold standard result. MSS result was confirmed by both standard PCR fragment analysis (Fig. 2A) and NGS (Fig. 2C), but the Idylla MSI assay called it MSI-H.

Table 2. Correlation between standard PCR analysis and NGS for MSI

Colorectal carcinoma (n=105)	Standard PCR analysis			Total
	MSS	MSI-L	MSI-H	
NGS				
Stable	89	5	0	94
Unstable	0	0	11	11
Total	89	5	11	105

PCR, polymerase chain reaction; NGS, next-generation sequencing; MSI, microsatellite instability; MSS, microsatellite stable; MSI-L, MSI-low; MSI-H, MSI-high.

Further evaluation of the cases that failed the NGS test

To investigate whether the Idylla MSI assay can accept a wider range of samples than NGS, we selected three cases that were confirmed as MSI-H in standard PCR test but failed in our NGS test. Among them, two cases showed instability on only two microsatellite markers (case Nos. 131 and 133) (Fig. 2D–H), while the other case (case No. 132) showed instability in all five markers (Table 4). Among them, only one case (case No. 132) showed concordant results and the other two showed discordant

Table 3. Comparison between the Idylla MSI assay results and the combined gold standard MSI results

Colorectal carcinoma (n=105)	Idylla MSI assay		Total
	MSS	MSI-H	
Combined gold standard MSI			
MSS	93 (98.9)	1 (1.1)	94
MSI-H	0	11 (100)	11
Total	93	12	105

Values are presented as number (%).

MSI, microsatellite instability; MSS, microsatellite stable; MSI-H, MSI-high.

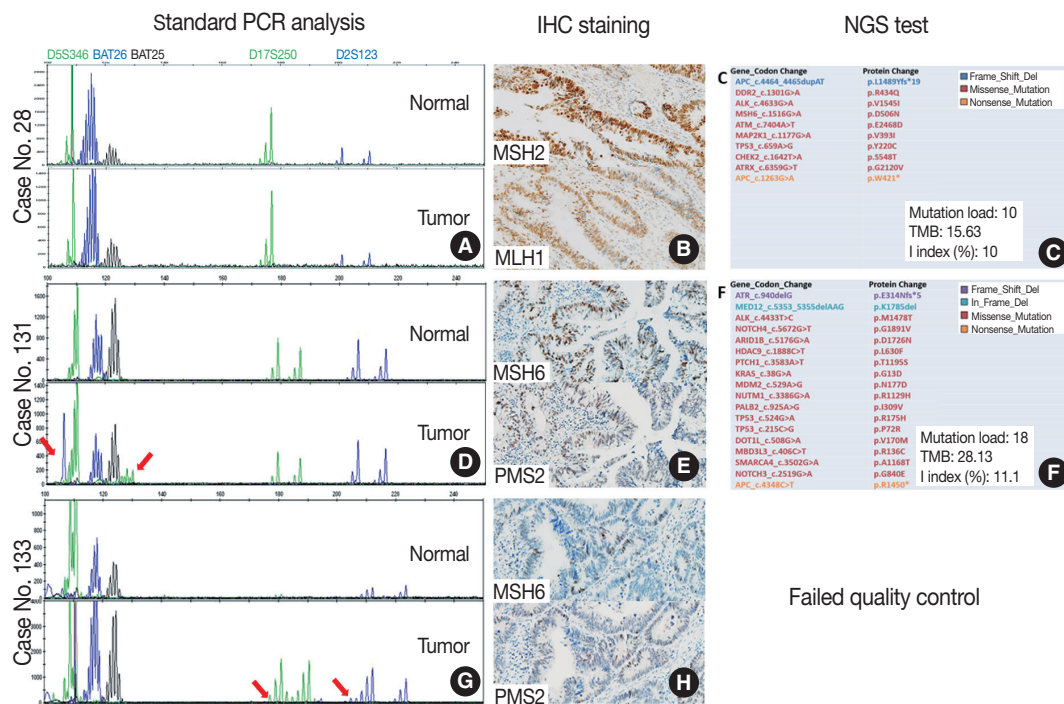


Fig. 2. Details of three cases with discrepant results between the Idylla microsatellite instability (MSI) assay and the standard polymerase chain reaction (PCR) test. (A–C) Case No. 28, MSI-high (MSI-H) according to the Idylla MSI assay. Standard PCR MSI test is consistent with microsatellite stable (MSS) (A). MSH2 and MLH1 expression is shown in immunochemical staining (B), and next-generation sequencing (NGS) results show MSS pattern (C). (D–F) Case No. 131, MSS (0/7) according to the Idylla MSI assay. Two markers show instability in standard PCR MSI test (arrows, D), and MSH6 and PMS2 protein expressions are shown (E). Repeated NGS shows MSS pattern (F). (G, H) Case No. 133, MSS (0/7) according to the Idylla MSI assay. Two markers show instability in standard PCR MSI test (arrows, G), and MSH6 and PMS2 expressions are shown (H). Repeated NGS analysis was failed. Mutation load, the number of total somatic mutations detected by our NGS panel; TMB, tumor mutation burden, the inferred number of somatic mutations per megabase; I index, the number of insertion or deletion mutations divided by the number of all mutations; IHC, immunohistochemistry.

Table 4. Analysis of the cases that failed in the NGS test

Case No.	Standard PCR analysis No. 1	Repeated NGS analysis	Immunohistochemical staining				Idylla MSI assay
			MSH2	MSH6	MLH1	PMS2	
131	MSI-H, 2/5	MSS	Positive	Positive	Positive	Positive	MSS, 0/7
132	MSI-H, 5/5	Not done	Negative	Negative	Positive	Positive	MSI-H, 6/7
133	MSI-H, 2/5	Failed	Positive	Positive	Positive	Positive	MSS, 0/7

NGS, next-generation sequencing; PCR, polymerase chain reaction; MSI, microsatellite instability; MSI-H, microsatellite instability-high; MSS, microsatellite stable.

Table 5. MSI detection ability of the Idylla MSI assay according to variable tumor cellularity

Case No.	Tumor cellularity (%)	Marker gene							Mutant marker/ Total makers
		<i>ACVR2A</i>	<i>BTBD7</i>	<i>DIDO1</i>	<i>MRE11</i>	<i>RYR3</i>	<i>SEC31A</i>	<i>SULF2</i>	
118	80	Mut	Mut	Mut	Mut	Mut	Mut	Mut	7/7
	60	Mut	Mut	Mut	Mut	No	Mut	Mut	6/7
	40	Mut	Mut	Mut	Mut	No	Mut	Mut	6/7
	20	Mut	Mut	Mut	Mut	No	Mut	Mut	6/7
	10	Mut	Mut	Mut	Mut	No	Mut	Mut	6/7
104	80	No	No	Mut	Mut	No	No	Mut	3/7
	60	No	No	Mut	Mut	Mut	No	Mut	4/7
	40	No	No	Mut	Mut	No	No	Mut	3/7
	20	No	No	Mut	Mut	No	No	Mut	3/7
	10	No	No	Mut	Mut	No	No	No	2/7
113	5	No	No	Mut	Mut	No	No	Mut	3/7
	2	No	No	Mut	Mut	No	No	No	2/7
	80	Mut	Mut	Mut	Mut	Mut	Mut	Mut	7/7
52	2	Mut	No	Mut	No	Mut	No	Mut	4/7
	80	Mut	Mut	Mut	No	Mut	Mut	Mut	6/7
	2	No	No	No	No	No	No	No	0/7

MSI, microsatellite instability; Mut, mutation detected; No, no mutation detected.

results. Interestingly, the two cases with discordant results were the cases where instability was observed in two markers in the standard PCR analysis. To resolve these discrepancies, additional immunohistochemical staining for MSH2, MSH6, MLH1, and PMS2 were performed and standard PCR analysis and NGS was repeated. Although repeated PCR MSI tests were not helpful due to the high background noise band (data not shown), protein expression of all the MMR proteins was preserved in the two cases (Fig. 2B, E), suggesting that those two cases were likely MSS. Furthermore, the second attempt of NGS was successful in case No. 131 and it showed MSS pattern although the tumor mutation burden was relatively high (28.13/Mb) (Fig. 2F). The second attempt of NGS was not successful in case No. 133. As expected, the MSI-H phenotype of the case with concordant standard PCR and Idylla MSI results was confirmed through the loss of MSH2 and MSH6 expression (Table 4).

Limit of detection analysis of the Idylla MSI assay

To determine the minimum tumor purity that does not affect the assay results, we selected a few MSI-H samples and macro-

dissected each sample in such a way that various levels of tumor purity could be achieved. Case No. 118 was successfully categorized as MSI-H when the tumor purity was lowered down to 10% (Table 5). Likewise, case Nos. 104 and 113 were successfully categorized as MSI-H even in samples with lower tumor purity of 2%. However, in case No. 52, which was diagnosed as MSI-H based on the presence of mutations in six out of seven markers, no single mutation was detected in all seven biomarkers when the tumor cellularity was 2%. In this particular case, there were several foci of lymphoid aggregates which may further dilute the tumor cells (Supplementary Fig. S1E).

DISCUSSION

In this study, the Idylla MSI assay demonstrated excellent diagnostic performance when we tested the fully automated kit with 115 CRC samples with rigorously confirmed MSI results. In addition, the test successfully detected MSI-H status in samples with very low tumor purity (down to 10%), although the tumor purity estimates were inevitably crude. Our findings suggest

that the Idylla MSI assay could be used in the clinic to determine MSI status, at least for CRC samples, and that macro-dissection may not be required in most CRC cases. Since the Idylla MSI assay does not require DNA extraction and reagent loading steps, the hands-on time could be greatly reduced.

The identification of MMR deficiency is important not only for the identification of the risk for Lynch syndrome but also for the appropriate treatment approach and prognosis for sporadic tumors.¹⁰ MMR deficiency can be diagnosed by PCR fragment analysis, NGS, and MMR protein IHC test.⁸ MMR IHC staining is used as a first-line screening method and is used as a good surrogate marker for MSI, but heterogeneity has previously been well described.^{10,11} PCR fragment analysis has been widely used as a standard method and NGS-based MSI detection is now increasing, but both methods are time-consuming and labor-intensive. The Idylla MSI assay offers a fully automated workflow from direct FFPE tissue input to a simple final report (Supplementary Fig. S2) and achieved a short turnaround time (about 150 minutes) and minimal hands-on time (less than 2 minutes). When we simulated actual hands-on time in maximum throughput environment (8 samples/run for the Idylla MSI assay, 32 samples/run for the standard MSI PCR assay, and 24 samples/run for the NGS in Illumina NextSeq platform), the hands-on time per sample was 30 seconds for the Idylla MSI assay, 5 minutes for the standard MSI PCR test, and 120 minutes for the NGS. Thus, the Idylla MSI assay may significantly save time and manpower. The downside of the Idylla MSI assay, however, is that only one sample can be processed in each instrument unit at a time. Thus, to increase sample throughput, multiple instruments are required (up to 8 instruments per one console, according to the manufacturer). Requirements for multiple instruments and usage of one sophisticated cartridge per one sample may make this test to be more expensive than the standard PCR assay.

Although the Idylla MSI assay results were concordant with gold standard results in most cases, there was one false-positive case (case No. 28). The gold standard result was MSS but the Idylla MSI assay categorized it as MSI-H based on the presence of mutations in four genes such as *ACVR2A*, *BTBD7*, *MRE11*, and *SULF2*. Since the MSS result was confirmed by both standard PCR fragment analysis and NGS, it is unlikely that the gold standard result was incorrect. Furthermore, cross-contamination or sample swapping was rigorously excluded through repeated analysis and DNA fingerprinting that is included in our NGS assay. It could be that the particular tumor harbored somatic mutations in the four genes, irrespective of MMR deficiency. Indeed, one MSS tumor (case No. 71) showed *MRE11* muta-

tion on the Idylla MSI assay but the assay categorized it as MSS because the total probability score was below the threshold. Thus, rare false MSI-H results may be possible in a particular MSS tumor harboring mutations in the genes covered by the Idylla MSI assay.

Most molecular techniques involving homogenized samples, in which the tumor cells and non-neoplastic cells are mixed, require tumor marking with subsequent macro-dissection to ensure sufficient tumor purity. Regarding this, the direct use of unstained FFPE tissues cut without macro-dissection could maximize the benefits of the fully automated Idylla MSI assay. In this study, we found that most FFPE samples may not require macro-dissection because the test reliably detected MSI-H in samples with low tumor purity (approximately 10%). However, since the ability to detect MSI-H was not perfectly consistent with the very low tumor purity (approximately 2%), we propose that the minimum required tumor purity would be approximately 10%. In addition, the age of the FFPE tissue material may not cause any significant problem in most cases because the test was successful in FFPE samples aged up to 9 years.

We also tested whether the Idylla MSI assay might accept poor quality samples better than the NGS assay by testing samples that were diagnosed as MSI-H with the standard PCR test but failed in our NGS analysis. All the Idylla MSI assay results were “valid” which means successful amplification of the adequate number of marker genes, suggesting that the Idylla MSI assay may accept some “difficult” samples better than NGS. Furthermore, MMR protein IHC study and repeated NGS analysis suggested that the Idylla MSI assay may sometimes be more accurate than the standard PCR MSI test because the two samples, which were MSS on the Idylla MSI assay but were MSI-H on the standard PCR test, showed unequivocal expression of four MMR proteins and a relatively low number of unstable markers (only two unstable markers out of five markers) in the standard PCR MSI test. In addition, in one of the two samples, MSS could be confirmed through repeated NGS analysis. However, the full validation of the performances of the Idylla MSI assay might be limited because of a relatively small size of the MSI-H sample group in our study.

In summary, the Idylla MSI assay is fast, accurate, and reliable, and thus might be clinically applicable. The fully automated workflow may offer a significant reduction in time and labor although the cost for consumables or cartridge is higher than that of the standard MSI PCR test. In addition, colonoscopic biopsy specimens in the case of initially metastatic disease may be easily processed because this test does not require a matched

normal tissue sample.

Electronic Supplementary Material

Supplementary materials are available at Journal of Pathology and Translational Medicine (<https://jpatholtm.org>).

ORCID

Miseon Lee: <https://orcid.org/0000-0002-6385-7621>

Sung-Min Chun: <https://orcid.org/0000-0002-3357-1382>

Chang Ohk Sung: <https://orcid.org/0000-0002-8567-456X>

Sun Y. Kim: <https://orcid.org/0000-0002-5886-3920>

Tae W. Kim: <https://orcid.org/0000-0001-9522-1997>

Se Jin Jang: <https://orcid.org/0000-0001-8239-4362>

Jihun Kim: <https://orcid.org/0000-0002-8694-4365>

Author Contributions

Conceptualization: JK.

Data curation: SMC, COS, SYK, TWK, SJJ, JK, ML.

Formal analysis: JK, ML.

Funding acquisition: JK.

Investigation: SMC, COS, SYK, TWK, SJJ, JK, ML.

Methodology: JK, ML.

Project administration: JK, ML.

Resources: SMC, COS, SYK, TWK, SJJ, JK, ML.

Supervision: JK, ML.

Validation: JK, ML.

Visualization: JK, ML.

Writing—original draft: JK, ML.

Writing—review & editing: JK, ML.

Conflicts of Interest

The Idylla MSI assay equipment rentals and cartridge supplies were supported by the SeongKohn Traders' Corp.

Funding

No funding to declare.

REFERENCES

1. Ryan E, Sheahan K, Creavin B, Mohan HM, Winter DC. The current value of determining the mismatch repair status of colorectal cancer: a rationale for routine testing. *Crit Rev Oncol Hematol* 2017; 116: 38-57.
2. Shi C, Washington K. Molecular testing in colorectal cancer: diagnosis of Lynch syndrome and personalized cancer medicine. *Am J Clin Pathol* 2012; 137: 847-59.
3. Cunningham JM, Christensen ER, Tester DJ, et al. Hypermethylation of the hMLH1 promoter in colon cancer with microsatellite instability. *Cancer Res* 1998; 58: 3455-60.
4. Battaglin F, Naseem M, Lenz HJ, Salem ME. Microsatellite instability in colorectal cancer: overview of its clinical significance and novel perspectives. *Clin Adv Hematol Oncol* 2018; 16: 735-45.
5. Sinicrope FA, Shi Q, Smyrk TC, et al. Molecular markers identify subtypes of stage III colon cancer associated with patient outcomes. *Gastroenterology* 2015; 148: 88-99.
6. Le DT, Uram JN, Wang H, et al. PD-1 blockade in tumors with mismatch-repair deficiency. *N Engl J Med* 2015; 372: 2509-20.
7. Kim JE, Chun SM, Hong YS, et al. Mutation burden and I index for detection of microsatellite instability in colorectal cancer by targeted next-generation sequencing. *J Mol Diagn* 2019; 21: 241-50.
8. Zhu L, Huang Y, Fang X, et al. A novel and reliable method to detect microsatellite instability in colorectal cancer by next-generation sequencing. *J Mol Diagn* 2018; 20: 225-31.
9. Samaison L, Grall M, Staroz F, Uguen A. Microsatellite instability diagnosis using the fully automated Idylla platform: feasibility study of an in-house rapid molecular testing ancillary to immunohistochemistry in pathology laboratories. *J Clin Pathol* 2019 Jun 23 [Epub]. <https://doi.org/10.1136/jclinpath-2019-205935>.
10. McCarthy AJ, Capo-Chichi JM, Spence T, et al. Heterogenous loss of mismatch repair (MMR) protein expression: a challenge for immunohistochemical interpretation and microsatellite instability (MSI) evaluation. *J Pathol Clin Res* 2019; 5: 115-29.
11. Joost P, Veurink N, Holck S, et al. Heterogenous mismatch-repair status in colorectal cancer. *Diagn Pathol* 2014; 9: 126.

Cytomorphological Features of Hyperchromatic Crowded Groups in Liquid-Based Cervicovaginal Cytology: A Single Institutional Experience

Youngeun Lee, Cheol Lee, In Ae Park, Hyoung Jin An, Haeryoung Kim

Department of Pathology, Seoul National University Hospital, Seoul National University College of Medicine, Seoul, Korea

Background: Hyperchromatic crowded groups (HCGs) are defined as three-dimensional aggregates of crowded cells with hyperchromatic nuclei, and are frequently encountered in cervicovaginal liquid-based cytology (LBC). Here, we aimed to examine the prevalence of HCGs in cervicovaginal LBC and the cytomorphological characteristics of various epithelial cell clusters presenting as HCGs. **Methods:** We first examined the prevalence of HCGs in a “routine cohort” of LBC cytology (n=331), consisting of all cervicovaginal LBCs accessioned over 3 days from outpatient clinics (n=179) and the screening population (n=152). Then we examined a second “high-grade epithelial cell abnormalities (H-ECA cohort)” (n=69) of LBCs diagnosed as high-grade squamous intraepithelial lesion (HSIL), squamous cell carcinoma (SCC), or adenocarcinoma during 1 year. **Results:** HCGs was observed in 34.4% of the routine cohort and were significantly more frequent in the epithelial cell abnormality category compared to the non-neoplastic category (p=.003). The majority of HCGs represented atrophy (70%). Of the 69 histologically confirmed H-ECA cases, all contained HCGs. The majority of cases were HSIL (62%), followed by SCC (16%). Individually scattered neoplastic cells outside the HCGs were significantly more frequent in SCCs compared to glandular neoplasia (p=.002). Despite the obscuring thick nature of the HCGs, examining the edges and the different focal planes of the HCGs and the background were helpful in defining the nature of the HCGs. **Conclusions:** HCGs were frequently observed in cervicovaginal LBC and were mostly non-neoplastic; however, neoplastic HCGs were mostly high-grade lesions. Being aware of the cytomorphological features of different HCGs is important in order to avoid potential false-negative cytology interpretation.

Key Words: Hyperchromatic crowded groups; Cervical neoplasms; Liquid-based cytology

Received: July 11, 2019 **Revised:** August 13, 2019 **Accepted:** August 14, 2019

Corresponding Author: Haeryoung Kim, MD, PhD, Department of Pathology, Seoul National University Hospital, Seoul National University College of Medicine, Basic Science Building 101, 103 Daehak-ro, Jongno-gu, Seoul 03080, Korea
Tel: +82-2-740-8322, Fax: +82-2-765-5600, E-mail: haeryoung.kim@snu.ac.kr

Hyperchromatic crowded groups (HCGs, also known as “microbiopsies”) are defined as three-dimensional aggregates of crowded cells with hyperchromatic nuclei.¹ They are commonly found in liquid-based cytology (LBC) samples—in almost 80% according to one study²—and are easily detected at low-power magnification.

Most of the time, HCGs represent normal or reactive conditions, such as endometrial cells, reactive endocervical cells, basal cells in severe atrophy, squamous metaplasia or tubal metaplasia, or even non-epithelial components such as neutrophil clusters, lymphoid follicles or bacterial colonies.³ However, they may also occasionally represent the other extreme of the benign-malignant spectrum, including high-grade squamous intraepithelial lesions (HSIL), squamous cell carcinomas, or glandular neoplasia. Thus, it is important to bear in mind that HCGs require

careful examination before being passed off as normal/benign. In fact, HCGs have been reported to be the most common reason for false-negative reports in cervicovaginal LBC.⁴

In this study, we aimed to evaluate the prevalence of HCGs in cervicovaginal LBC and examine the cytomorphological characteristics of various epithelial cell clusters presenting as HCGs.

MATERIALS AND METHODS

Subjects

In order to examine the prevalence of HCG in everyday practice, we first reviewed all cervicovaginal LBC slides accessioned at Seoul National University Hospital during 3 days in January 2012 (“routine cohort”), including specimens from the outpatient clinics and from the screening population (health promo-

tion center). All LBC slides were prepared by the BD SurePath system (BD Diagnostics, Burlington, NC, USA).

We collected a second cohort (“high-grade epithelial cell abnormalities [H-ECA] cohort”) of all cervicovaginal LBC cases diagnosed as HSIL, squamous cell carcinoma, adenocarcinoma, or atypical glandular cell (AGC) from January 2012 to December 2012 at Seoul National University Hospital, in order to examine in more detail the cytomorphological characteristics of neoplastic HCGs. Among a total of 1,130 retrieved cases, we included only cases that were confirmed by histological examination (concurrent or subsequent biopsies or operative specimens), and we also excluded all conventional smears. The remaining 69 cases were subjected to detailed cytomorphological review and the patient age information was obtained from the pathology database.

Cytological review

All the cervicovaginal smears were reviewed by two pathologists (H.K. and Y.L.). The cytological details examined included the cytological diagnosis, presence of endocervical/transformation zone (EC/TZ) components, presence and the nature (neoplastic versus non-neoplastic) of HCGs, and the presence of scattered single neoplastic cells in the background. We defined HCGs as dense cellular aggregates of at least 10 cells and excluded HCGs consisting of neutrophil clusters and bacterial colonies.

Statistical analyses

Statistical analyses were performed using SPSS statistics ver. 25.0 (IBM Corp., Armonk, NY, USA). The student t-test, Pearson chi-square test, and Fisher exact test were used. A p-value of less than .05 was considered statistically significant.

Ethics statement

This study was approved by the Institutional Review Board of Seoul National University Hospital (#H-1905-090-1034) and informed consent was waived due to the retrospective nature of the study.

RESULTS

Prevalence of HCGs in routine cervicovaginal LBC

A total of 331 cases were collected in the routine cohort, of which 152 cases (45.9%) were from the screening population and the remaining 179 cases (54.1%) were from outpatient clinics. The cases consisted of eight cases (2.4%) and 323 cases (97.6%) in the ECA and negative for intraepithelial lesion or malignancy (NILM) categories, respectively (Fig. 1). The ECA

cases of the routine cohort consisted of one squamous cell carcinoma, one adenocarcinoma, one AGC, one low-grade squamous intraepithelial lesion (LSIL), and four atypical squamous cells of uncertain significance (ASC-US). The AGC case was subsequently confirmed as endocervical adenocarcinoma by histology. In the routine cohort, HCGs were observed in 114 cases (34.4%). The frequency of HCGs was significantly higher in the ECA category (7/8, 87.5%) compared to the NILM category (107/323, 33.1%; $p = .003$).

The majority of HCGs in the NILM group comprised atrophic parabasal cell clusters ($n = 75$, 70.1%), and the remainder were endocervical or metaplastic cells ($n = 25$, 23.4%) and endometrial cells ($n = 7$, 6.5%). The HCGs in atrophy were characterized by flat monolayer sheets of parabasal cells with nuclear overlapping in individual focal planes. The constituent parabasal cells had dark nuclei and scant cytoplasm, but the nuclei showed regular nuclear contours and were frequently even, smudgy and degenerated (Fig. 2A). Maturation of parabasal cells at the edges of HCGs and the streaming pattern with preserved polarity were helpful clues in classifying the HCGs as atrophic.

Endocervical cells frequently presented as a large HCG fragments, and focusing up and down revealed the regular honeycomb arrangement with distinct cytoplasmic borders (Fig. 2B). Reactive endocervical cells often demonstrated prominent nucleoli, mild nuclear size variation and even occasional mitotic figures (Fig. 2C). However, the presence of a streaming pattern, smooth and round nuclear outlines and mild nuclear hyperchromasia were indicative of reactive cellular changes. Metaplastic HCGs showed dense cytoplasm and spindled cytoplasmic projections.

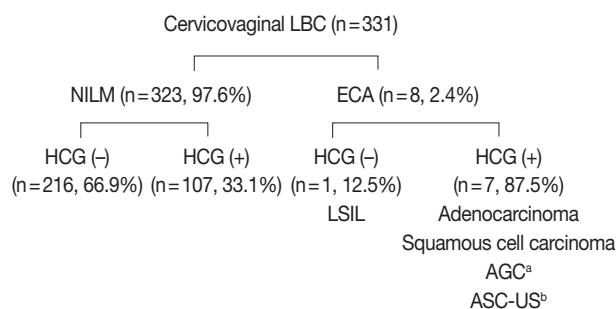


Fig. 1. Summary of the routine cervicovaginal liquid-based cytology (LBC) cases. Hyperchromatic crowded groups (HCGs) were significantly more frequent in the epithelial cell abnormality (ECA) category compared to the negative for intraepithelial lesion or malignancy (NILM) category, and neoplastic HCGs were high-grade lesions. LSIL, low-grade squamous intraepithelial lesion; AGC, atypical glandular cell; ASC-US, atypical squamous cells of uncertain significance. ^aSubsequently diagnosed as adenocarcinoma; ^bOnly non-neoplastic HCGs were observed.

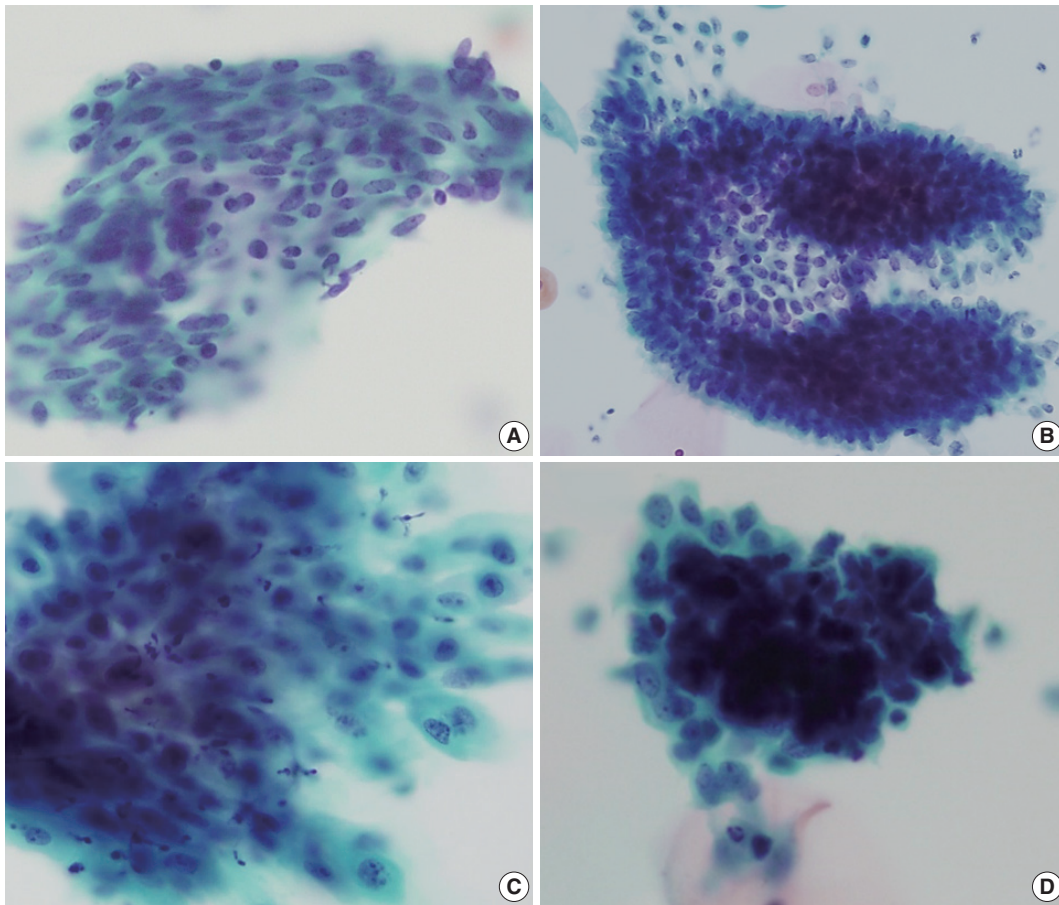


Fig. 2. Cytological features of non-neoplastic hyperchromatic crowded group (HCG). (A) Atrophic HCGs consisted of bland-looking parabasal cells with streaming patterns. (B) Regular honeycomb arrangement of endocervical cells. (C) Reactive endocervical cells demonstrating mild nuclear size variation and nucleoli but smooth nuclear membranes. (D) Biphasic pattern observed in endometrial cell clusters.

Endometrial cells appeared as very dense cellular clusters, and although the centers of HCGs were too dark to appreciate the cytomorphology even by examining different focal planes, the biphasic gland-stroma pattern was a helpful feature for identifying the endometrial cells (Fig. 2D). The periphery of the HCGs were lined by glandular cells with high nuclear:cytoplasmic ratio and small, hyperchromatic nuclei.

In the ECA group, all HCGs in the squamous cell carcinoma and glandular lesions were neoplastic HCGs. However, all cases diagnosed as ASC-US ($n = 4$) demonstrated only non-neoplastic HCGs, and there were no HCGs in the LSIL case. All neoplastic HCGs were seen in the outpatient clinic setting, and were not seen in the general screening population.

As expected, the mean age of subjects with atrophic HCGs (62.8 ± 7.9 years) were significantly higher compared to those with endometrial HCGs (39.5 ± 4.8 years) in the NILM group ($p < .001$). Interestingly, EC/TZ components were present in all 114 HCG-positive cases, while 34 of 217 HCG-negative cases

(15.7%) did not contain EC/TZ components ($p < .001$). On comparing the screening and outpatient populations, no statistically significant differences were seen in the age distribution or the frequency of HCGs.

Prevalence and characteristics of neoplastic HCGs

All 69 cases of the H-ECA cohort contained HCGs. The H-ECA cohort consisted of 63 uterine lesions (91.3%) (HSIL [$n = 43$], squamous cell carcinoma [$n = 11$], endometrial cancer [$n = 7$], endocervical cancer [$n = 2$]) and six extrauterine (8.7%) (ovarian [$n = 4$], colorectal [$n = 2$]) lesions (Fig. 3). The endometrial lesions comprised four endometrioid carcinomas, one clear cell carcinoma, one serous carcinoma, and one carcinosarcoma. All extrauterine lesions were adenocarcinomas.

All HCGs (100%) in the glandular neoplasia were neoplastic HCGs. In contrast, in the squamous lesions, neoplastic HCGs were observed in 45 cases (83.3%). Neoplastic HCGs were seen in all of the squamous cell carcinomas, while they were seen in 34

of HSILs (79.1%). The remaining nine (20.9%) HSILs showed individually scattered HSIL cells without neoplastic HCGs.

Neoplastic squamous HCGs (HSIL and squamous cell carcinoma)

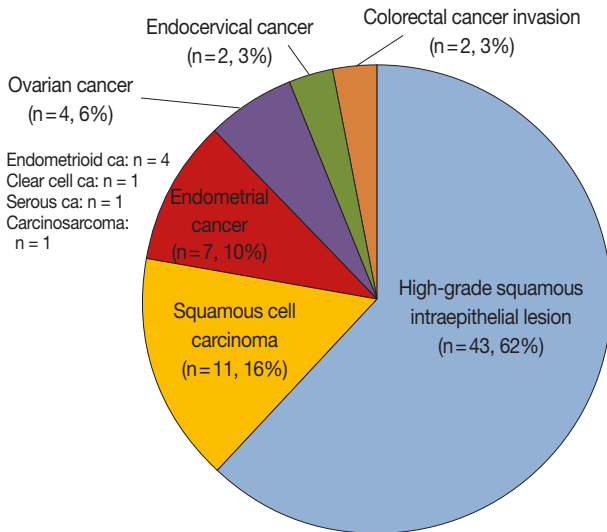


Fig. 3. Summary of the high-grade epithelial cell abnormalities cohort. The majority were squamous lesions (78%).

noma) were characterized by neoplastic cells with anisocytosis, increased nuclear:cytoplasmic ratio, and hyperchromatic nuclei with coarse chromatin (Fig. 4A, B). Tumor diathesis was seen in squamous cell carcinomas, and the presence of scattered atypical dyskeratotic cells were helpful features in recognizing the HCG as squamous (Fig. 4C). Neoplastic endocervical glandular HCGs demonstrated acinar patterns within the HCGs and the neoplastic cells were often columnar cells with pseudostratification (Fig. 4D). Smaller sheets and strips of neoplastic cells were present outside the HCGs with more obvious rosette-like patterns (Fig. 4E). The tumor cells frequently demonstrated macronucleoli, and scattered single cells were observed in one endocervical adenocarcinoma case. When the squamous and glandular HCGs were compared, squamous HCGs tended to show flattening of cells at periphery of HCG and oval-to-round nuclei (Fig. 4A, B), while the glandular HCGs demonstrated acinar patterns within the HCGs and cigar-shaped nuclei (Fig. 4D). HCGs of endometrioid carcinomas were characterized by tight clusters of smaller neoplastic cells (Fig. 4F). The nuclear pleomorphism was subtle in the well-differentiated tumors, while more obvious

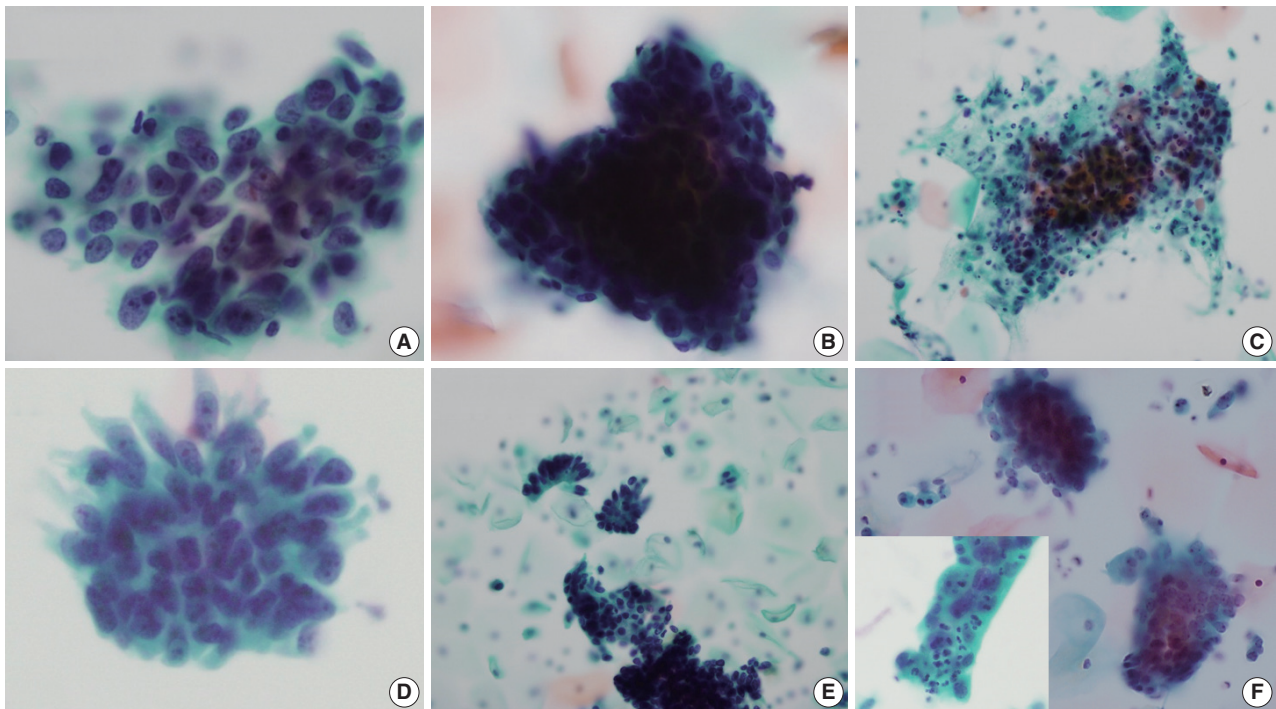


Fig. 4. Cytological features of neoplastic hyperchromatic crowded group (HCG). (A–C) HCGs of squamous cell carcinoma demonstrate dense cellular clusters with chaotic arrangement, and the individual cells are markedly hyperchromatic. The periphery of the HCG is flattened. When present, tumor diathesis and scattered dyskeratotic cells are helpful features in recognizing squamous cell carcinomas (C). (D, E) HCGs of endocervical adenocarcinomas. A vague acinar arrangement is seen within the HCG with feathering of the border (D). Smaller strips and rosettes of tumor cells are helpful clues in the diagnosis (E). (F) HCGs of well-differentiated endometrioid carcinoma were tight clusters of neoplastic cells that were smaller than endocervical adenocarcinoma. More obvious nuclear atypia were present in high-grade tumors and intra-cytoplasmic neutrophils were also present (inset).

nuclear atypia was present in high-grade endometrioid carcinomas. Intracytoplasmic neutrophils (“bags of polys”) were also seen in one case (Fig. 4F, inset). The ovarian and colorectal carcinoma cases all showed glandular cell clusters: the background of the ovarian cancer metastases were clean, while the two colorectal adenocarcinomas demonstrated a necrotic and inflammatory background, suggestive of direct invasion of the uterine cervix by the tumor.

When we examined the presence of individually scattered neoplastic cells in the background, invasive squamous cell carcinomas more frequently demonstrated neoplastic single cells compared to glandular neoplasia (10/11 vs 4/15, respectively; $p = .002$). Glandular lesions demonstrating scattered neoplastic cells were all primary uterine lesions (3 endometrial carcinomas and 1 endocervical adenocarcinoma), and extrauterine neoplasms all presented as cellular clusters on cervicovaginal cytology.

DISCUSSION

HCGs have received more attention in cervicovaginal cytology since the introduction of the LBC test, as the HCGs are more visible against the monolayer background with the LBC method, compared to conventional smears. As LBC is being increasingly used (in Korea, the proportion of cervicovaginal LBC tests has increased from 7.6% in 2004 to 25.3% in 2015),^{5,6} it is important to be aware that HCGs may occasionally be the causes of false-negative or false positive cytology interpretation and to become familiar with the morphological characteristics of different HCGs.

In this study, HCGs were observed in 34% of routine cervicovaginal LBC samples, although less than the previously reported literature.² The majority of HCGs were non-neoplastic cell clusters as previously reported, and the non-neoplastic HCGs were mostly parabasal cell clusters in atrophy. However, the small number of neoplastic HCGs in this study were all high-grade lesions, suggesting that HCGs in cervicovaginal LBC should be carefully evaluated in order to avoid serious false-negative interpretations.²⁻⁴ Conversely, non-neoplastic HCGs may also be over-interpreted as abnormal; for example, specimens from the lower uterine segment have been reported to be over-diagnosed as positive in patients with histories of endocervical adenocarcinomas.⁷ Therefore, although the cytological evaluation of HCGs is often difficult due to the dense obscuring hyperchromasia of the clusters, it is still important to discriminate between neoplastic and non-neoplastic HCGs. One important tip is to evaluate the cytomorphology at the periphery of the HCGs, where the cells

may be more spread out into a single layer. For example, we observed that atrophic cells are flattened at the edges of HCGs into monolayer sheets where the streaming pattern and the bland nuclear features are more easily appreciable. As another example, endocervical adenocarcinomas may show the typical feathery pattern of columnar cells at the edge of the HCGs. Secondly, it is useful to examine each focal plane of the HCG by focusing up and down. By examining each focal plane, it is possible to appreciate the lack of nuclear overlapping in atrophic cell clusters where the parabasal-like cells are stacked in multilayer sheets, and in the case of adenocarcinoma, vague acinar patterns may be visible within the HCGs. Finally, examining the scattered cells and the background outside the HCGs is extremely important. We found scattered neoplastic cells in the majority of squamous cell carcinomas in addition to the tumor diathesis. On the other hand, scattered neoplastic cells were relatively rare in glandular lesions; however, when present, the cytological features of the scattered cells showed the typical features of glandular neoplasia which helped the diagnosis.

In this study, all cases with HCGs in the routine cohort contained EC/TZ components, while about 15% of HCG-negative cases did not demonstrate EC/TZ components. The presence of EC/TZ components in LBC implies that the cervix has been properly sampled, and thus increasing the likelihood of detecting ECAs when present. Chivukula et al.² reported that most HCGs were endocervical cell aggregates and that ECA was detected only when HCGs were present.

In efforts to solve the diagnostic dilemma of HCG, cell block preparations and immunohistochemistry for p16 have been studied on cases showing HCGs.^{8,9} These methods were particularly helpful in identifying neoplastic HCGs from menstrual contamination. An image analysis study of HCGs, where the area, shape and color intensity of HCGs were evaluated, demonstrated little discriminative value in defining the neoplastic or benign nature of HCGs.¹⁰

To conclude, we examined the prevalence of HCGs in routine cervicovaginal LBC and described the morphological features of different types of HCGs. Examining the edges of HCGs, each plane of focus and scattered cells outside HCGs were helpful in the interpretation of the HCGs.

ORCID

Youngeun Lee: <http://orcid.org/0000-0002-0000-1615>

Cheol Lee: <http://orcid.org/0000-0001-5098-8529>

In Ae Park: <http://orcid.org/0000-0001-6667-3484>

Hyoung Jin An: <http://orcid.org/0000-0002-4009-836X>
 Haeryoung Kim: <http://orcid.org/0000-0002-4205-9081>

Author Contributions

Conceptualization: HK.
 Data curation: YL, HK.
 Investigation: YL, HK.
 Methodology: YL, HK.
 Resources: YL, HK, IAP, CL, HJA.
 Supervision: HK.
 Visualization: YL, HK.
 Writing—original draft: YL, HK.
 Writing—review & editing: YL, HK, CL, IAP.

Conflicts of Interest

The authors declare that they have no potential conflicts of interest.

Funding

This work was supported by the Basic Science Research Program through NRF funded by the Ministry of Education (NRF-2016R1D1A1A09919042).

REFERENCES

1. DeMay RM. Common problems in Papanicolaou smear interpretation. *Arch Pathol Lab Med* 1997; 121: 229-38.
2. Chivukula M, Austin RM, Shidham VB. Evaluation and significance of hyperchromatic crowded groups (HCG) in liquid-based paps. *Cytojournal* 2007; 4: 2.
3. Croll E, Rana DN, Walton LJ. Hyperchromatic crowded cell groups in gynaecological liquid-based cytology samples. *Br J Biomed Sci* 2010; 67: 154-63.
4. Gupta N, John D, Dudding N, Crossley J, Smith JH. Factors contributing to false-negative and potential false-negative cytology reports in SurePath liquid-based cervical cytology. *Cytopathology* 2013; 24: 39-43.
5. Oh EJ, Jung CK, Kim DH, et al. Current cytology practices in Korea: a nationwide survey by the Korean Society for Cytopathology. *J Pathol Transl Med* 2017; 51: 579-87.
6. Lim SC, Yoo CW. Current status of and perspectives on cervical cancer screening in Korea. *J Pathol Transl Med* 2019; 53: 210-6.
7. Feratovic R, Lewin SN, Sonoda Y, et al. Cytologic findings after fertility-sparing radical trachelectomy. *Cancer* 2008; 114: 1-6.
8. Diaz-Rosario LA, Kabawat SE. Cell block preparation by inverted filter sedimentation is useful in the differential diagnosis of atypical glandular cells of undetermined significance in ThinPrep specimens. *Cancer* 2000; 90: 265-72.
9. Ge Y, Mody DR, Smith D, Anton R. p16(INK4a) and ProEx C immunostains facilitate differential diagnosis of hyperchromatic crowded groups in liquid-based Papanicolaou tests with menstrual contamination. *Acta Cytol* 2012; 56: 55-61.
10. Evered A, Edwards J, Powell G. Image analysis of hyperchromatic crowded cell groups in SurePath cervical cytology. *Cytopathology* 2013; 24: 113-22.

Concurrent Anti-glomerular Basement Membrane Nephritis and IgA Nephropathy

Kwang-Sun Suh, Song-Yi Choi, Go Eun Bae, Dae Eun Choi¹, Min-Kyung Yeo

Departments of Pathology and ¹Nephrology, Chungnam National University School of Medicine, Daejeon, Korea

Anti-glomerular basement membrane (GBM) nephritis is characterized by circulating anti-GBM antibodies and crescentic glomerulonephritis (GN) with deposition of IgG along the GBM. In a limited number of cases, glomerular immune complexes have been identified in anti-GBM nephritis. A 38-year-old female presented azotemia, hematuria, and proteinuria without any pulmonary symptoms. A renal biopsy showed crescentic GN with linear IgG deposition along the GBM and mesangial IgA deposition. The patient was diagnosed as concurrent anti-GBM nephritis and IgA nephropathy. Therapies with pulse methylprednisolone and cyclophosphamide administration were effective. Concurrent cases of both anti-GBM nephritis and IgA nephropathy are rare among cases of anti-GBM diseases with deposition of immune complexes. This rare case of concurrent anti-GBM nephritis and IgA nephropathy with literature review is noteworthy.

Key Words: Anti-glomerular basement membrane disease; Immunoglobulin A; Crescentic glomerulonephritis

Received: June 11, 2019 **Revised:** July 31, 2019 **Accepted:** August 5, 2019

Corresponding Author: Min-Kyung Yeo, MD, PhD, Department of Pathology, Chungnam National University School of Medicine, 266 Munhwa-ro, Jung-gu, Daejeon 35015, Korea
Tel: +82-42-280-7196, Fax: +82-42-280-8199, E-mail: mkyeo83@gmail.com

Anti-glomerular basement membrane (GBM) disease manifests as rapidly progressive glomerulonephritis (RPGN) characterized by necrotizing glomerulonephritis (GN) with crescentic proliferation. The non-collagenous domain of the α -3 chain of type IV collagen is identified as the autoantigen, and linear IgG deposition along the GBM aid diagnosis of anti-GBM disease. In rare cases, an association of anti-GBM disease with deposition of immune complexes has been reported. Herein, a case of concurrent anti-GBM nephritis and IgA nephropathy is presented.

CASE REPORT

A 38-year-old Korean woman noticed gross hematuria in April 2016. Laboratory analysis revealed a serum creatinine (Cr) level of 0.65 mg/dL; a serum total protein of 7.9 g/dL; a serum albumin of 4.4 g/dL; a serum anti-GBM antibody of 49 U/mL; a urine spot protein/Cr ratio of 0.360 g/g; and many urine spot erythrocytes. She was recommended further workup and treatment, but she refused. She experienced anorexia and weakness in June 2016. Her serum Cr level was 1.7 mg/dL at the second

hospital visit. She was asked for hospitalization, but she refused treatment. She was admitted due to weakness and fever (38.1°C) at the third hospital visit in July 2016. Laboratory analysis at this visit revealed a serum Cr level of 5.45 mg/dL; a serum total protein of 7.5 g/dL; a serum albumin of 3.5 g/dL; a serum anti-GBM antibody of 187.2 U/mL; a urine spot protein/Cr ratio of 1.4 g/g; and many urine spot erythrocytes. Serum antinuclear antibody, anti-double stranded DNA, anti-neutrophil cytoplasmic antibody (ANCA), and antibodies to HIV, hepatitis B, and hepatitis C were all negative. There was no evidence of lung involvement based on chest computed tomography and no respiratory symptoms.

A renal biopsy contained 16 glomeruli with five global scleroses, six fibrocellular crescents, and five cellular crescents (Fig. 1A). An immunofluorescence study showed linear deposition of IgG along the GBM (Fig. 1B) and granular deposition of IgA in mesangial spaces (Fig. 1C). Electron microscopy showed a diffusely wrinkled GBM and mesangial electron-dense deposition (Fig. 1D).

The pathologic diagnosis was “concurrent anti-GBM crescentic

GN and IgA nephropathy,” which was treated with intravenous methylprednisolone (500 mg/day for three successive days) with cyclophosphamide (500 mg/day) followed by oral prednisolone (50 mg/day). Plasmapheresis was avoided due to the possibility of side effects. Three months after the treatment, the anti-GBM

antibody titer gradually decreased (anti-GBM titer, 15.6 U/mL) and renal function improved (Cr, 2.08 mg/dL) (Fig. 2).

This study was approved by the Institutional Review Board of Chungnam National University Hospital with a waiver of informed consent (IRB No. 2016-11-009) and performed in accor-

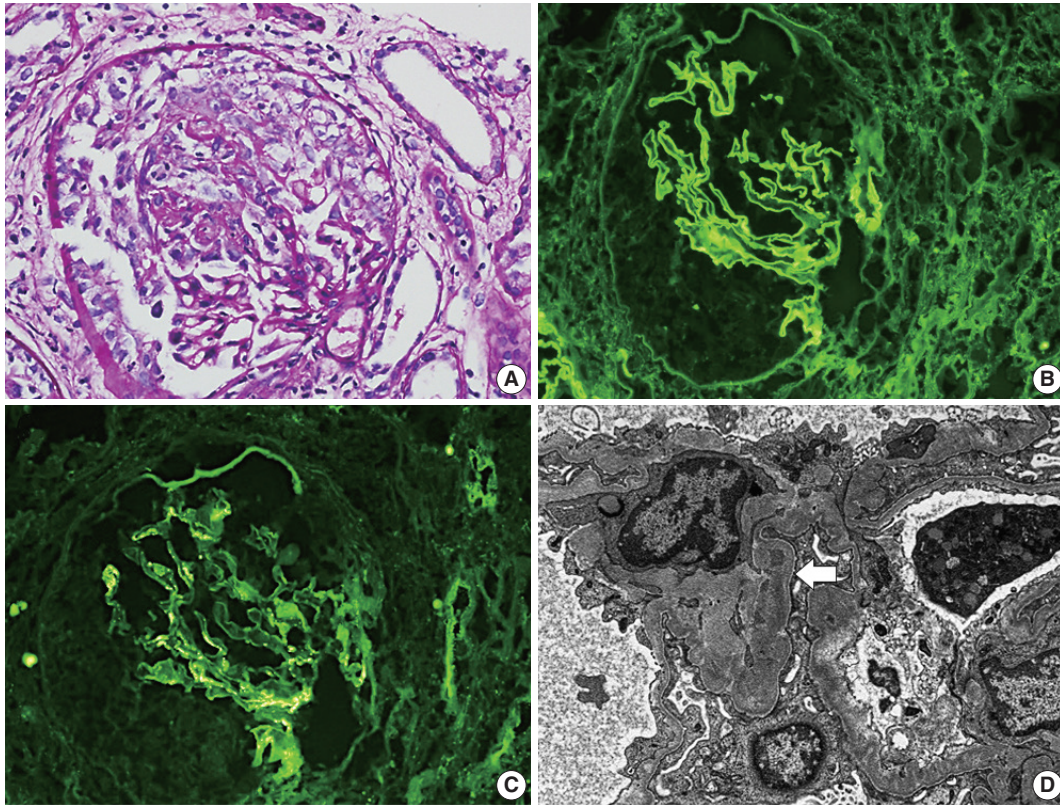


Fig. 1. (A) Light microscopy shows encircling cellular crescents (periodic acid–Schiff staining). Immunofluorescence shows linear deposition of IgG along the glomerular basement membrane (GBM) (B) and granular deposition of IgA in mesangial spaces (C). (D) Electron microscopy shows a diffusely wrinkled GBM and mesangial electron-dense deposition (arrow) (uranyl acetate/lead citrate staining, $\times 8,000$).

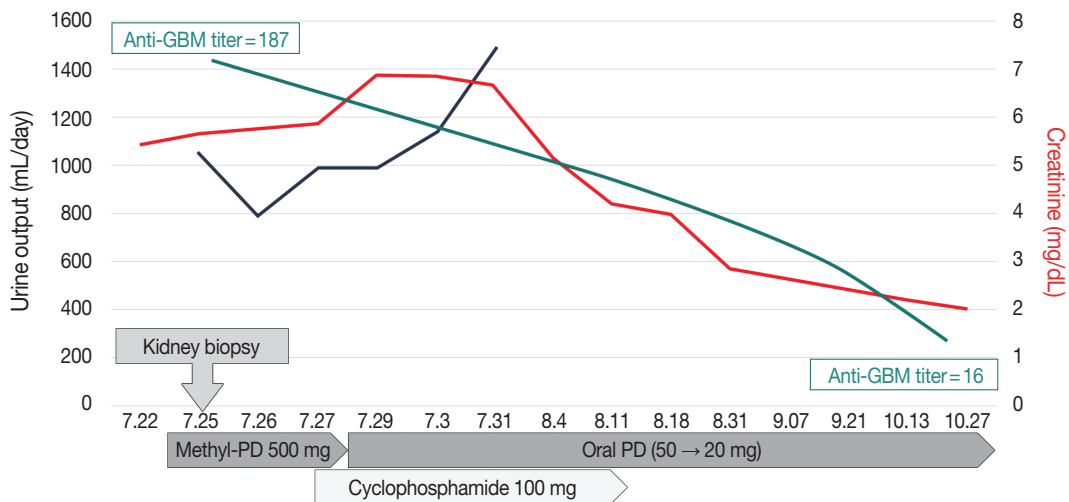


Fig. 2. Clinical course of the patient. GBM, glomerular basement membrane; PD, prednisolone.

dance with the 1964 Helsinki declaration and its later amendments.

DISCUSSION

RPGN is classified into three categories as anti-GBM disease, immune complex disease, and ANCA-associated disease. Among these three categories, anti-GBM disease is the rarest and severest form of crescentic GN and is characterized by linear IgG deposition along the GBM with circulating anti-GBM antibodies.¹ Overlapping features of crescentic GN are identified as coexistence of anti-GBM disease and ANCA antibodies, or anti-GBM disease and immune complex-mediated GN.^{2,3} ANCA antibodies are detected in 21% to 43% of anti-GBM disease patients and clinical characteristics of dual antibody-positive patients are documented.^{3,4} However, concurrent anti-GBM disease and immune complex-mediated GN is rarely reported and the most frequent form of combined immune complex GN is membranous

nephropathy.² Concurrent anti-GBM disease and IgA nephropathy is rare and clinical characteristics are not well understood.

Herein, a case of concurrent anti-GBM nephritis and IgA nephropathy is presented. A literature review for concurrent anti-GBM disease and IgA nephropathy using PubMed (<http://www.ncbi.nlm.nih.gov/pubmed>) was performed resulting in identification of a total of nine cases from nine articles between 1995 and 2016 (Table 1, Supplementary Table S1).^{2,5-12}

The average age and sex of concurrent anti-GBM disease and IgA nephropathy in reported cases was 43 years old with a male:female ratio of 1:1.5. Cases were reported in China (n = 5), the United States (n = 2), Canada (n = 1), and Japan (n = 1). None of the cases was previously diagnosed as immune complex GN including IgA nephropathy. A recent history of hematuria or proteinuria was shown in 40% of cases and a history of upper respiratory tract infection was present in 20% of cases. None showed symptoms of hemoptysis or pulmonary involvement based on image analysis. Oliguria was seen in 10% of cases. The mean proteinuria, serum Cr levels, and anti-GBM antibody titer (among available cases) were 2.6 g/day, 5.0 mg/dL, and 180 EU/mL. The ANCA autoantibody was not identified. The percentage of fibrocellular or cellular crescents in renal biopsies was 59%. All cases were treated with steroids and some cases with combined cytotoxic immunosuppressive agents, including cyclophosphamide, mycophenolate mofetil, or methotrexate. Plasmapheresis was applied to 30% of cases. More than half (60%) of cases showed improved renal function and dialysis dependence was shown in 30% of cases.

Cui et al.² compared clinical and laboratory data of patients suffering anti-GBM disease associated with depositions of immune complexes (10 cases) with data from anti-GBM disease alone (37 cases). No significant differences in clinical and pathological findings were observed. In comparison with anti-GBM disease associated with depositions of immune complexes reported by Cui et al.,² this present review of cases with concurrent anti-GBM disease and IgA nephropathy showed a tendency of better prognosis. Symptoms of oliguria were reported less commonly in concurrent anti-GBM disease and IgA nephropathy (10%) than in anti-GBM disease with depositions of immune complexes (40%). Percentage of crescent formation in cases of concurrent anti-GBM disease and IgA nephropathy (59%) is less than that in cases of anti-GBM disease with deposition of immune complexes (93.8%). Dialysis independence was more frequent in concurrent anti-GBM disease and IgA nephropathy (60%) than in anti-GBM disease with immune complexes (10%).

The connection between anti-GBM disease and IgA nephrop-

Table 1. Clinical characteristics of 10 cases (including the present case) of concurrent anti-GBM nephritis and IgA nephropathy in the literature

Characteristic	Percent
Male:Female ratio	4:6 (1:1.5)
Age, mean (range, yr)	43 (27–60)
History of upper respiratory tract infection	20
History of hematuria or proteinuria	40
Symptoms or signs	
Hemoptysis or abnormal chest findings	0
Oliguria	10
Nephrotic syndrome	20
Laboratory findings	
Proteinuria, mean (g/day)	2.6
Hematuria	100
Creatinine, mean (mg/dL)	5.0
Anti-GBM antibody titer, mean (EU/mL)	180
Percentage of crescents, mean	59
Treatment	
Intravenous methyl-PD + Oral-PD	100
Cyclophosphamide	60
Mycophenolate mofetil	20
Methotrexate	10
Plasmapheresis	30
Prognosis	
Improved	60
Not improved	40
Expired (due to gastrointestinal bleeding)	10
Dialysis	
Independent	60
Dependent	30

GBM, glomerular basement membrane; PD, prednisolone.

athy is uncertain. IgA nephropathy is the most common immune complex-mediated GN and clinical features vary from asymptomatic hematuria to RPGN.¹³ Occurrence of anti-GBM disease superimposed on underlying symptomatic IgA nephropathy could be a possible explanation. No cases were confirmed as IgA nephropathy before diagnosis of anti-GBM nephritis in the present review; however, a history of upper respiratory tract infection or microscopic hematuria was noted in some cases. Pathological changes of GBM components triggered by IgA-related immune complex deposition is another hypothesis.¹⁴ Anti-GBM antibodies might alter the permeability of GBM to allow circulating immune complex deposition in the mesangium.²

Based on the present review of a limited number of cases, concurrent anti-GBM disease and IgA nephropathy seems to have a better prognosis than anti-GBM disease alone or anti-GBM disease with immune complexes. In order to understand concurrent anti-GBM disease and IgA nephropathy as more than just a simple coincidence of the two diseases, more cases need to be analyzed with an in-depth examination of underlying pathogenic relationships between anti-GBM disease and IgA nephropathy.

Electronic Supplementary Material

Supplementary materials are available at Journal of Pathology and Translational Medicine (<https://jpatholtm.org>).

ORCID

Kwang-Sun Suh: <https://orcid.org/0000-0003-3874-864X>
 Song-Yi Choi: <https://orcid.org/0000-0002-8496-5613>
 Go Eun Bae: <https://orcid.org/0000-0001-9288-1383>
 Dae Eun Choi: <https://orcid.org/0000-0003-2870-3958>
 Min-kyung Yeo: <https://orcid.org/0000-0001-8873-0021>

Author Contributions

Conceptualization: KSS, MKY.
 Resources: SYC, DEC.
 Supervision: GEB.
 Writing—original draft: MKY.
 Writing—review and editing: MKY, KSS.

Conflicts of Interest

The authors declare that they have no potential conflicts of interest.

Funding

This work was supported by Chungnam National University Hospital Research Fund, 2018.

REFERENCES

- Jennette JC, D'Agati VD, Olson JL, Silva FG. *Heptinstall's pathology of the kidney*. Philadelphia: Lippincott Williams & Wilkins, 2014; 661-2.
- Cui Z, Zhao MH, Wang SX, Liu G, Zou WZ, Wang HY. Concurrent antiglomerular basement membrane disease and immune complex glomerulonephritis. *Ren Fail* 2006; 28: 7-14.
- Rutgers A, Slot M, van Paassen P, van Breda Vriesman P, Heeringa P, Tervaert JW. Coexistence of anti-glomerular basement membrane antibodies and myeloperoxidase-ANCAs in crescentic glomerulonephritis. *Am J Kidney Dis* 2005; 46: 253-62.
- Alchi B, Griffiths M, Sivalingam M, Jayne D, Farrington K. Predictors of renal and patient outcomes in anti-GBM disease: clinicopathologic analysis of a two-centre cohort. *Nephrol Dial Transplant* 2015; 30: 814-21.
- Trpkov K, Abdulkareem F, Jim K, Solez K. Recurrence of anti-GBM antibody disease twelve years after transplantation associated with de novo IgA nephropathy. *Clin Nephrol* 1998; 49: 124-8.
- Wechsler E, Yang T, Jordan SC, Vo A, Nast CC. Anti-glomerular basement membrane disease in an HIV-infected patient. *Nat Clin Pract Nephrol* 2008; 4: 167-71.
- Wang A, Wang Y, Wang G, Zhou Z, Xun Z, Tan X. Mesangial IgA deposits indicate pathogenesis of anti-glomerular basement membrane disease. *Mol Med Rep* 2012; 5: 1212-4.
- Yamaguchi H, Takizawa H, Ogawa Y, Takada T, Yamaji I, Ura N. A case report of the anti-glomerular basement membrane glomerulonephritis with mesangial IgA deposition. *CEN Case Rep* 2013; 2: 6-10.
- Gao B, Li M, Xia W, Wen Y, Qu Z. Rapidly progressive glomerulonephritis due to anti-glomerular basement membrane disease accompanied by IgA nephropathy: a case report. *Clin Nephrol* 2014; 81: 138-41.
- Troxell ML, Houghton DC. Atypical anti-glomerular basement membrane disease. *Clin Kidney J* 2016; 9: 211-21.
- Ge YT, Liao JL, Liang W, Xiong ZY. Anti-glomerular basement membrane disease combined with IgA nephropathy complicated with reversible posterior leukoencephalopathy syndrome: an unusual case. *Am J Case Rep* 2015; 16: 849-53.
- Xu D, Wu J, Wu J, et al. Novel therapy for anti-glomerular basement membrane disease with IgA nephropathy: a case report. *Exp Ther Med* 2016; 11: 1889-92.
- Emancipator SN, Lamm ME. IgA nephropathy: pathogenesis of the most common form of glomerulonephritis. In: Rubin E, Damjanov I, eds. *Pathol reviews*. Clifton: The Humana Press, 1990; 113-28.
- Kamimura H, Honda K, Nitta K, et al. Glomerular expression of alpha2(IV) and alpha5(IV) chains of type IV collagen in patients with IgA nephropathy. *Nephron* 2002; 91: 43-50.

Adenocarcinoma Arising in an Ectopic Hamartomatous Thymoma with HER2 Overexpression

Harim Oh, Eojin Kim, Bokyoung Ahn, Jeong Hyeon Lee, Youngseok Lee, Yang Seok Chae, Chul Hwan Kim, Yoo Jin Lee

Department of Pathology, Korea University Anam Hospital, Seoul, Korea

Ectopic hamartomatous thymoma (EHT) is a rare tumor which occurs almost exclusively in the supraclavicular or suprasternal area. Since first described by Smith and McClure in 1982,¹ EHT has been reported in a total of 81 cases, which were mostly benign tumors. However, very rarely, a malignant tumor occurs in EHT, and only four cases have been reported.^{2–4} We report a case of a 52-year-old man with adenocarcinoma arising from EHT.

CASE REPORT

A 52-year-old man visited the hospital with a 1-year history of a supraclavicular mass which had grown to a size of 4 cm over the past 3–4 months. The radiologic findings on contrast-enhanced T1 weighted oropharynx magnetic resonance imaging showed a well-defined enhancing mass involving the left pectoralis major, suggesting a neurogenic tumor, complicated dermoid cyst or a reactive lymphadenopathy. Surgical removal was performed for diagnostic and therapeutic purposes. There has been no evidence of recurrence or metastasis in 6 months of follow up.

Grossly, the resected mass measured 3.1 × 3.1 × 1.8 cm. On section, the cut surface showed a well-circumscribed, multi-lobulated, whitish-gray, heterogenous, solid mass with focal cystic changes (Fig. 1A).

Microscopically, the tumor could be largely divided into two portions. The periphery of the tumor displayed a haphazard blending of epithelial and spindle cells with focal adipose tissue

(Fig. 1B). The dominant portion was spindle cell proliferation with moderate cellularity. These cells were arranged in a fascicular and storiform pattern with oval-to-tapered nuclei with eosinophilic cytoplasm. There was no evidence of significant atypia or mitotic activity. Some small lymphocytes were admixed with the spindle cell component. There were also epithelial islands consisting of elongated strands or anastomosing networks, and some cystic spaces with focal squamous differentiation. These islands were perceptibly merged into spindle cells. Small amounts of mature adipocytes were scattered in various portions of the tumor.

In the central portion of the tumor, areas of atypical glandular proliferation forming solid and cribriform architecture with an infiltrative edge were identified (Fig. 1C). The cells were oncocytoïd with abundant, granular, eosinophilic cytoplasm, which are findings consistent with the features of apocrine cells and bearing some resemblance to ductal-type carcinoma. Unlike cells of the tumor periphery, the cells of the central portion had large pleomorphic nuclei with coarse chromatin and prominent nucleoli (Fig. 1D). Mitotic figures were identified and counted at an average of 3/high-power field, but atypical mitoses were not found.

On immunohistochemistry, both spindle cells and epithelial cells in the benign portion were reactive with pan-cytokeratin. The delicate spindle cells were positive for CD34, but negative for S-100. Both the spindle cells and the epithelial components of all areas of the tumor showed nuclear staining for androgen receptor (Fig. 1E).

EHT shows a biphasic pattern, so our differential diagnosis included other malignant lesions. Based on the CD34 and S100 immunohistochemistry results, we excluded synovial sarcoma and malignant peripheral nerve sheath tumor with epithelial differentiation. The tumor did not have chondromyxoid stroma,

Received: May 20, 2019 Revised: June 4, 2019

Accepted: June 23, 2019

Corresponding Author: Yoo Jin Lee, MD

Department of Pathology, Korea University Anam Hospital, 73 Incheon-ro, Seongbuk-gu, Seoul 02841, Korea

Tel: +82-2-920-5595, Fax: +82-2-927-6576, E-mail: yujinn87@korea.ac.kr

which can distinguish EHT from mixed tumor of the skin.

Notably, the dysplastic area showed complete and circumferential intense membrane staining of human epidermal growth factor receptor 2 (HER2) and scored 3+ in accordance with the

HER2 analysis criteria for breast cancer (Fig. 1F). *HER2* gene amplification was not performed.

Because the lesion had recently grown in size and the histological features showed a distinct malignant area with typical

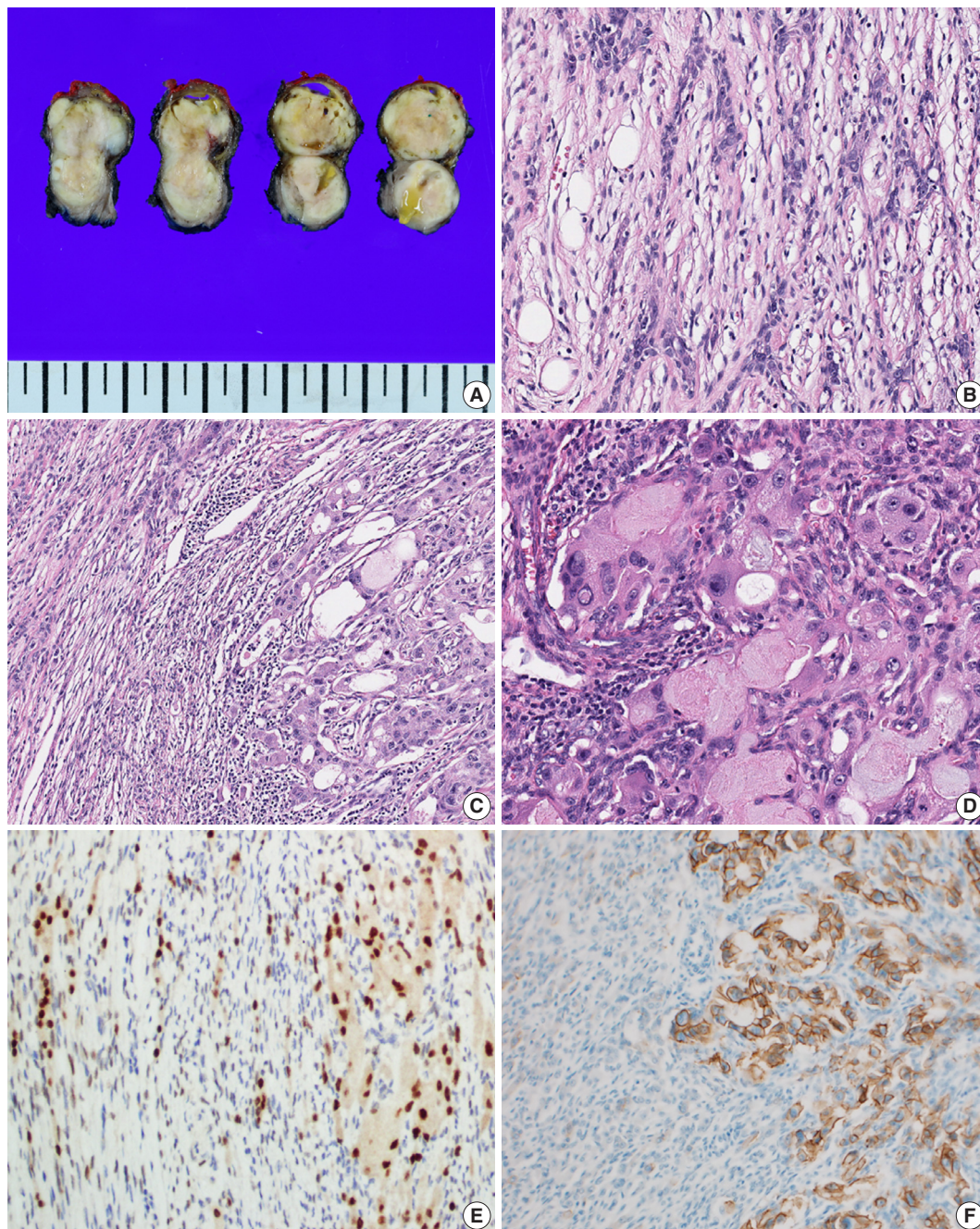


Fig. 1. Representative images of adenocarcinoma arising in ectopic hamartomatous thymoma (EHT). (A) Gross findings show a well-circumscribed, multi-lobulated, whitish-gray, heterogenous, solid mass with focal cystic changes. (B) The periphery of the tumor is composed of epithelial cells, spindle cells and adipose tissue, typical features of EHT. (C) The area of atypical glandular proliferation (right) is distinct from the background EHT (left). (D) The malignant components have large pleomorphic nuclei with prominent nucleoli and abundant eosinophilic cytoplasm. (E) Androgenic receptor immunostain shows nuclear positivity in both the benign and malignant areas. (F) HER2 overexpression is only identified in the malignant portion (right).

EHT, we diagnosed this tumor as an adenocarcinoma arising in EHT.

Ethics statement

This report was approved by the Institutional Review Board of Korea University Anam Hospital (2018AN0340), and informed consent was waived.

DISCUSSION

EHT is a rare tumor, and only 81 cases have been reported thus far. It is generally known as benign, but there have been a few reports of malignancy.²⁻⁴ Three malignant cases had a portion of EHT with a distinct adenocarcinoma component. Consistent with these three cases, the present case demonstrated an area of atypical glandular proliferation with a punctuated cribriform or solid architecture where infiltration was identified, which was diagnosed as invasive adenocarcinoma arising in EHT.

According to the literature, a relatively high prevalence of HER2 overexpression was reported in ductal-type carcinoma ex pleomorphic adenoma,⁵ and HER2 overexpression was only restricted to the malignant portion.⁶ Also, the HER2 positivity was closely related to the aggressive behavior of carcinoma ex pleomorphic adenoma.⁵ These findings suggest that HER2 overexpression had an important role in the malignant transformation of pleomorphic adenoma and progression of carcinoma ex pleomorphic adenoma. Likewise, we could suggest that HER2 overexpression may explain the morphological similarity of the malignant area to ductal-type carcinoma (e.g., pleomorphic and oncocytic tumor cells), and HER2 might have a potential role in the malignant transformation of EHT.

One previous report associated EHT with the androgenic receptor.⁷ This implies that EHT is a tumor affected by androgenic stimuli and is further supported by the fact that EHT occurs exclusively in the adult male.⁷ Moreover, as the androgenic receptor was positive in both the benign and malignant areas of the tumor, we can suggest that the androgenic receptor is related to the occurrence of EHT.

To the best of our knowledge, this is the first case in which HER2 overexpression was found in a malignancy arising in EHT. Patients with HER2 overexpression have a therapeutic advantage because of the availability of targeted therapy, such as trastuzumab, once the mutation is confirmed. Therefore, identification of HER2 overexpression in adenocarcinoma arising from EHT could not only provide important information for understanding the pathogenesis of malignant transformation of EHT, but it can

also indicate treatment with trastuzumab as a potential therapeutic target agent.

ORCID

Harim Oh: <https://orcid.org/0000-0003-4904-4015>

Eojin Kim: <https://orcid.org/0000-0003-3111-6754>

Bokyung Ahn: <https://orcid.org/0000-0002-0229-2276>

Jeong Hyeon Lee: <https://orcid.org/0000-0003-2041-4617>

Youngseok Lee: <https://orcid.org/0000-0002-9762-4957>

Yang Seok Chae: <https://orcid.org/0000-0002-8801-0910>

Chul Hwan Kim: <https://orcid.org/0000-0003-2026-8824>

Yoo Jin Lee: <https://orcid.org/0000-0003-3830-7051>

Author Contributions

Conceptualization: HO, YJL.

Data curation: EK, BA.

Investigation: HO, BA.

Project administration: JHL.

Resources: YL, YSC.

Supervision: YJL, CHK.

Validation: YL, YSC.

Visualization: EK, JHL.

Writing—Original Draft Preparation: HO.

Writing—Review & Editing: YJL.

Conflicts of Interest

The authors declare that they have no potential conflicts of interest.

Funding

No funding to declare.

REFERENCES

1. Smith PS, McClure J. Unusual subcutaneous mixed tumour exhibiting adipose, fibroblastic, and epithelial components. *J Clin Pathol* 1982; 35: 1074-7.
2. Michal M, Zamecnik M, Gogora M, Mukensnabl P, Neubauer L. Pitfalls in the diagnosis of ectopic hamartomatous thymoma. *Histopathology* 1996; 29: 549-55.
3. Sato K, Thompson LDR, Miyai K, Kono T, Tsuda H. Ectopic hamartomatous thymoma: a review of the literature with report of new cases and proposal of a new name: biphenotypic branchioma. *Head Neck Pathol* 2018; 12: 202-9.
4. Michal M, Neubauer L, Fakan F. Carcinoma arising in ectopic

- hamartomatous thymoma: an ultrastructural study. *Pathol Res Pract* 1996; 192: 610-8.
5. Glisson B, Colevas AD, Haddad R, et al. HER2 expression in salivary gland carcinomas: dependence on histological subtype. *Clin Cancer Res* 2004; 10: 944-6.
 6. Di Palma S, Skalova A, Vanieek T, Simpson RH, Starek I, Leivo I. Non-invasive (intracapsular) carcinoma ex pleomorphic adenoma: recognition of focal carcinoma by HER-2/neu and MIB1 immunohistochemistry. *Histopathology* 2005; 46: 144-52.
 7. Weinreb I, O'Malley F, Ghazarian D. Ectopic hamartomatous thymoma: a case demonstrating skin adnexal differentiation with positivity for epithelial membrane antigen, androgen receptors, and BRST-2 by immunohistochemistry. *Hum Pathol* 2007; 38: 1092-5.

Peritoneal Fluid Cytology of Disseminated Large Cell Neuroendocrine Carcinoma Combined with Endometrioid Adenocarcinoma of the Endometrium

Yong-Moon Lee, Min-Kyung Yeo¹, Song-Yi Choi¹, Kyung-Hee Kim¹, Kwang-Sun Suh¹

Department of Pathology, Dankook University School of Medicine, Cheonan; ¹Department of Pathology, Chungnam National University School of Medicine, Daejeon, Korea

Primary large cell neuroendocrine carcinoma (LCNEC) of the endometrium is extremely rare¹⁻³ and the cytomorphology has not been well described. Recently, we experienced a case of combined LCNEC with endometrioid carcinoma (ECa) showing peritoneal dissemination that was confirmed by histology and peritoneal fluid cytology. The purpose of this report is to delineate cytologic characteristics of LCNEC in an effusion specimen.

CASE REPORT

A 62-year-old woman was admitted for evaluation of continuous vaginal bleeding for 1 month. She was in a menopausal state since the age of 50 years with gravida 2–para 2, and had no specific remarkable past medical history. Her initial laboratory test was unremarkable. Ascites was noticed on physical examination. On ultrasonography, the uterine corpus was enlarged with the endometrium thickened to 15 mm. Endometrial curettage showed low-grade ECa. Intraoperative peritoneal fluid sampling demonstrated small-sized tumor cell clusters measuring approximately 100–150 µm in diameter and discohesive polyhedral single tumor cells admixed with karyorrhectic debris, which made a definitive diagnosis difficult. In contrast to mesothelial cells and lymphocytes in the background, tumor cells had large nuclei with an irregular nuclear membrane, vesicular nuclei, relatively prominent nucleoli, and notable cytoplasm (Fig. 1A–C). A panel of

immunohistochemical stains was performed on the cell block material, and atypical cells were positive for CD56 (Fig. 1D) and synaptophysin, but not for chromogranin and CD45. These findings were consistent with neuroendocrine carcinoma (NEC). An en-bloc resection was performed. On microscopic examination, there were foci of transition between a low-grade ECa and a loosely cohesive carcinoma component in the endometrium (Fig. 2A) invading the superficial myometrium (Fig. 2B). The loosely cohesive tumor component showed pseudoglandular and cord-like growth patterns. The tumor cells had relatively abundant cytoplasm, vesicular nuclei, and prominent nucleoli (Fig. 2C). There were tumor emboli in lymphovascular spaces of the myometrium. These cells were positive for CD56 (Fig. 2D) and synaptophysin (Fig. 2E), but negative for CD45 and CD99. Some tumor cells were positive for epithelial membrane antigen (Fig. 2F) and cytokeratin. According to these findings, a diagnosis of combined LCNEC with a low-grade ECa was made. The patient died of the disease 32 days after operation.

Ethics statement

Approval for this case report was obtained from the Institutional Review Board (IRB) of Chungnam National University Hospital (CNUH-IRB 2017-9-49) with a waiver of informed consent.

DISCUSSION

LCNEC is characterized by the presence of polygonal cells with a neuroendocrine growth pattern in at least part of the tumor and expression of one or more of the neuroendocrine markers (chromogranin, CD56, and synaptophysin) in more than 10%

Received: June 11, 2019 Revised: July 19, 2019

Accepted: July 29, 2019

Corresponding Author: Kwang-Sun Suh, MD, PhD

Department of Pathology, Chungnam National University School of Medicine,
266 Munhwa-ro, Jung-gu, Daejeon 35015, Korea
Tel: +82-42-280-7196, Fax: +82-42-280-7189, E-mail: kssuh@cnu.ac.kr

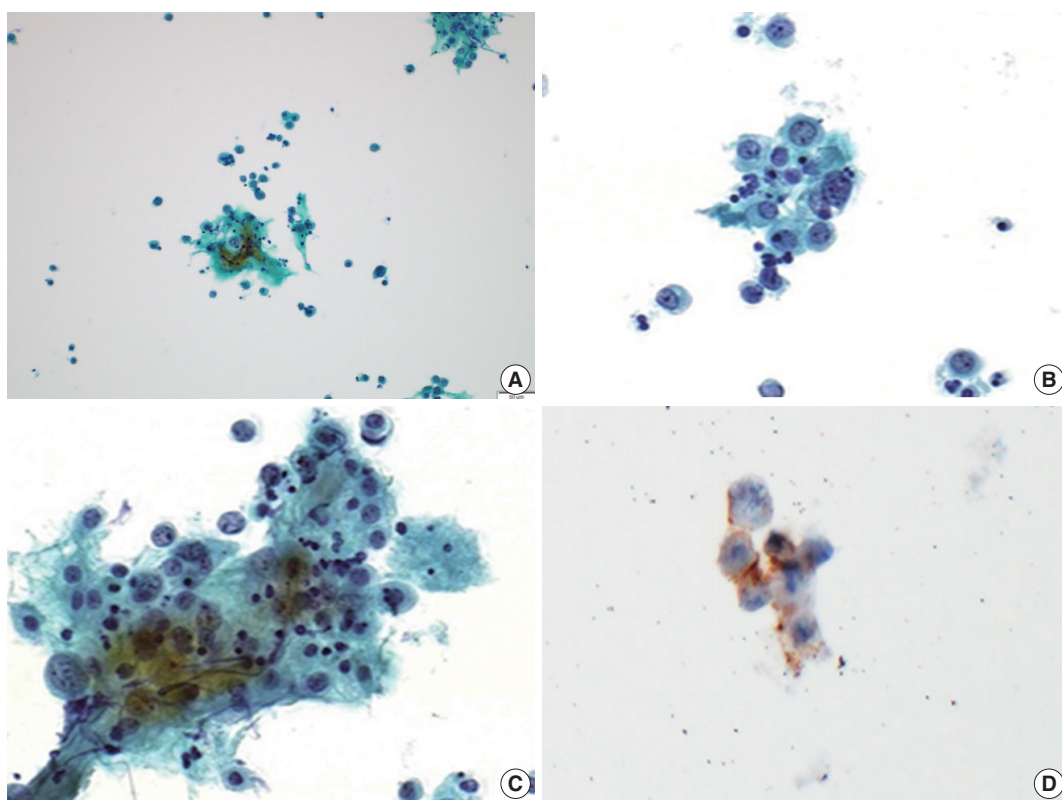


Fig. 1. Cytopathologic features of large cell neuroendocrine carcinoma in a peritoneal fluid smear. (A) Loose clusters of tumor cells measuring 100 to 150 μm are present. (B, C) These tumor cells are polyhedral with abundant eosinophilic cytoplasm, nuclei are either vesicular or hyperchromatic, chromatin is heterogeneous, and nucleoli are variably prominent. (D) These cells show positive reactions for CD56.

of tumor cells.¹ Due to the rarity of LCNECs in the female genital tract,¹⁻³ a specific diagnosis of LCNEC is usually not possible in effusion specimens. Additional difficulties that may be encountered in effusion cytology include overlapping morphology among similar neoplastic entities, scant cellularity, and predominance of apoptosis or cellular debris. Cytopathologic diagnosis of LCNEC is more challenging than small cell neuroendocrine carcinoma due to rare nuclear molding (13%), frequent apoptosis (67%), and prominent nucleoli (86%) in LCNEC.⁴ The cytologic findings of LCNEC of the uterine cervix are characterized by loosely cohesive clusters or single tumor cells with hyperchromatic nuclei and necrotic materials in the background. The ovoid nuclei are 3–5 times larger than nuclei of small lymphocytes and have coarsely clumped chromatin and two or more prominent nucleoli. The tumor cells have a moderate amount of cytoplasm.⁵⁻⁷

A cytopathologic differential diagnosis of our case included serous carcinoma, small cell NEC (SCNEC), and undifferentiated carcinoma. Serous carcinoma is characterized by marked exfoliation of high-grade tumor cells either in the form of cellular clusters or single cells. Psammoma bodies can be seen.⁸ SCNEC is com-

posed of relatively uniform small hyperchromatic nuclei with characteristic nuclear molding and scant cyanophilic cytoplasm.⁹ In this case, cellular overlapping, an acinar arrangement, and papillary configuration were not distinctive. Dedifferentiated carcinoma is composed of a mixture of undifferentiated carcinoma and either the International Federation of Gynecology and Obstetrics grade 1 or 2 ECa.¹ Undifferentiated carcinoma grows as sheets of noncohesive atypical tumor cells without any nested or trabecular architecture and displays chromogranin and/or synaptophysin staining in a minority of tumor cells.¹⁰ In this case, the tumor components showed a cord-like growth pattern and were positive for CD56 and synaptophysin.

In high-grade NEC metastases, the three architectural patterns of the cytomorphologic spectrum that have been presented within body cavities are (1) a predominance of small clusters of tumor cells (seen more often in LCNEC cases), (2) a predominance of large clusters of tumor cells (mainly in SCNEC), and (3) a predominance of single tumor cells (seen in both SCNECs and LCNECs).⁴ The small clustering pattern is seen in 73% of LCNEC and 41% of SCNEC cases.⁴ Our case presented predominantly with small clusters of tumor cells measuring less

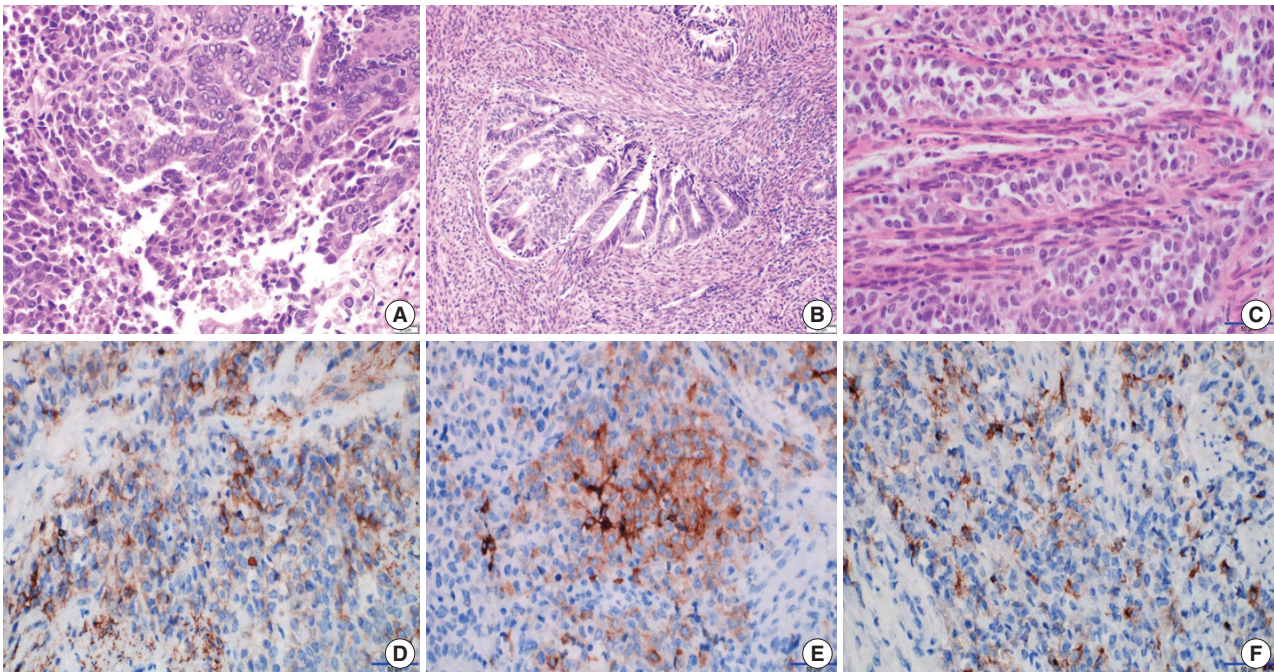


Fig. 2. Microscopic and immunohistochemical findings. The endometrium shows foci of transition between a low-grade endometrioid adenocarcinoma and a loosely cohesive carcinoma component (A) with a cribriform pattern of growth invading the myometrium (B). (C) The loosely cohesive tumor component shows a cord-like growth pattern and the tumor cells have relatively abundant eosinophilic cytoplasm with a large polyhedral nucleus and prominent nucleoli. Immunohistochemically, these tumor cells show positive reactions for CD56 (D) and synaptophysin (E). (F) Some tumor cells are positive for epithelial membrane antigen.

than 150 μm (approximately 100 to 150 μm) and discohesive single tumor cells.

ORCID

Yong-Moon Lee: <https://orcid.org/0000-0002-4302-9263>

Min-Kyung Yeo: <https://orcid.org/0000-0001-8873-0021>

Song-Yi Choi: <https://orcid.org/0000-0002-8496-5613>

Kyung-Hee Kim: <https://orcid.org/0000-0003-0214-0296>

Kwang-Sun Suh: <https://orcid.org/0000-0003-3874-864X>

Author Contributions

Conceptualization: KHK, KSS.

Data curation: YML, MKY.

Funding acquisition: KSS.

Writing—original draft: YML, KSS.

Writing—review & editing: MKY, SYC, KSS.

Conflicts of Interest

The authors declare that they have no potential conflicts of interest.

Funding

This study was supported by the research fund of Chungnam National University.

REFERENCES

1. Kurman RJ, Carcangiu ML, Herrington CS, Young RH. WHO classification of tumours of female reproductive organs. 4th ed. Lyon: IARC Press, 2014; 131-3.
2. Chun YK. Neuroendocrine tumors of the female reproductive tract: a literature review. *J Pathol Transl Med* 2015; 49: 450-61.
3. Deodhar KK, Kerkar RA, Suryawanshi P, Menon H, Menon S. Large cell neuroendocrine carcinoma of the endometrium: an extremely uncommon diagnosis, but worth the efforts. *J Cancer Res Ther* 2011; 7: 211-3.
4. Khalbuss WE, Yang H, Lian Q, Elhosseiny A, Pantanowitz L, Monaco SE. The cytomorphologic spectrum of small-cell carcinoma and large-cell neuroendocrine carcinoma in body cavity effusions: a study of 68 cases. *Cytojournal* 2011; 8: 18.
5. Lee WY. Exfoliative cytology of large cell neuroendocrine carcinoma of the uterine cervix. *Acta Cytol* 2002; 46: 1176-9.
6. Niwa K, Nonaka-Shibata M, Satoh E, Hirose Y. Cervical large cell

- neuroendocrine carcinoma with cytologic presentation: a case report. *Acta Cytol* 2010; 54(5 Suppl): 977-80.
7. Kuroda N, Wada Y, Inoue K, et al. Smear cytology findings of large cell neuroendocrine carcinoma of the uterine cervix. *Diagn Cytopathol* 2013; 41: 636-9.
 8. Kobayashi TK, Norimatsu Y, Buccoliero AM. Cytology of the body of the uterus. In: Gray W, Kocjan G, eds. *Diagnostic cytopathology*. 3rd ed. London: Churchill Livingstone Elsevier, 2010; 709-11.
 9. Tabbara SO, Khalbuss WE. Other malignant neoplasms. In: Nayar R, Wilbur DC, eds. *The Bethesda system for reporting cervical cytology*. 3rd ed. Cham: Springer, 2015; 244-59.
 10. Altrabulsi B, Malpica A, Deavers MT, Bodurka DC, Broaddus R, Silva EG. Undifferentiated carcinoma of the endometrium. *Am J Surg Pathol* 2005; 29: 1316-21.

Comment on “Prognostic Role of Claudin-1 Immunohistochemistry in Malignant Solid Tumors: A Meta-Analysis”

Bolin Wang, Yan Huang¹

Weifang Medical University, Weifang; ¹Department of Oncology, Affiliated Hospital of Weifang Medical University, Weifang, China

Dear Editor,

With great interest, we read the article “Prognostic Role of Claudin-1 Immunohistochemistry in Malignant Solid Tumors: A Meta-Analysis”.¹ The authors stated that low claudin-1 immunohistochemistry expression is significantly correlated with worse survival in various malignant tumors. The results of the meta-analysis are encouraging. Nevertheless, there are still some shortcomings that need to be addressed.

Firstly, literature search is an important step in meta-analysis. If the collection is incomplete, it will lead to obvious selective bias. I want to know whether this is an independent collection in the process of literature collection and how the authors resolved the differences of opinion.

Secondly, the authors seem to have forgotten the key step: quality assessment. We doubt the quality of the attached literature. If the quality of the literature is poor, it will directly affect the value of the results.

Finally, overall survival and disease-free survival are two key endpoints. The authors point out that to avoid bias, articles with a follow-up date of 60 months were extracted. So we want to know if literature collection excluded articles that had follow-up period less than 60 months. Also, we want to know that

the overall survival rate and disease-free survival rate refer to the 5-year survival rate? If not, we recommend that it be shown in the text or table.

Nevertheless, we are grateful to the authors for their efforts in studying the association between claudin-1 immunohistochemistry and malignant solid tumors.

ORCID

Bolin Wang: <https://orcid.org/0000-0001-8086-0681>

Yan Huang: <https://orcid.org/0000-0002-1599-9086>

Conflicts of Interest

The authors declare that they have no potential conflicts of interest.

REFERENCE

1. Pyo JS, Kim NY, Cho WJ. Prognostic role of claudin-1 immunohistochemistry in malignant solid tumors: a meta-analysis. *J Pathol Transl Med* 2019; 53: 173-9.

Received: July 23, 2019 Accepted: September 25, 2019

Corresponding Author: Yan Huang, MD
Department of Oncology, Affiliated Hospital of Weifang Medical University, Weifang
261031, China
Tel: +86-159-2176-8060, E-mail: Yanhuangdr@163.com

Response to Comment on “Prognostic Role of Claudin-1 Immunohistochemistry in Malignant Solid Tumors: A Meta-Analysis”

Jung-Soo Pyo, Nae Yu Kim¹, Won Jin Cho²

Departments of Pathology and ¹Internal Medicine, Eulji University Hospital, Eulji University School of Medicine, Daejeon;
²Department of Urology, Chosun University Hospital, Chosun University School of Medicine, Gwangju, Korea

This study aimed to elucidate the prognostic roles of claudin-1 immunohistochemistry in various malignant tumors through a meta-analysis. Data from all included studies were extracted by two independent authors (J.S.P. and N.Y.K.). Any disagreements for extracting data were resolved by consensus. In the present study, to review more articles, we used the narrow exclusion criteria. Therefore, discordance for the literature collection did not occur. We assessed the risk of bias for all included studies according to the Newcastle-Ottawa Scale. The detailed information was shown in Table 1. All data for survivals were a 5-year survival rate. If the extractable data only included the survival curve, survival rates at 5-year were obtained from the survival curve.

ORCID

Jung-Soo Pyo: <https://orcid.org/0000-0003-0320-8088>

Nae Yu Kim: <https://orcid.org/0000-0002-0461-6385>

Won Jin Cho: <https://orcid.org/0000-0001-9827-5173>

Conflicts of Interest

The authors declare that they have no potential conflicts of interest.

Received: September 23, 2019 Accepted: September 26, 2019

Corresponding Author: Won Jin Cho, MD

Department of Urology, Chosun University Hospital, Chosun University School of Medicine, 365 Pilmun-daero, Dong-gu, Gwangju 61453, Korea

Tel: +82-62-220-3210, Fax: +82-62-232-3210, E-mail: uro2097@gmail.com

Table 1. The Newcastle-Ottawa Scale for the quality assessment of eligible studies

Study	Selection			Demonstration that outcome of interest was not present at start of study	Comparability		Outcome		Score
	Representativeness of the exposed cohort	Selection of the non-exposed cohort	Ascertainment of exposure		Comparability of cohorts on the basis of the design or analysis	Assessment of outcome	Was follow-up long enough for outcomes to occur	Adequacy of follow-up of cohorts	
Ma et al. (2014) ¹	NA	NA	NA	*	*	*	*	*	5
Morohashi et al. (2007) ²	NA	NA	NA	*	*	*	*	*	5
Matsuo et al. (2011) ³	NA	NA	NA	*	*	*	*	*	5
Resnick et al. (2005) ⁴	NA	NA	NA	*	-	*	*	*	4
Shibutani et al. (2013) ⁵	NA	NA	NA	*	*	*	*	*	5
Yoshida et al. (2011) ⁶	NA	NA	NA	*	*	*	*	*	5
Miyamoto et al. (2008) ⁷	NA	NA	NA	*	*	*	*	*	5
Xiong et al. (2011) ⁸	NA	NA	NA	*	*	*	*	*	5
Li et al. (2015) ⁹	NA	NA	NA	*	*	*	*	*	5
Sappayatosok and Phattaratip (2015) ¹⁰	NA	NA	NA	*	*	*	*	*	5
Fritzsche et al. (2008) ¹¹	NA	NA	NA	*	*	*	*	*	5
Shin et al. (2011) ¹²	NA	NA	NA	*	*	*	*	*	5
Bouchagier et al. (2014) ¹³	NA	NA	NA	*	*	*	*	*	5
Higashi et al. (2007) ¹⁴	NA	NA	NA	*	-	*	*	*	4
Chae et al. (2014) ¹⁵	NA	NA	NA	*	-	*	*	*	4
Chao et al. (2009) ¹⁶	NA	NA	NA	*	-	*	*	*	4
Merikallo et al. (2011) ¹⁷	NA	NA	NA	*	*	*	*	*	5
Zhang et al. (2013) ¹⁸	NA	NA	NA	*	*	*	*	*	5
Huang et al. (2014) ¹⁹	NA	NA	NA	*	*	*	*	*	5
Jung et al. (2011) ²⁰	NA	NA	NA	*	*	*	*	*	5
Tzelepi et al. (2008) ²¹	NA	NA	NA	*	*	*	*	*	5
Hoellen et al. (2017) ²²	NA	NA	NA	*	*	*	*	*	5

NA, not available; *, criteria satisfied; -, criteria not satisfied.

REFERENCES

1. Ma F, Ding X, Fan Y, et al. A CLDN1-negative phenotype predicts poor prognosis in triple-negative breast cancer. *PLoS One* 2014; 9: e112765.
2. Morohashi S, Kusumi T, Sato F, et al. Decreased expression of claudin-1 correlates with recurrence status in breast cancer. *Int J Mol Med* 2007; 20: 139-43.
3. Matsuoka T, Mitomi H, Fukui N, et al. Cluster analysis of claudin-1 and -4, E-cadherin, and beta-catenin expression in colorectal cancers. *J Surg Oncol* 2011; 103: 674-86.
4. Resnick MB, Konkin T, Routhier J, Sabo E, Pricolo VE. Claudin-1 is a strong prognostic indicator in stage II colonic cancer: a tissue microarray study. *Mod Pathol* 2005; 18: 511-8.
5. Shibutani M, Noda E, Maeda K, Nagahara H, Ohtani H, Hirakawa K. Low expression of claudin-1 and presence of poorly-differentiated tumor clusters correlate with poor prognosis in colorectal cancer. *Anticancer Res* 2013; 33: 3301-6.
6. Yoshida T, Kinugasa T, Akagi Y, et al. Decreased expression of claudin-1 in rectal cancer: a factor for recurrence and poor prognosis. *Anticancer Res* 2011; 31: 2517-25.
7. Miyamoto K, Kusumi T, Sato F, et al. Decreased expression of claudin-1 is correlated with recurrence status in esophageal squamous cell carcinoma. *Biomed Res* 2008; 29: 71-6.
8. Xiong L, Wen Y, Miao X, Yang Z. Expressions of cell junction regulatory proteins and their association with clinicopathologic parameters in benign and malignant gallbladder lesions. *Am J Med Sci* 2011; 342: 388-94.
9. Li WJ, Zhang ZL, Yu XM, Cai XL, Pan XL, Yang XY. Expression of claudin-1 and its relationship with lymphatic microvessel generation in hypopharyngeal squamous cell carcinoma. *Genet Mol Res* 2015; 14: 11814-26.
10. Sappayatosok K, Phattaratatip E. Overexpression of claudin-1 is associated with Advanced clinical stage and invasive pathologic characteristics of oral Squamous Cell Carcinoma. *Head Neck Pathol* 2015; 9: 173-80.
11. Fritzsche FR, Oelrich B, Johannsen M, et al. Claudin-1 protein expression is a prognostic marker of patient survival in renal cell carcinomas. *Clin Cancer Res* 2008; 14: 7035-42.
12. Shin HI, Kim BH, Chang HS, Kim CI, Jung HR, Park CH. Expression of claudin-1 and -7 in clear cell renal cell carcinoma and its clinical significance. *Korean J Urol* 2011; 52: 317-22.
13. Bouchagier KA, Assimakopoulos SF, Karavias DD, et al. Expression of claudins-1, -4, -5, -7 and occludin in hepatocellular carcinoma and their relation with classic clinicopathological features and patients' survival. *In Vivo* 2014; 28: 315-26.
14. Higashi Y, Suzuki S, Sakaguchi T, et al. Loss of claudin-1 expression correlates with malignancy of hepatocellular carcinoma. *J Surg Res* 2007; 139: 68-76.
15. Chae MC, Park CK, Keum DY, Hwang I, Kwon KY, Jang BC. Prognostic significance of claudin 4 in completely resected adenocarcinoma of the lung. *Korean J Thorac Cardiovasc Surg* 2014; 47: 262-8.
16. Chao YC, Pan SH, Yang SC, et al. Claudin-1 is a metastasis suppressor and correlates with clinical outcome in lung adenocarcinoma. *Am J Respir Crit Care Med* 2009; 179: 123-33.
17. Merikallio H, Kaarteenaho R, Pääkkö P, et al. Impact of smoking on the expression of claudins in lung carcinoma. *Eur J Cancer* 2011; 47: 620-30.
18. Zhang Z, Wang A, Sun B, Zhan Z, Chen K, Wang C. Expression of CLDN1 and CLDN10 in lung adenocarcinoma in situ and invasive lepidic predominant adenocarcinoma. *J Cardiothorac Surg* 2013; 8: 95.
19. Huang J, Li J, Qu Y, et al. The expression of claudin 1 correlates with beta-catenin and is a prognostic factor of poor outcome in gastric cancer. *Int J Oncol* 2014; 44: 1293-301.
20. Jung H, Jun KH, Jung JH, Chin HM, Park WB. The expression of claudin-1, claudin-2, claudin-3, and claudin-4 in gastric cancer tissue. *J Surg Res* 2011; 167: e185-91.
21. Tzelepi VN, Tsamandas AC, Vlotinou HD, Vagianos CE, Scopa CD. Tight junctions in thyroid carcinogenesis: diverse expression of claudin-1, claudin-4, claudin-7 and occludin in thyroid neoplasms. *Mod Pathol* 2008; 21: 22-30.
22. Hoellen F, Waldmann A, Banz-Jansen C, et al. Claudin-1 expression in cervical cancer. *Mol Clin Oncol* 2017; 7: 880-4.

CORRIGENDUM

Journal of Pathology and Translational Medicine 2019; 53: 415
<https://doi.org/10.4132/jptm.2019.08.12>

JPTM

Correction of Ethics Statement: Metastatic Insulinoma Presenting as a Liver Cyst

Hua Li, Tony El Jabbour, Ankesh Nigam¹, Hwajeong Lee
Departments of Pathology and Laboratory Medicine and ¹General Surgery, Albany Medical Center, Albany, NY, USA

To the Editor:

We found an error in our published article.

Li H, Jabbour TE, Nigam A, Lee H. Metastatic insulinoma presenting as a liver cyst. *Journal of Pathology and Translational Medicine* 2019; 53(2): 148-151. <https://doi.org/10.4132/jptm.2019.01.15>.

On page 148, the ethics statement in the last paragraph should read “Anonymous case reports are exempt category reviews by the institutional review board (IRB) at Albany Medical Center, Albany, NY, USA. The IRB does not require consent of the patient for an anonymous case review. Therefore, a formal IRB consent waiver was not required and was not obtained. Our study follows the principles of the Declaration of Helsinki.”

We apologize for the error.

